GEOLOGICAL SURVEY OF CANADA
OPEN FILE 7423

Indicator minerals in till and bedrock samples from the Pine Point Mississippi Valley-type district, Northwest Territories

N.M. Oviatt, M.B. McClenaghan, R.C. Paulen, S.A. Gleeson, S.A. Averill, and S. Paradis

2013

Natural Resources Canada | Ressources naturelles Canada

Canada

GEOLOGICAL SURVEY OF CANADA
OPEN FILE 7423

Indicator minerals in till and bedrock samples from the Pine Point Pb-Zn Mississippi Valley-type district, Northwest Territories

N.M. Oviatt[1], M.B. McClenaghan[2], R.C. Paulen[2], S.A. Gleeson[1], S.A. Averill[3], and S. Paradis[4]

[1]Department of Earth and Atmospheric Sciences, University of Alberta, Edmonton, Alberta
[2]Geological Survey of Canada, Ottawa, Ontario
[3]Overburden Drilling Management, Ottawa, Ontario
[4]Geological Survey of Canada, Sidney, British Columbia

doi:10.4095/293031

This publication is available for free download through GEOSCAN (http://geoscan.ess.nrcan.gc.ca/).

Recommended citation
Oviatt, N.M., McClenaghan, M.B., Paulen, R.C., Gleeson, S.A., Averill, S.A., and Paradis, S., 2013. Indicator minerals in till and bedrock samples from the Pine Point Pb-Zn Mississippi Valley-type district, Northwest Territories; Geological Survey of Canada, Open File 7423. doi:10.4095/293031

Publications in this series have not been edited; they are released as submitted by the author.

Contribution to the Geological Survey of Canada's Geo-mapping for Energy and Minerals (GEM) Program (2008–2013)

TABLE OF CONTENTS

Figures

Tables

INDICATOR MINERALS IN TILL AND BEDROCK SAMPLES FROM THE PINE POINT MISSISSIPPI VALLEY-TYPE DISTRICT, NORTHWEST TERRITORIES

N.M. Oviatt[1*], M.B. McClenaghan[2], R.C. Paulen[2], S.A. Gleeson[1], S.A. Averill[3], and S. Paradis[4]

[1]Department of Earth and Atmospheric Sciences, University of Alberta, Edmonton, Alberta T6G 2R3
[2]Geological Survey of Canada, 601 Booth Street, Ottawa, Ontario K1A 0E
[3]Overburden Drilling Management, Unit 107, 15 Capella Court, Ottawa, Ontario K2E 7X1
[4]Geological Survey of Canada, 9860 West Saanich Road, P.O. Box 6000, Sidney, British Columbia V8L 4B2
*Author email: oviatt@ualberta.ca

ABSTRACT

An indicator mineral study was conducted within the Pine Point Mississippi Valley-type (MVT) district in Northwest Territories to document the abundance, morphology, size and, chemistry of the indicator minerals present in the deposits and in till down-ice of the deposits. Till and bedrock samples for this study were collected in 2010 and 2011. Heavy mineral concentrates (specific gravity >3.2) were isolated from till samples and indicator minerals were picked from this fraction. Indicator minerals identified for the Pine Point MVT deposits include sphalerite, galena, smithsonite, cerussite, and pyrite. Sphalerite and galena are the most useful indicator minerals because they are the most abundant in ore and till samples down-ice and they are sufficiently physically robust that they survive glacial transport.

INTRODUCTION

As long-term demand for metals and minerals is expected to grow (Stothart, 2011) base metal deposits have once more become a major exploration target in Canada. Since indicator mineral and till geochemical methods have proven to be successful exploration tools in glaciated terrain (e.g. Averill, 2001; McClenaghan, 2005) focus has shifted to apply these exploration methods to Mississippi Valley-type (MVT) deposits. Canada is one of the most mineral resource-rich countries in the world and one of the largest producers of minerals and metals (Stothart, 2011). Prior to 2002, the production of Pb and Zn in Canada from MVT deposits was 30%, however, current Canadian production is nil (Sangster, 2002). To improve Pb and Zn exploration in glaciated areas, the Geological Survey of Canada (GSC), in collaboration with the University of Alberta, Overburden Drilling Limited, Tamerlane Ventures Incorporated, and Teck Resources Limited have initiated a study of the till geochemistry and indicator mineral signature of the Pine Point MVT district, Northwest Territories. Till geochemistry data from this study are presented in GSC Open File 7320 (Oviatt et al., 2013); the focus of this report is to present indicator mineral data. Indicator mineral data for stream sediment samples (Fig. 1), also collected as part of this study, have been reported in GSC Open File 7267 (McClenaghan et al., 2012a). Stream sediment and water geochemical data will be reported in a subsequent open file.

LOCATION AND PHYSIOGRAPHY

The Pine Point mining district is on the south shore of Great Slave Lake, Northwest Territories, on the eastern margin of the Western Canada Sedimentary Basin (WCSB). The district is approximately 180 km due south of Yellowknife, in the Buffalo Lake topographic map sheet (NTS 85B) and approximately 50 km east of the town of Hay River. The Buffalo River flows north into Great Slave Lake on the western side of the study area. Black spruce bogs characterize the area and local relief does not exceed 15 m (Lemmen et al., 1994). The Pine Point mine site and open pits can be accessed via Highway 6 and mine roads by truck or ATV in the summer.

EXPLORATION HISTORY

The Pine Point mining district was discovered by prospectors heading north during the Klondike gold rush (1896–1898). They staked claims on a gossanous outcrop at Sulphur Point on the shore of Great Slave Lake (Fig. 1). Little work was conducted on these claims until 1929 when the Northern Lead Zinc Company, which included Cominco Limited, was formed, (Campbell, 1966). The focus of Northern Lead Zinc Company's 1929-1930 exploration program was to determine if the known orebodies were connected beneath the surface and to define the ore grade of the subcropping mineralization. The Great Depression in the early 1930s halted all exploration in the area. Between 1940 and 1947, Cominco Limited directed a drilling program to delineate orebodies associated with basement faulting (Campbell, 1966). In 1963, an induced polarization geophysical survey was conducted in the area, which led to the discovery of orebodies that did not subcrop (Hannigan, 2006). The Pine Point mines opened in 1964 and were one of Canada's most profitable Pb-Zn mining districts until 1987 when

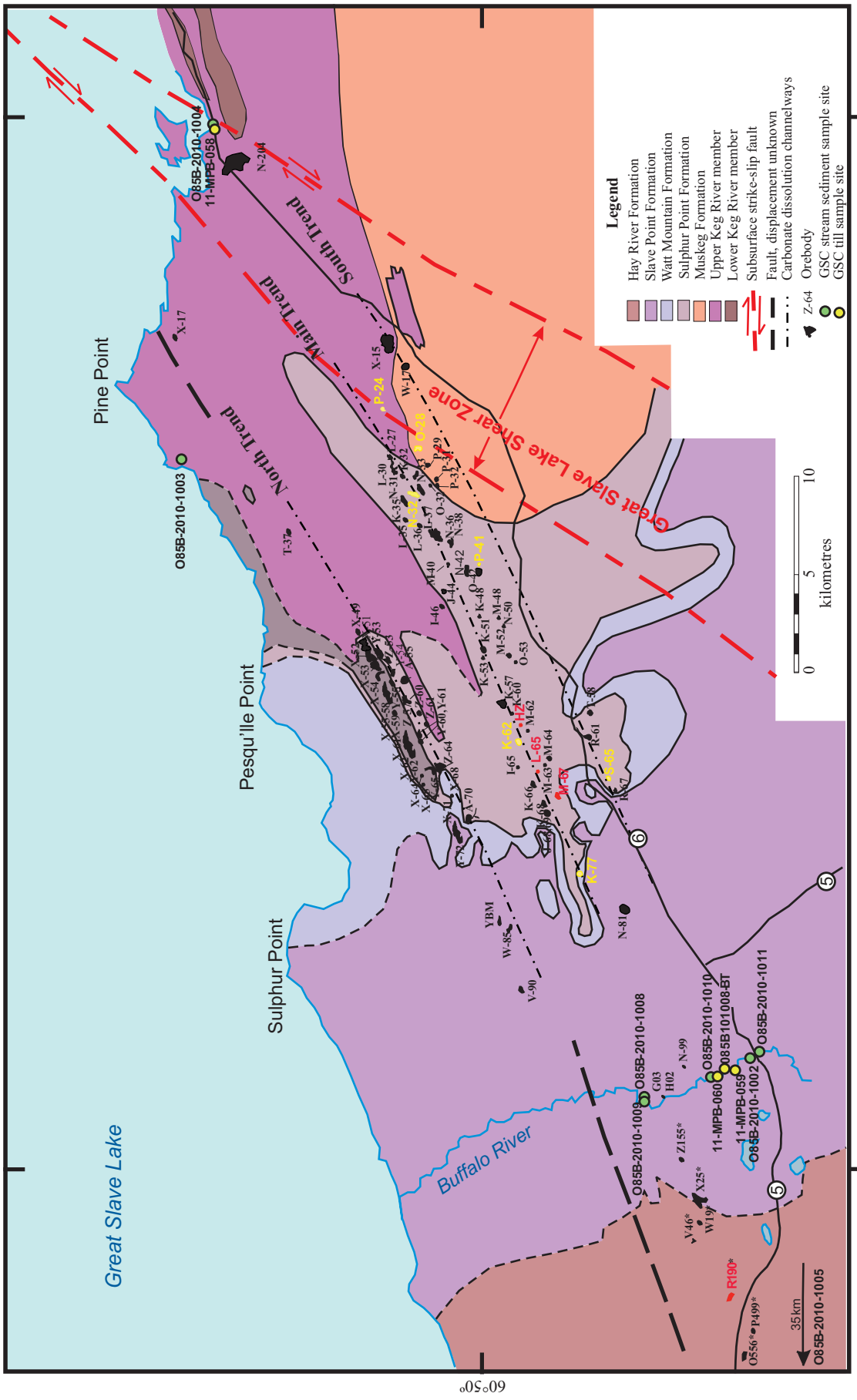

Figure 1. Regional bedrock geology map of the Pine Point area showing the three main trends (North, Main, and South) and their orebodies (modified from Hannigan, 2007). Till samples were collected from open pits at deposits labelled in yellow and at yellow dots. Bedrock samples were collected from deposits labelled in red; stream sediment samples were collected from locations indicated by green dots.

they were shut down. Between 1975 and 1981, Westmin Resources Limited conducted drilling programs approximately 25 km west of Cominco's open pits and discovered nine additional deposits (Hannigan, 2007). None of these western deposits have been mined. Tamerlane Ventures Incorporated optioned the unmined Westmin Resources deposits at Pine Point in 2008 and are currently exploring and assessing the feasibility of several of these deposits (Hannon et al., 2012).

Soil surveys have been conducted in the district to characterize Zn-rich shale that occurs in the region and determine whether or not these rocks are a source for the Zn metal in the Pine Point deposits. The high concentration of Zn that still remains in this shale indicates that it was likely not the source of the mineralization at Pine Point (Macqueen and Ghent, 1975; Brabec, 1983).

GEOLOGY

Bedrock Geology

The Pine Point district is underlain by rocks of the eastern margin of the WCSB. Bedrock of the Pine Point district consists of 350 to 600 m thick, Ordovician to Devonian strata that overlie Archean and Proterozoic crystalline basement rocks (Skall, 1975; Kyle, 1977, 1981; Rhodes et al., 1984; Okulitch, 2006; Hannigan, 2007). All the MVT deposits are hosted in middle Devonian Givetian carbonate strata within and adjacent to the Presqu'ile reef-like barrier complex, which is 200 m at its thickest point. The rocks of the Presqu'ile separate the deep marine rocks to the north from the shallow marine rocks to the south (Rhodes et al., 1984; Hannigan, 2007). At Pine Point, the Presqu'ile barrier consists of two superimposed buildups, the Upper Keg River (or Lower Pine Point Group of Skall (1975); Pine Point Formation of Rhodes et al. (1984)) and the succeeding Sulphur Point formations (Hannigan, 2006). These rocks sit on the shallow-water carbonate platform of the Lower Keg River Formation. The Watt Mountain and Slave Point formations overlie strata of the Presqu'ile barrier. The Upper Keg River Formation includes the lower two-thirds of the barrier and consists of flat, lensoidal beds of carbonate sandstone and mudstone, and fine, dense, grey-brown to buff-brown dolomite with abundant carbonaceous fossils (Skall, 1975; Hannigan, 2007). The overlying Sulphur Point Formation consists of a build-up of bioherms, bioclastic limestone, and carbonate sandstone (Rhodes et al., 1984; Hannigan, 2007) that has undergone alteration into a coarse crystalline, vuggy dolomite, known as Presqu'ile dolomite, and is the host of the majority of the ore bodies (Skall, 1975; Hannigan, 2007).

The Great Slave Lake Shear Zone (GSLSZ) is a crustal-scale structure that cross-cuts basement and Paleozoic bedrock in an area of highly deformed and sheared rocks that extend for approximately 700 km from Northwest Territories southwest into northeastern British Columbia (Eaton and Hope, 2003). It is considered to be a boundary between the Churchill and Slave cratonic provinces (Morrow et al., 2006). Lead isotopic studies (Nelson et al., 2002; Paradis et al., 2006) indicate that mineralizing fluids likely originated in the basement using the GSLSZ as a conduit. This event would likely have occurred in the Phanerozoic when the fault zone was reactivated during the Laramide orogeny (Morrow et al., 2006). The Pine Point deposits are concentrated within 3 northeast–southwest-trending zones, referred to as the North trend, Main trend, and South trend (Fig. 1). The McDonald Fault, a component of the GSLSZ, cuts through the basement rocks immediately below and subparallel to these three trends (Skall, 1975; Kyle, 1981). It has been interpreted that tectonic activity associated with the MacDonald Fault may have had a part in creating these trends (Skall, 1977).

Surficial Geology

The low-relief geomorphology of the Pine Point district is the result of the relatively flat bedrock topography overlain by glacial sediments formed and deposited by the Keewatin sector of the Laurentide Ice Sheet. The landscape surrounding the Pine Point district has glacially streamlined features (e.g. flutings) that mostly reflect the last phase of ice flow. Till cover occurs as a continuous blanket that generally increases in thickness from east to west across the Pine Point district (Lemmen, 1990). Till deposits at the eastern margin of the district range from <1 m to 3 m thick, and gradually thicken westward to >25 m at the western Pine Point open pits. Rice et al. (2013) discuss the Quaternary stratigraphy in detail at Pit K-62, where the till thickness exceeds 23 m. Till is locally thicker where karst collapse structures have created depressions in the bedrock surface. Historic drillhole data indicates that till is up 100 m thick in places (Lemmen, 1990). Commonly, till in the area has a silt to fine sand matrix with very little clay (Lemmen, 1998a,b).

The Pine Point region was deglaciated between 10.0 and 9.6 ka BP (^{14}C: Dyke, 2004) and subsequently was inundated by glacial Lake McConnell (Smith, 1994). Most till surfaces are winnowed, and there was extensive reworking of the till into glaciolacustrine littoral sediments over much of the area (Lemmen, 1990). Glaciolacustrine deposits occur as shorelines and beach ridges, some of which have been reworked into eolian dunes. A corrected age of 11.1 ± 1.1 ka BP was measured by optically stimulated luminescence on the crest of a large sand dune in the Breynat Point map area (NTS 85B15) (Oviatt and Paulen, 2013) and this date (with optical dating uncertainty) is consistent with

deglacial chronologies dated in eolian sediments in southern Northwest Territories (Wolfe et al., 2005) and northwestern Alberta (Wolfe et al., 2007). At approximately 7.8 ka BP (^{14}C), it is speculated that basin uplift in the region restored Great Slave Lake to its current position (Dyke and Prest, 1987; Dyke, 2004).

Surficial mapping was carried out in the Pine Point area by the GSC from 1989 to 1994, mainly to expand the knowledge of glacial Lake McConnell and associated deposits (Lemmen, 1998a,b). Surficial geology maps were published for Buffalo Lake (NTS 85B) and Klewi River (NTS 85A), and a single phase of ice flow to the west was identified (Lemmen, 1990). There is very little published information on the ice-flow history of the region or southern Great Slave Lake in general (Prest et al., 1968; Paulen et al., 2009). Additional research on glacial Lake McConnell was conducted east of the area by Smith (1994). As part of this GEM research project, a surficial map was produced for the western half of the Pine Point deposits (Oviatt and Paulen, 2013).

Mississippi Valley-Type Deposits

The ore field consists of 100 drill-defined orebodies (Hannigan, 2007) that cover an area of approximately 1600 km2. The orebodies range from 100,000 to 17.5 million tonnes and have an average grade of 2% Pb and 6.2% Zn (Hannigan, 2007). The total geological resource (produced and remaining proven resource) is estimated to be 95.4 Mt (Hannigan, 2007). The MVT deposits consist of tabular and prismatic bodies that are hosted by and crosscut more than one carbonate strata unit, i.e., Upper Keg River Member (or Pine Point Group), Sulphur Point Formation, Muskeg Formation, Buffalo River Formation, Watt Mountain Formation, and Slave Point Formation. Sulphide mineralization occurs as open-space cavity-fills of breccia, fractures, and vugs, as well as locally as replacements of carbonate and disseminations.

Sulphide minerals consist of galena and sphalerite with minor pyrite and marcasite (Hannigan, 2007). Galena occurs as isolated crystals (Fig. 2) or as massive aggregates (Fig. 3), and as skeletal crystals within colloform sphalerite (Fig. 4). Sphalerite is present as very fine-crystalline colloform textures (Fig. 5) or occurs as isolated crystals (1–5 mm). Sphalerite crystals range from a dark brown to black, Fe-rich variety to a light honey-brown colour (Fig. 6). Sphalerite, galena, and pyrite also occur as brecciated clasts (Fig. 7). Minor minerals include marcasite, pyrite, sulphur, pyrrhotite, celestite, barite, gypsum, anhydrite, and fluorite (Hannigan, 2007). Bitumen is also present in the host Paleozoic carbonate rocks. Table 1 provides a summary for the ore minerals associated with the Pine Point Pb-Zn deposits.

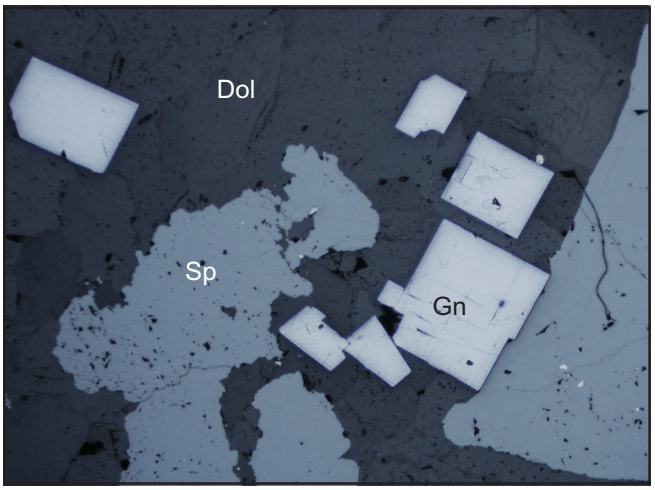

Figure 2. Cubic galena grains in a polished thin section of sample 10-MPB-R76 from deposit HZ. Field of view is 4 mm.

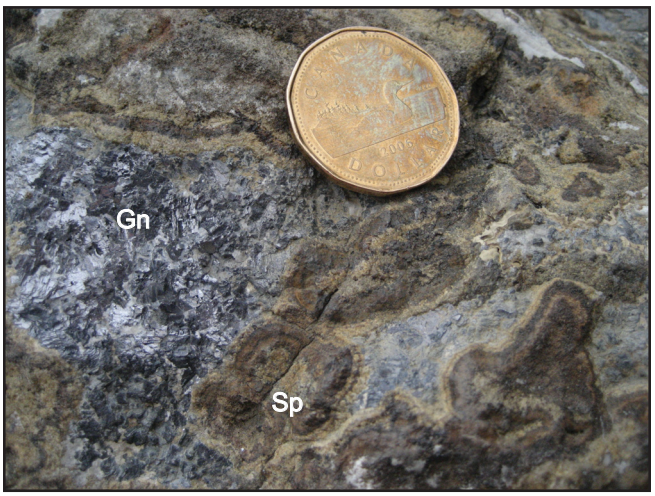

Figure 3. Massive galena with colloform sphalerite from a grab sample collected from a waste rock pile beside deposit O-42. Gn = galena, Sp = sphalerite. Canadian one dollar coin (26.5 mm) for scale.

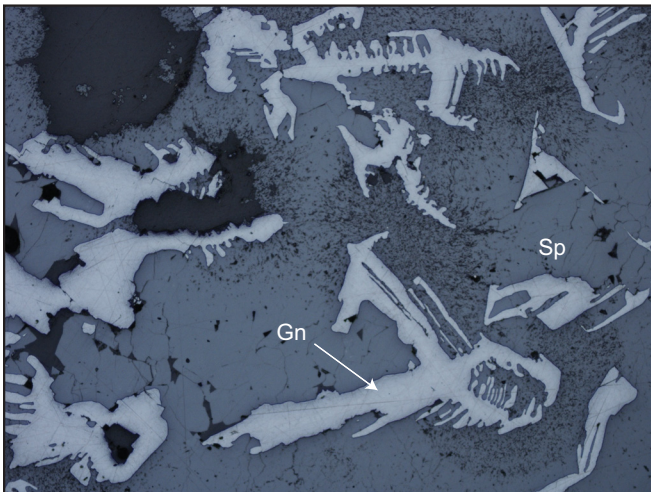

Figure 4. Photomicrograph of skeletal galena in a polished thin section of bedrock sample 10-MPB-R67 from deposit HZ. Reflected light. Gn = galena, Sp = sphalerite. Field of view is 4 mm.

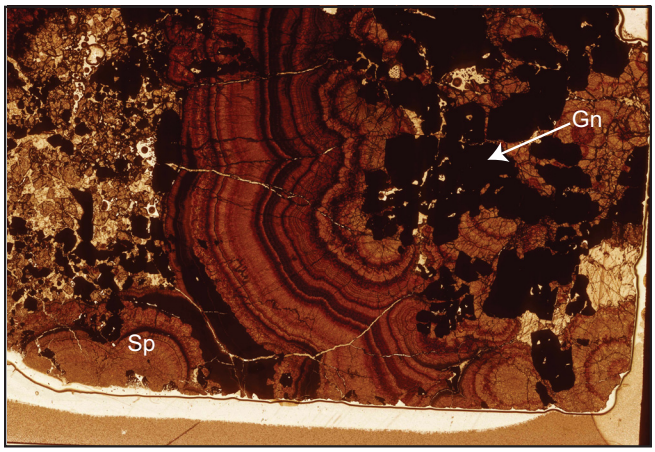

Figure 5. Colloform sphalerite and galena in a polished thin section of sample 10-MPB-R46A from deposit O-28. Image is a colour scan. Gn = galena, Sp = sphalerite. Field of view is 10 cm.

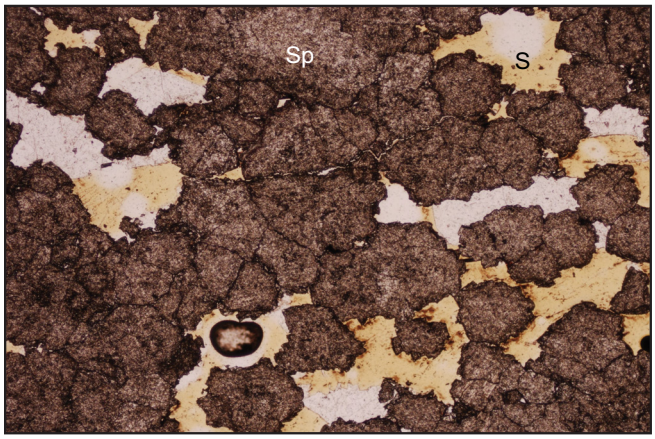

Figure 6. Photomicrograph of subhedral, honey-brown sphalerite grains in a polished thin section of drill core sample 10-MPB-R63 from deposit R190. Interstitial space is filled with native sulphur. S = sulphur, Sp = sphalerite. Field of view is 4 mm.

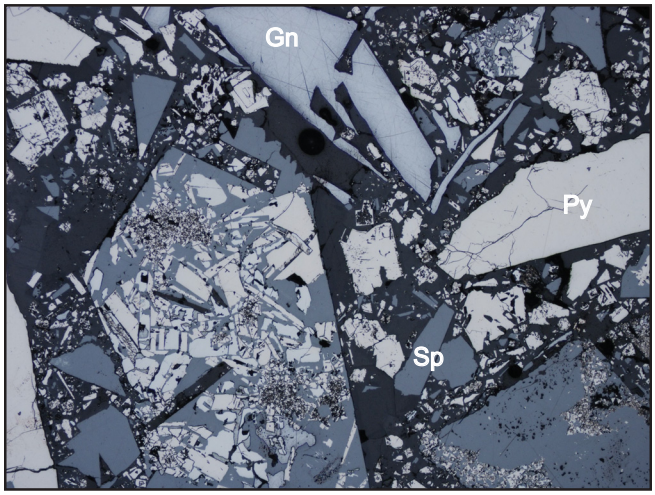

Figure 7. Photomicrograph of brecciated grains of galena (Gn), pyrite (Py), and sphalerite (Sp) in drill core sample 10-MPB-R17 from deposit R190. Some brecciated sphalerite grains contain fragments of galena and pyrite. Reflected light. Field of view is 4 mm.

Table 1. Summary of potential indicator minerals in the Pine Point MVT district deposits (summarized from Hannigan, 2007). The size range of each mineral observed in polished thin section, bedrock heavy mineral concentrates, and till heavy mineral concentrates in this study is also listed.

Mineral	Formula	Reported by Hannigan (2007)	Found in PTS in this Study*	Found in Bedrock HMC in this Study*	Found in Till in this Study*
Major and Minor Minerals in the Ore					
sphalerite	(Zn,Fe)S	yes	0.1-1.5	0.05-2	0.075-2
galena	PbS	yes	0.05-5	0.025-2	0.025-2
pyrite	FeS_2	yes	0.01-0.5	0.025-0.5	0.025-0.5
marcasite	FeS_2	yes	no	0.025-0.5	0.025-0.5
Trace and Rare Minerals in the Ore					
smithsonite	$ZnCO_3$	no	no	no	0.25-2
cerussite	$PbCO_3$	no	no	no	0.25-1
celestite	$SrSO_4$	yes	no	no	no
chalcopyrite	$CuFeS_2$	no	yes	no	0.25-0.5
pyrrhotite	$Fe_{(1-x)}S_{(x=0-0.17)}$	yes	no	no	no
barite	$BaSO_4$	yes	no	no	0.25-0.5
anhydrite	$CaSO_4$	yes	no	no	no
fluorite	CaF_2	yes	no	no	no

* measurements in mm

METHODS

Till and bedrock sampling were conducted in the summers of 2010 and 2011. Field data, including till sample location, depth, and site photos as well as a detailed description of till sampling methods, are reported in GSC Open file 7320 (Oviatt et al., 2013).

Bedrock Sampling

A total of 75 bedrock samples were collected from diamond drill core and waste rock piles adjacent to open pits. Fresh drill core samples were collected from five orebodies: R190, M-67, L-65, HZ, and O-28 (Fig. 1). These bedrock samples were collected to determine the characteristics of the sulphide minerals typical of the Pine Point deposits. Fifteen of the bedrock samples identified in Appendix A1 were submitted to Overburden Drilling Management Limited (ODM), Ottawa, Ontario, for recovery of the heavy mineral fraction and picking of indicator minerals. Fifty-seven of the bedrock samples were made into polished thin sections (PTS) at Vancouver Petrographics, Langley, British Columbia, for petrography and electron microprobe analysis (EMP). Field collection data for bedrock samples are listed in Appendix A1. Photographs and descriptions of bedrock hand samples, including a polished slab and PTS, are included in Appendix A2.

Till Sampling

In 2010 and 2011, a total of 15 till samples were collected across the Pine Point district at a regional scale

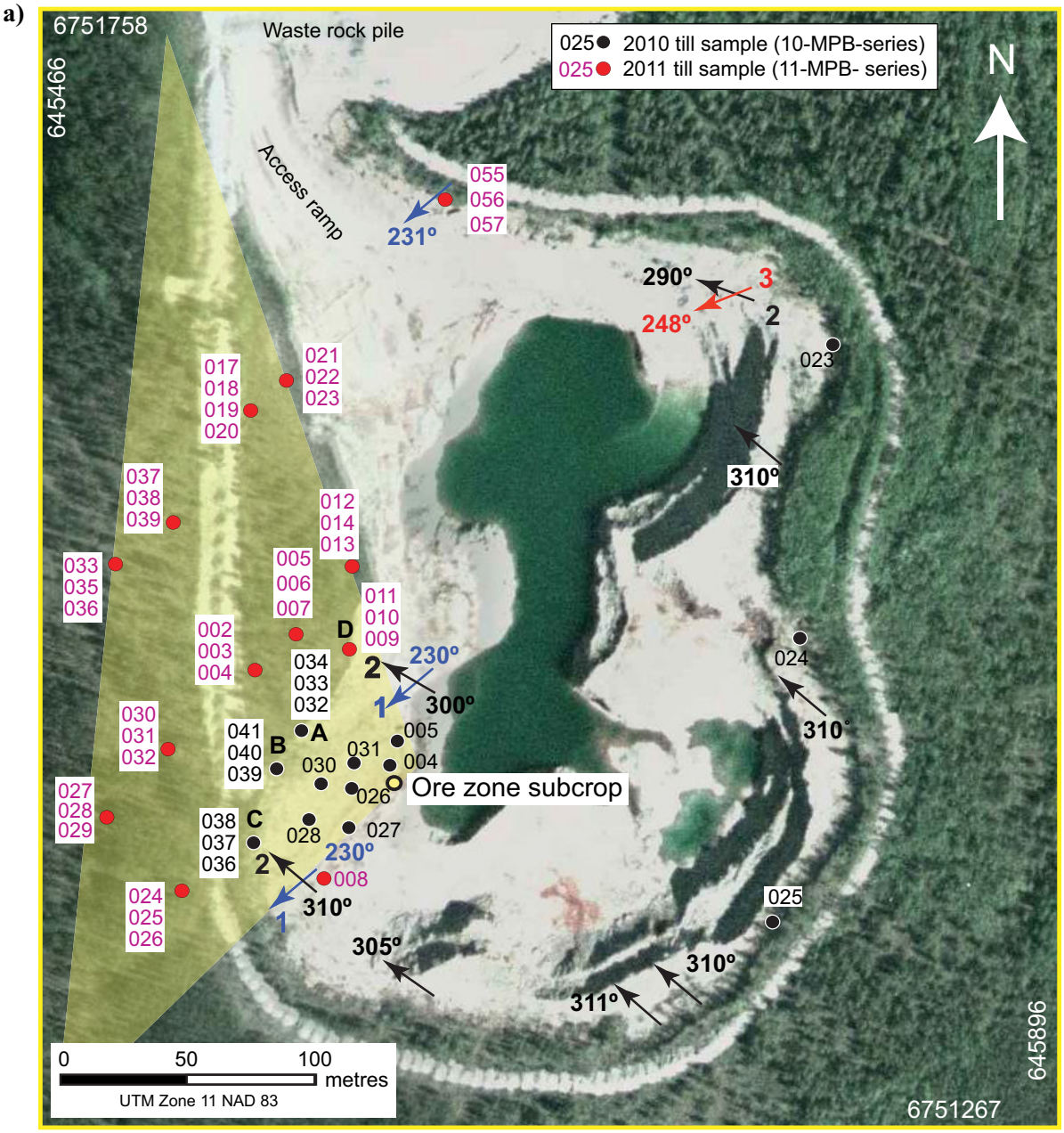

Figure 8. Locations of till samples: **a)** proximal to the former open pit at deposit O-28; and **b)** farther west. Samples collected in 2010 (10-MPB- series) are shown with black numbers and samples collected in 2011 (11-MPB- series) are shown with pink numbers. Three vertical samples were collected from excavated pits at ~1, 2, and 3 m below the natural land surface. 'A', 'B', 'C', and 'D' indicate locations of vertical sections in the western pit wall, which were sampled in 2010 and are referred to in the text. Arrows indicate direction of ice flow: (1) blue = oldest, (2) black, (3) red = youngest ice flow.

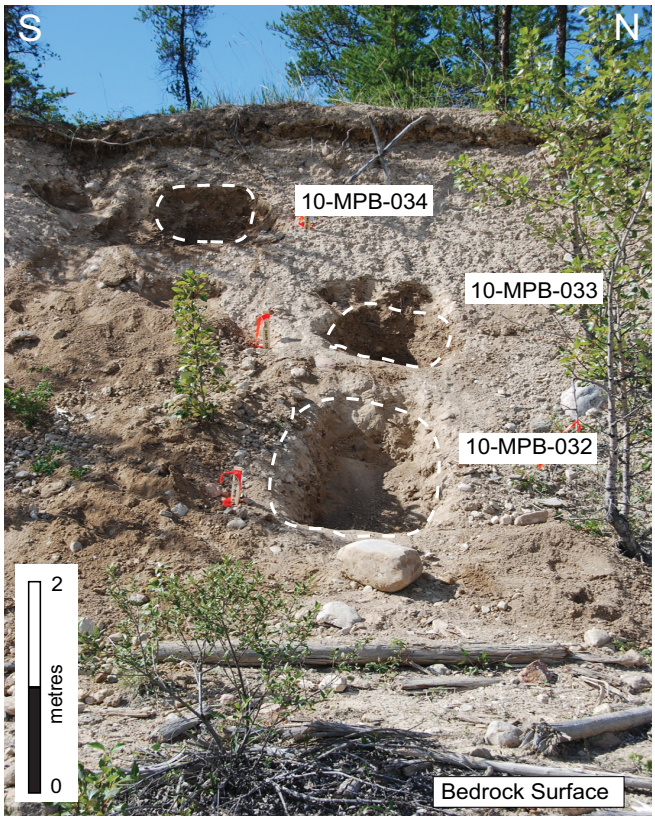

Figure 9. Till samples collected immediately down-ice of deposit O-28 at section A (see Fig. 8 for location). The till section is approximately 6 m high; till samples were collected at ~1, 3, and 5 m below the natural land surface.

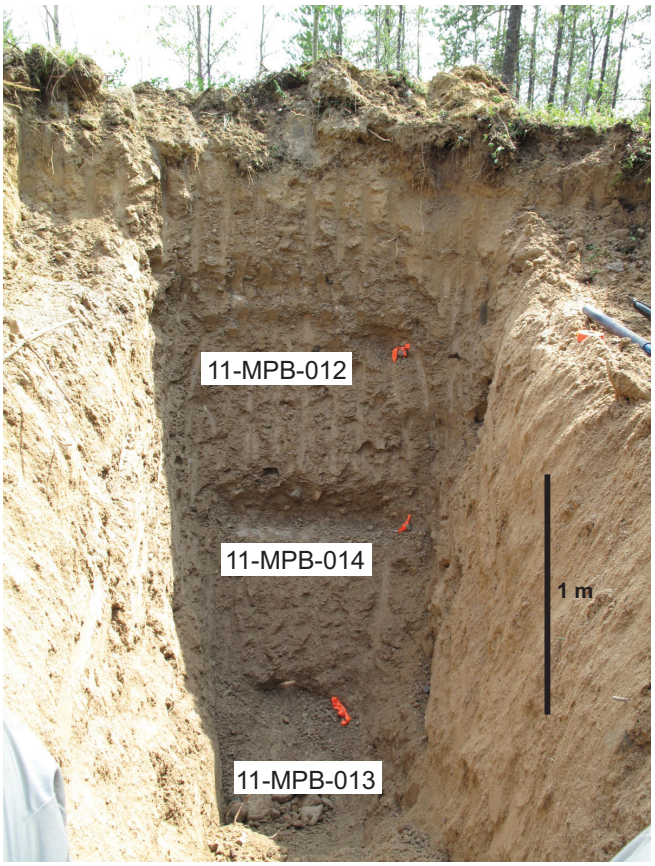

Figure 10. Till samples collected from trenches west and northwest the west wall of Pit O-28. See Figure 8 for location.

and 64 till samples (excluding field duplicates) were collected proximal to deposit O-28 (Fig. 8). Deposit O-28 was chosen for detailed till sampling because (1) mineralization subcropped and thus was directly eroded by glaciers; (2) no known subcropping Pb-Zn orebodies occur directly up-ice (east) of deposit O-28, thus till samples collected to the east should reflect background; (3) multiple striated outcrops on the pit shoulders provide detailed ice-flow information; (4) till is of moderate thickness (~6 m), compared to deposits farther west (>15 m), providing the opportunity to sample till from surface to bedrock in the third dimension; (5) till occurs at the surface, with only minor deposits from inundation of glacial Lake McConnell; and (6) the natural land surface is relatively undisturbed from past mining and exploration activities. Field data for all till samples collected for this study are listed in Appendix A3.

Till samples were collected up-ice, overlying, and down-ice of the ore zone at deposit O-28, relative to three prominent ice-flow trajectories preserved in striations on the pit shoulders (Fig. 8a). Up-ice till samples (10-MPB-023, -024, -025) were collected on the east side of the pit at the till/bedrock interface and were used to establish background concentrations. Eight till samples (10-MPB-004, -005, -026 to -028, -030, -031, 11-MPB-008) were collected overlying and just down-ice of the O-28 ore zone on the stripped bedrock surface exposed on the west side of the open pit (Fig. 8b).

In 2010, three vertical sections of till (labeled "A", "B", and "C" in Fig. 8a) were sampled in the upper west wall of pit O-28 to collect till samples ~50 m down-ice of mineralization. Three till samples were collected from each section at ~1, 3, and 5 m depths below the natural land surface (Fig. 9). Based on the preliminary indicator mineral results for these samples (10-MPB-032 to 034, -036 to 041), additional till samples were collected in 2011 in a pattern that widens westward (Fig. 8a, yellow triangle) from the ore zone (samples 11-MPB-002 to 007, -009 to 014, -017 to 033, -035 to 044, -046 to 054). These till samples were collected from ~3 m deep trenches (Fig. 10) to document vertical patterns in the till composition. An additional section of till was sampled in the upper west wall of the pit (see "D", Fig. 8a). This section was sampled in the same manner as sections A, B, and C. Till samples were also collected from open pits at deposits P-24 (samples 10-MPB-013, -014), N-32 (samples 10-MPB-020, -021), and P-41 (samples 10-MPB-009, -017, -018) (Fig. 1) to document variations in the till geochemistry

and indicator mineral size and morphology related to other deposits in the district.

Broadly spaced surface till samples (Fig. 1) were collected to document regional-scale signals of the Pb-Zn deposits. Sample 11-MPB-058 was collected from Paulette Creek, 15 km up-ice of the eastern most Pb-Zn deposit, to determine background concentrations of indicator minerals. Seven till samples were collected from surface till exposed at pits K-62 (samples 11-PTA-037, -042), S-65 (sample 11-MPB-062), K-77 (sample 11-MPB-061), and in sections along the Buffalo River (samples 11-MPB-059, -060, 085B101008BT) to establish regional down-ice indicator mineral concentrations in till.

Field duplicate till samples were collected from the same sample intervals at two different locations to assess field variability. Sample 11-MPB-034 (depth 1.0–1.5 m) is a duplicate of 11-MPB-033 (depth 2.0–2.5 m). Sample 11-MPB-016 is a duplicate of 11-MPB-009 (both at ~5 m depth).

Sample Processing and Indicator Mineral Picking

The bedrock samples submitted to ODM were subject to electric pulse disaggregation and processed to produce heavy mineral concentrates (HMC). Before disaggregation, ODM geologists described each bedrock sample and these descriptions are reported in McClenaghan et al. (2012a). Polished thin sections (PTS) for 52 bedrock samples were described and are reported in Appendix A2. Sample processing and indicator mineral picking procedures used by ODM, as well as the weights of all fractions produced and indicator mineral abundances for Pine Point bedrock samples are reported in McClenaghan et al. (2012a). Sphalerite, galena, and other mineral grains indicative of the Pine Point MVT deposits were counted in each bedrock sample. Indicator mineral data from bedrock samples were normalized to 1 kg weight because processing weights varied from 41.0 to 274.7 g. Normalized indicator mineral data from bedrock samples are listed in Appendix B1 and these values are described below.

Sixteen quartz blank bedrock samples were inserted into the batch at the beginning and after each bedrock sample to monitor cross contamination between samples during processing. These samples include the letters QBlk in their sample number. The results for these 16 samples are reported along with the bedrock samples in McClenaghan et al. (2012a).

Bulk till samples were also processed at ODM to recover the heavy mineral fraction. Sphalerite, galena, and other minerals indicative of the Pine Point MVT deposits as well as other routine indicator mineral suites (magmatic massive sulphide indicator minerals (MMSIMs®), kimberlite indicator minerals, gold grains) were counted in each till sample. Sample processing and indicator mineral picking procedures used by ODM, as well as the weights of all fractions produced, and indicator mineral abundances for Pine Point till samples are reported in McClenaghan et al. (2012a). Samples were processed in order from least to most metal-rich, rather than in numerical order, to limit cross contamination between metal-rich and metal-poor samples. Raw ODM data are reported in the order the samples were processed in McClenaghan et al. (2012a). Indicator mineral data from till samples were normalized to 10 kg because till sample weights collected and processed varied between 5.5 and 15 kg. Normalized indicator mineral data from till samples are listed in Appendix B2 and are discussed in the results section of this paper.

Four 'blank' sand samples were inserted into each of the 2010 and 2011 till batches prior to processing to monitor the quality of processing and picking at the lab: samples 10-MPB-002, -022, -029, and 085B-2010-1001BT in the 2010 batch and 11-MPB-001, -015, -044, -063 in the 2011 batch. The blank samples are weathered Silurian-Devonian granite (grus) of the South Nepisiguit River Plutonic Suite (Wilson, 2007) collected in the Miramichi Highlands approximately 66 km west of Bathurst, New Brunswick (McClenaghan et al., 2012b). The material is unconsolidated and has the appearance of moderately sorted, monolithologic sand. It does not contain any precious or base metal indicator minerals (Plouffe et al., in press). Results for these eight blank samples are reported along with those for the till samples (Appendix B2).

Electron Microprobe Analysis

Selected sulphide minerals in PTS were analyzed at the University of Alberta using the CAMECA SX100 and the JEOL 8900 electron probe microanalyzers. Selected indicator mineral grains from till samples were mounted in 25 mm epoxy grain mounts prior to electron microprobe analysis (EMP). Maps for both grain mounts from the till sample collected immediately adjacent to the ore zone at Pit O-28 (sample 10-MPB-004), are included in Appendix C1. Elements determined include Mn, S, Zn, Fe, Pb, Ag, As, Sb, Se, Hg, Ge, and Cu. Operating conditions are listed in Appendix C2. The detection limits are reported as three standard deviations from the total background counts. Values that were below detection limit were removed before calculations and plotting. Raw EMP data for bedrock analysis and till grains from sample 10-MPB-004 are listed in Appendix C3.

QUALITY CONTROL

Bedrock Blank Samples

Table 2 is a summary of the non-normalized grain

Table 2. Summary of sphalerite, galena, and pyrite abundance in the 0.25–0.5 mm heavy mineral and pan concentrate fractions of bedrock samples and in quartz blanks that were processed prior to and after each bedrock sample at Overburden Drilling Management Limited.

Sample Number	Sphalerite 0.25-0.5 mm	Galena 0.25-0.5 mm	Pyrite 0.25-0.5 mm	Additional Grains 0.25-0.5 mm	Pan Concentrate Grains
10-MPB-QBlk5	0	0	0	0	1 pyrite grain
10-MPB-R25	10,000	15	0	0	~200 grains marcasite, ~2000 grains galena, ~5000 grains sphalerite
10-MPB-QBlkR25	0	0	0	0	1 grain pyrite, 1 grain galena
10_MPB-R32	20000	150	2	0	~25000 grains galena, 1% sphalerite
10-MPB-QBlkR32	0	0	0	0	5 grains pyrite, ~15 grains galena
10-MPB-R37	0	0	35000	0	90% pyrite
10-MPB-QBlkR37	0	0	0	1 hornblende grain and 2 metal turnings	~500 grains pyrite, 9 grains galena
10-MPB-R38	0	0	30000	0	60% pyrite, 10% marcasite, ~25 grains galena
10-MPB-QBlkR38	0	0	0	0	~200 grains pyrite
10-MPB-R43	60000	1200	1	0	2% galena, 60% sphalerite
10-MPB-QBlkR43	0	0	0	0	~100 grains pyrite, ~30 grains galena, ~40 grains sphalerite
10-MPB-R21	70000	8000	0	0	20% galena, 70% sphalerite
10-MPB-QBlkR21	0	0	0	0	~20 grains pyrite, ~150 grains galena, ~40 grains sphalerite
10-MPB-R30	120000	400	0	0	~100 grains pyrite, 2% galena, 80% sphalerite
10-MPB-QBlkR30	2	0	0	1 hornblende grain	~50 grains pyrite, ~500 grains galena, ~500 grains sphalerite
10-MPB-R17	20000	1500	30000	0	70% pyrite, 2% galena, 10% sphalerite
10-MPB-QBlkR17	0	0	0	2 metal turnings	~200 grains pyrite, ~50 grains galena, ~30 grains sphalerite
10-MPB-R59	70000	12000	0	0	~200 grains pyrite, 80% galena, 5% sphalerite
10-MPB-QBlkR59	0	0	0	0	~30 grains pyrite, ~700 grains galena, ~200 grains sphalerite
10-MPB-R12	7000	5000	0	0	70% marcasite, 5% galena, 10% sphalerite
10-MPB-QBlkR12	0	0	0	0	~200 grains marcasite, ~500 grains galena, ~50 grains sphalerite
10-MPB-R15	55000	60000	6000	0	40% marcasite, 10% galena, 20% sphalerite
10-MPB-QBlkR15	0	0	0	2 metal turnings	~100 grains pyrite, ~350 grains galena, ~40 grains sphalerite
10-MPB-R15	55000	60000	6000	0	40% marcasite, 10% galena, 20% sphalerite
10-MPB-QBlkR15	0	0	0	2 metal turnings	~100 grains pyrite, ~350 grains galena, ~40 grains sphalerite
10-MPB-R05	35000	100000	35000	0	50% pyrite, 10% galena, 25% sphalerite
10-MPB-QBlkR05	0	0	0	0	~150 grains pyrite, ~500 grains galena, ~30 grains sphalerite
10-MPB-R58	200000	200000	0	0	20% galena, 70% sphalerite
10-MPB-QBlkR58	1	1	0	2 metal turnings	~30 grains pyrite, ~250 grains galena, ~150 grains sphalerite
10-MPB-R34	150000	180000	0	0	30% galena, 40% sphalerite
10-MPB-QBlkR34	0	0	0	0	~15 grains pyrite, ~1000 grains galena, ~40 grains sphalerite
10-MPB-R57	100000	300000	0	0	80% galena, 20% sphalerite
10-MPB-QBlkR57	0	2	0	1 metal turning	2 grains pyrite, ~2500 grains galena, ~100 grains sphalerite

counts for the quartz blanks and disaggregated bedrock samples. Sulphide grain contamination was detected in the 0.25 to 0.5 mm fraction of three blank samples:

1) *Sample 10-MPB-R30blk* contains 2 sphalerite grains and was processed after bedrock sample 10-MPB-R30, which contains approximately 80% massive colloform sphalerite.
2) *Sample 10-MPB-R58blk* contains 1 grain of sphalerite and 1 grain of galena in the 0.25 to 0.5 mm fraction. Bedrock sample 10-MPB-R58 was processed before this blank and it contains the highest abundance of sphalerite and galena grains of all bedrock samples processed. The pan fraction for sample 10-MPB-R58blk contains approximately 150 grains of sphalerite, 250 grains of galena, and 30 grains of pyrite.
3) *Sample 10-MPB-R57blk* contains 2 grains of galena and was processed after bedrock sample 10-MPB-R57, which contains approximately 80% galena. The pan concentrate for sample 10-MPB-R57blk contains approximately 100 grains of sphalerite, 2500 grains of galena, and 2 grains of pyrite.

In contrast to the 0.25–0.5 mm fraction, significant contamination (100s of grains) was detected in the pan concentrate fraction of every blank sample that was processed. The first blank sample at the beginning of the batch contained 1 pyrite grain. Processing a quartz blank after each bedrock sample allows carryover from the previous sulphide-bearing sample to be "caught" by the blank, thus limiting carry-over contamination to the next bedrock sample. This significant level of contamination between samples, as indicated by the pan concentrate results, indicates that in future the electric pulse disaggregation equipment at ODM should be totally dismantled and thoroughly cleaned after disaggregation of any sulphide-rich sample.

Till Field Duplicates

Table 3 shows a comparison of the number of indicator minerals (normalized to 10 kg) recovered from dupli-

Table 3. Comparison of indicator mineral counts recovered from the pan concentrate, 0.25–0.5 mm, 0.5–1.0 mm, and 1.0–2.0 mm fractions of Bathurst blanks and the till samples processed immediately before each blank, as well as the original field versus duplicate till samples. Counts have been normalized to 10 kg sample weight.

Sample Number	Sample Status	0.25-0.50 mm						0.5-1.0 mm		1.0-2.0 mm		Pan Concentrate	
		Sphalerite grains/ 10 kg	Pyrite grains/ 10 kg	Galena grains/ 10 kg	Smithsonite grains/10 kg	Barite grains/ 10 kg	Cerussite grains/ 10 kg	Sphalerite grains/ 10 kg	Galena grains/ 10 kg	Sphalerite grains/ 10 kg	Galena grains/ 10 kg	Sphalerite grains/ 10 kg	Galena grains/ 10 kg
Field duplicates													
11-MPB-009		2308	615	62	0	0	0	46	15	1	0	0	76923
11-MPB-016	Field Duplicate of 11-MPB-009	2	2	1	0	0	0	0	0	0	0	0	23
11-MPB-033		3	41	0	0	0	0	2	0	0	0	0	41
11-MPB-034	Field duplicate of 11-MPB-033	0	1	4	0	0	0	0	3	0	0	0	159
Bathurst blanks													
start of batch													
085B-2010-1001BT	Bathurst blank #6	0	0	0	0	0	0	0	0	0	0	0	2
10-MPB-034	till sample	0	29	0	0	0	0	0	0	0	0	0	1
10-MPB-002	Bathurst blank #110	0	0	0	0	0	0	0	0	0	0	0	0
10-MPB-020	till sample	15789	8421	4211	5	0	0	263	158	3	26	105	20%
10-MPB-022	Bathurst blank #110	3	0	2	0	0	0	2	0	0	1	0	101
10-MPB-013	till sample	980392	57692	192308	57692	0	0	19231	24038	962	7692	0	95%
10-MPB-029	Bathurst blank #19	19	1	13	0	0	0	13	8	1	6	0	206
11-MPB-006	till sample	63	2	15	0	0	0	13	2	0	1	0	394
11-MPB-001	Bathurst blank #43	0	0	0	0	0	0	0	0	0	0	0	0
11-MPB-053	till sample	2	9	31	0	0	0	0	5	1	0	0	385
11-MPB-015	Bathurst blank #15	0	0	0	0	0	0	0	0	0	0	0	0
11-MPB-020	till sample	0	4	0	0	0	0	0	0	0	0	0	4
11-MPB-044	Bathurst blank #56	0	0	0	0	0	0	0	0	0	0	0	0
start of batch													
11-MPB-063	Bathurst blank #63	0	0	0	0	0	0	0	0	0	0	0	0

cate field samples. There are significant differences between the original sample and its duplicate, particularly for the content of galena in pan concentrates:

1) *Sample 11-MPB-009* contains 76,923 grains of galena in the pan concentrate while its field duplicate, sample 11-MPB-016, contains 23 grains. The grain counts for sample 11-MPB-034 and its duplicate, 11-MPB-033, are consistent in sphalerite, pyrite, and smithsonite.
2) *Sample 11-MPB-034* contains 159 galena grains in the pan concentrate and its duplicate, sample 11-MPB-033, contains 41 grains. Sample 11-MPB-009 contains 2308 grains of sphalerite and 615 grains of pyrite in the 0.25–0.5 mm fraction of till, while its duplicate, sample 11-MPB-016, contains 2 grains of sphalerite and pyrite in the same fraction.

These results indicate there are significant differences between duplicates proximal to the Pb-Zn mineralization. These differences may reflect inhomogeneity of the metal-rich till and the fact that samples were not collected from exactly the sample depth in the trench. It may be impossible to provide an accurate means for assessing lab precision for heavy mineral counts. In future, it is recommended that field duplicates be collected as a large sample from exactly the same hole or location in a section, at the same depth, and then homogenized and split in the field.

Till Blank Samples

Table 3 lists the indicator mineral count data for Bathurst blank samples inserted into the 2010 and 2011 batches and the till samples that were processed immediately before each blank. Two blank samples, 10-MPB-022 and 10-MPB-029, contain significant contamination (highlighted in yellow in Table 3). Note that the till samples processed prior to each of these two blank samples were extremely metal-rich, containing 10,000s to 100,000s of galena and sphalerite grains. The metal content of these two metal-rich till samples is unusually high. However, they serve to illustrate there is a carry-over problem at the processing lab and that it can be detected using blank samples within a till batch. This evidence of contamination was communicated to the processing lab, and modifications for cleaning of the processing equipment were made that will help to reduce this level of contamination in the future batches. These data demonstrate the values of inserting blank samples and monitoring for possible sample contamination.

RESULTS

The results and discussion focus on indicator minerals in the 0.25–0.5 mm non-ferromagnetic fraction of till and bedrock, unless otherwise noted.

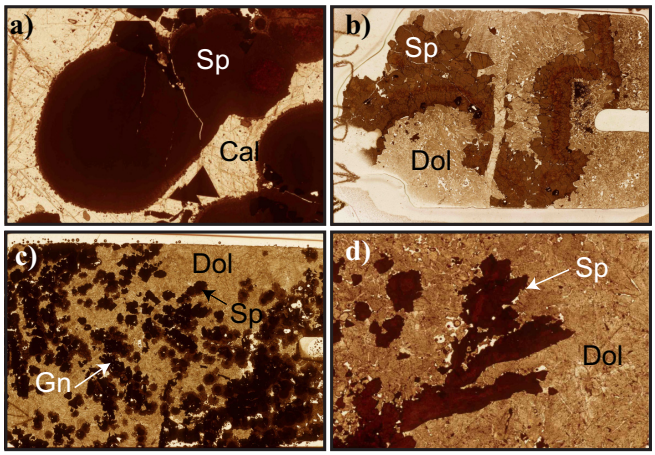

Figure 11. Photomicrographs showing the varying types and textures of sphalerite grains observed in samples: **a)** honey-brown sphalerite in sample 10-MPB-R02, **b)** banded honey-brown sphalerite in sample 10-MPB-R41, **c)** snow-on-roof honey-brown sphalerite in sample 10-MPB-R67, and **d)** dendritic, blackjack to reddish brown sphalerite in sample 10-MPB-R75. Plane polarized light. Cal = calcite, Dol = dolomite, Gn = galena, Sp = sphalerite. Field of view for each thin section is 4 mm.

Sphalerite

Bedrock

Sphalerite in PTS occurs as (1) honey-brown, (2) blackjack (Fe-rich), (3) colloform, and (4) cleiophane varieties. Different textures observed are (1) snow-on-roof, (2) banded sphalerite, (3) dendritic, and (4) acicular (Fig. 11). All sphalerite varieties occur as brecciated fragments in some samples. Honey-brown and blackjack varieties occur as isolated crystals or as aggregates. Colloform sphalerite is present in most bedrock samples. The bands of colloform sphalerite range from 50 to 1500 µm in thickness, while the individual botryoids range in size from 100 µm to >3 cm. The size range of sphalerite crystals in PTS was 100 to 1500 µm, though some crystals up to 0.5 cm were observed in hand sample. Very fine, powdery yellow sphalerite (cleiophane) occurs in some bedrock samples and usually has skeletal galena radiating outwards from the middle of the grain.

In bedrock heavy mineral concentrates (HMC), sphalerite grains were primarily recovered from the 0.25 to 0.5 mm fraction. The largest concentration of grains was recovered from sample 10-MPB-R21, a bedrock sample that contains approximately 60% sphalerite and 20% galena in hand sample. Grains were also recovered from the pan concentrate fraction of every bedrock sample. The size range of sphalerite grains in bedrock HMC ranges from 25 µm to 2 mm.

Each of the four varieties of sphalerite was analyzed by EMP on 80 to 85 grains randomly selected from PTS. Care was taken to obtain data points from each grain variety as well as each different texture

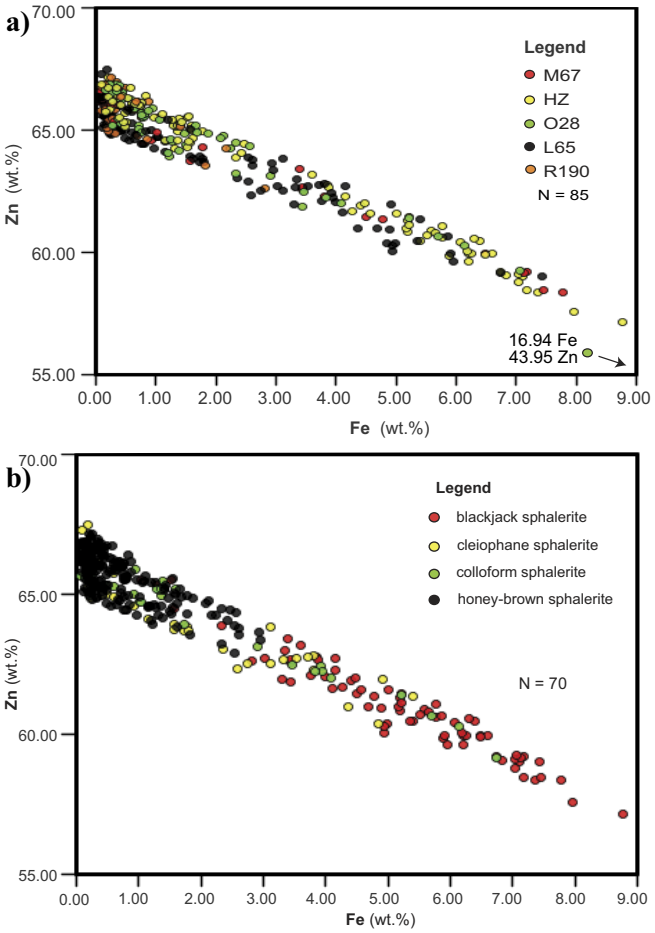

Figure 12. Relationship of Zn and Fe content in sphalerite from **(a)** the five deposits considered in this study and **(b)** different varieties of sphalerite from all five deposits.

(Appendix C3). The concentration of Zn in sphalerite in bedrock samples in this study ranges from 43.95 to 67.48 wt.%. Iron concentrations in sphalerite grains range from 0.02 to 16.94 wt.%, and that of S ranges from 32.03 to 39.19 wt.%. Minor elements Cd and Pb have concentrations ranging from 0.18 to 0.51 wt.% and <DL (detection limit) to 0.87 wt.%, respectively. Trace elements In, Cu, Sb, and Ge have concentrations that range from 0.01–0.03, 0.55, 0.07, and 0.09 wt.%, respectively. Zinc concentrations are highest in grains from deposits R190 and O-28 (Fig. 12a). Cleiophane sphalerite has the highest concentration of Zn. Sphalerite with the highest concentrations of Zn (i.e. cleiophane sphalerite) have the lowest concentrations of Fe (0.094–5.4 wt.%) and blackjack sphalerite has the highest concentrations of Fe (1.03–16.94 wt.%) (Fig. 12b). Sphalerite in bedrock samples from the M-67 deposit has the most diverse trace element geochemistry. In comparison to other orebodies sampled in this study, this deposit contains sphalerite with below detection limit concentrations of Ge, Ag, In, Sb, Pb, Cu, and Hg. Sphalerite from deposit HZ has higher concentrations of Sb (0.016–0.036 wt.%), Cu (0.011–

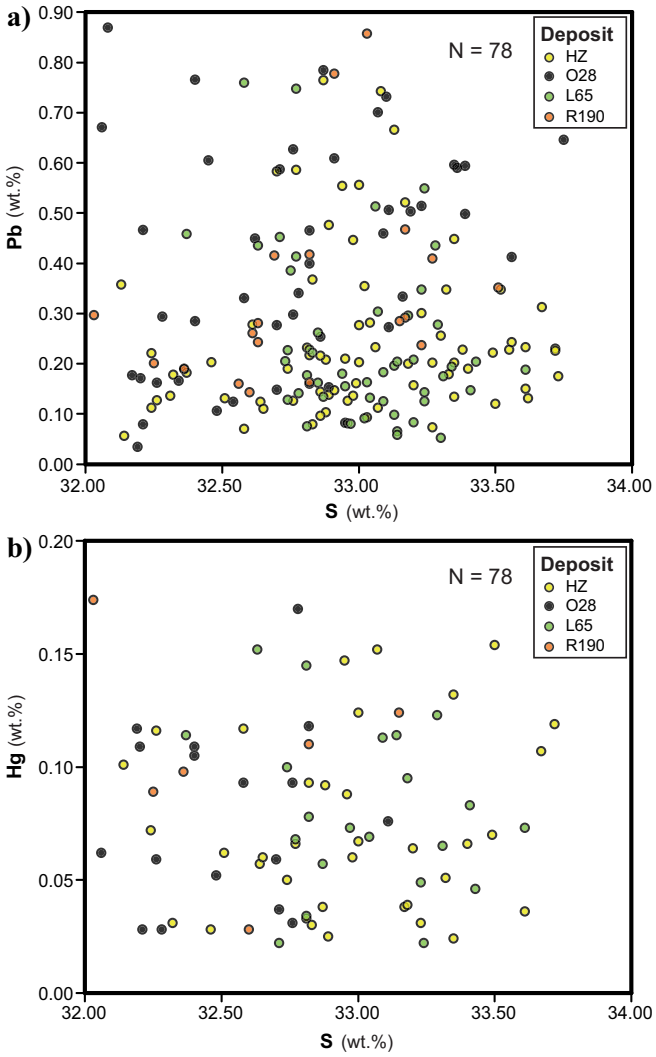

Figure 13. Concentrations of **(a)** Pb versus S and **(b)** Hg versus S determined by EMP analysis utilizing sphalerite grains from bedrock samples from four deposits.

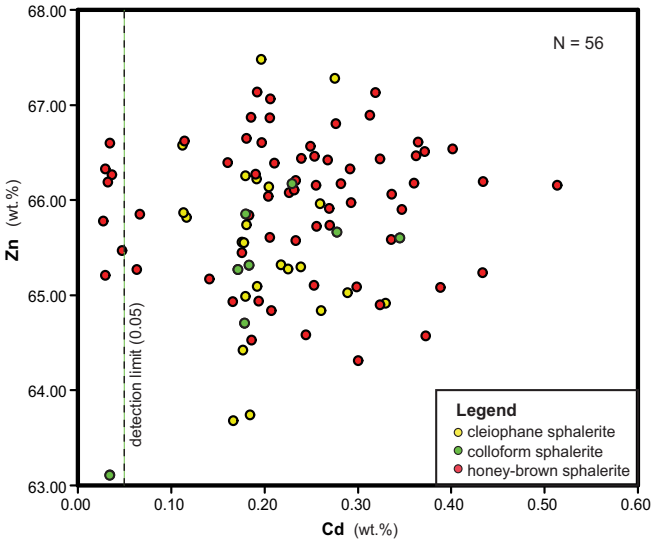

Figure 14. Concentrations of Zn and Cd determined by electron microprobe analysis in several varieties of sphalerite grains from bedrock samples. Blackjack sphalerite is absent from these graphs because Cd contents are not within 3 standard deviations of the detection limit of 0.18 wt.%.

0.035 wt.%), and Hg (0.024–0.154 wt.%), compared to the other deposits studied (Fig. 13). Honey-brown (0.03–0.51 wt.%), colloform (0.03–0.35 wt.%), and cleiophane (0.11–0.33 wt.%) varieties of sphalerite have the highest concentrations of Cd while blackjack sphalerite has below detection limit concentrations of Cd (Fig. 14). Lead concentrations vary among all the varieties of sphalerite, but are often higher in cleiophane (0.25–0.79 wt.%) and colloform sphalerite (0.13–0.77 wt.%).

Till

The majority of sphalerite grains recovered from till range in size from 0.25 to 1.0 mm, although grains up to 2.0 mm in size were recovered from till samples. The pan concentrate does contain some sphalerite grains, but these are limited to till samples collected proximal to the deposit (Table 4). Till samples collected on the bedrock bench (not including samples 10-MPB-004 and 10-MPB-005, which overlie the deposit) contain 38 to 114 grains in the 0.25 to 0.5 mm fraction. Figure 15 shows the distribution of sphalerite grains in till around deposit O-28. Background concentration in till is 0 to 1 grain. Sphalerite grains recovered from till in this study vary in colour from honey brown (Fe-poor) to black (Fe-rich) (Fig. 16).

Background values are determined by taking the average of till samples 10-MPB-023, -024, -025, and 11-MPB-058, which are all located up-ice (east) of the O-28 deposit. Till sample 10-MPB-004, which overlies the deposit, contains 35,398 grains, and till samples 10-MPB-005 (80 m down–ice) and 1-MPN-028 (120 m down-ice) contain 4839 and 3226 grains, respectively. The latter two till samples were collected near the bedrock surface, down-ice (to the southwest) of the ore zone, in the direction of the first ice-flow trajectory.

Till samples from the Buffalo River (samples 11-MPB-059, -060, and 085B-2010-1008) contain between 0 and 6 grains of sphalerite. Till samples from deposit P-24 contain 28,8462 to 98,0392 sphalerite grains and samples from deposit N-32 contain between 15,789 and 42,105 sphalerite grains. Regional till sample 11-MPB-061, collected at deposit K-77, contains 459 grains and sample 11-MPB-062, collected at deposit S-65, contains no sphalerite grains.

EMP of sphalerite grains from till samples indicate that these grains have similar concentrations to those recovered from bedrock samples (Appendix C3). Zinc concentration ranges from 64.06 to 67.27 wt.%, while S concentration ranges from 32.24 to 34.13 wt.%. The concentrations for Mn, Fe, Ge, and Se from grains recovered from till samples are similar to sphalerite

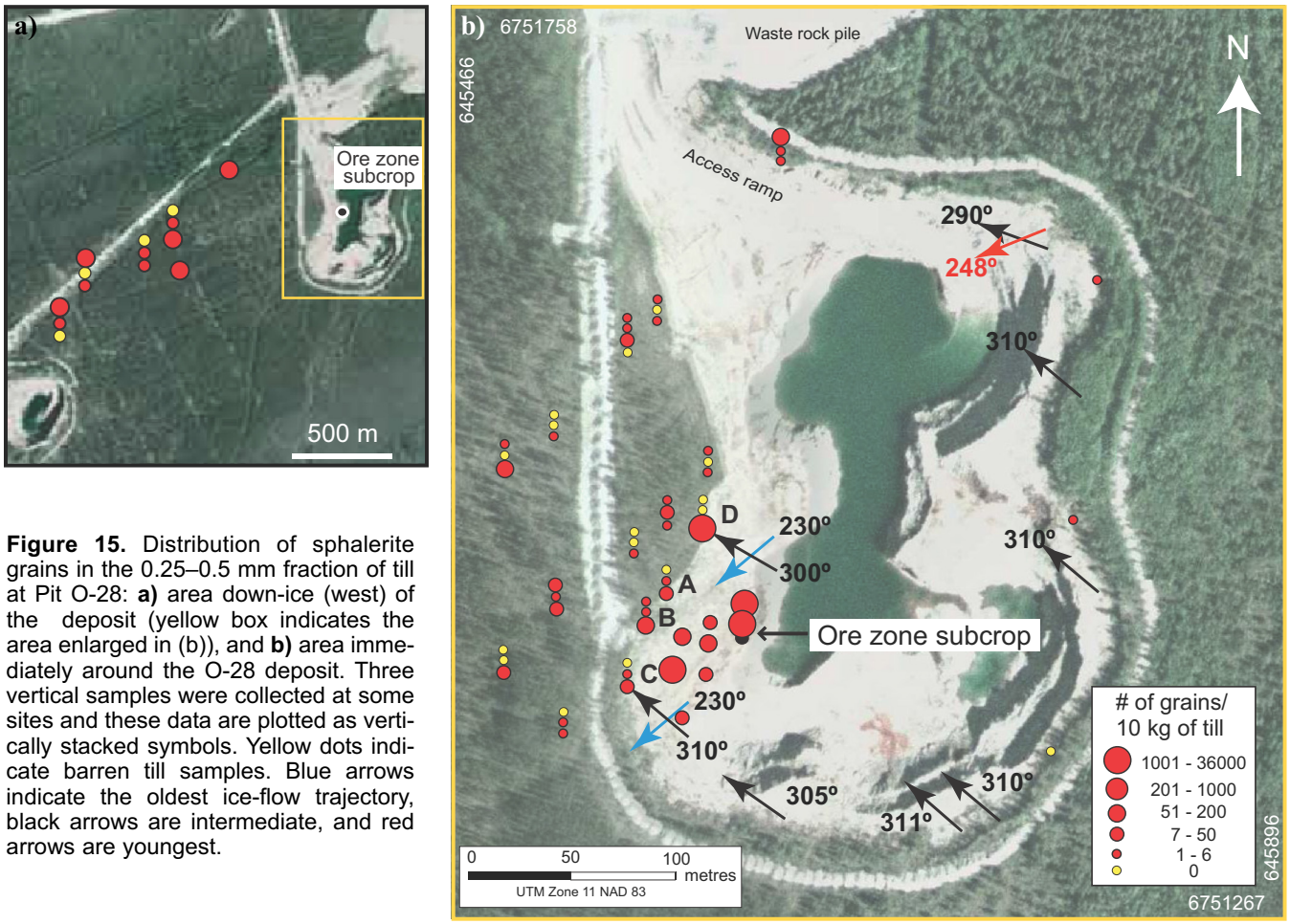

Figure 15. Distribution of sphalerite grains in the 0.25–0.5 mm fraction of till at Pit O-28: **a)** area down-ice (west) of the deposit (yellow box indicates the area enlarged in (b)), and **b)** area immediately around the O-28 deposit. Three vertical samples were collected at some sites and these data are plotted as vertically stacked symbols. Yellow dots indicate barren till samples. Blue arrows indicate the oldest ice-flow trajectory, black arrows are intermediate, and red arrows are youngest.

Figure 16. Photograph of sphalerite grains from the 1–2 mm heavy mineral fraction of till sample 10-MPB-004.

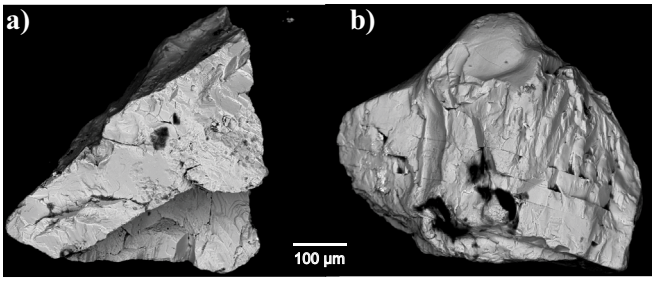

Figure 17. Secondary electron images showing the morphology of sphalerite grains in till samples: **a)** an angular grain from sample 10-MPB-004 and **b)** a subangular grain from sample 11-MPB-029.

grains recovered from bedrock. Sphalerite grains recovered from till samples have lower concentrations of As, Ag, Cd, In, Sb, Pb, Cu, and Hg on average in comparison to sphalerite grains recovered from bedrock samples. Secondary electron images of the 0.25–0.5 mm sphalerite grains reveal that the grain morphology for sphalerite in till ranges from subrounded to angular (Fig. 17). Table 5 compares indicator mineral grain counts recovered from till with sample distance from the orebody at O-28. Most grains recovered from till samples proximal to the deposit are angular to subangular, while some grains from samples 250 m down-ice in the southwest direction are subrounded to rounded.

Galena

Bedrock

Cubic and skeletal galena are the two main varieties that are observed in PTS. Different textures of galena identified in PTS are dendritic, fracture filling (late galena), and massive aggregates forming bands (Fig.

Table 4. Listing of indicator minerals recovered from the pan concentrate, and 0.25–0.5 mm, 0.5–1.0 mm, and 1.0–2.0 mm size fractions of till samples. Counts have been normalized to 10 kg sample weight.

	Sphalerite				Galena				Pyrite				Smithsonite			
Sample	No. grains pan	No. grains 0.25-0.5 mm	No. grains 0.5-1.0 mm	No. grains 1.0-2.0 mm	No. grains pan	No. grains 0.25-0.5 mm	No. grains 0.5-1.0 mm	No. grains 1.0-2.0 mm	No. grains pan	No. grains 0.25-0.5 mm	No. grains 0.5-1.0 mm	No. grains 1.0-2.0 mm	No. grains pan	No. grains 0.25-0.5 mm	No. grains 0.5-1.0 mm	No. grains 1.0-2.0 mm
085B-2010-1001BT	0	0	0	0	1	0	0	0	2	0	0	0	0	0	0	0
085B-2010-1008BT	0	0	0	0	0	0	0	0	465	6	0	0	0	0	0	0
10-MPB-002	0	0	0	0	0	0	0	0	0	0	0	0	0	0	0	0
10-MPB-004	88	35398	265	16	60%	53097	8850	708	0	26549	0	0	0	133	0	0
10-MPB-005	81	4839	121	3	30%	2419	121	12	0	3226	0	0	0	65	0	0
10-MPB-009	0	889	59	21	5%	37	10	4	0	2222	0	0	0	0	0	0
10-MPB-013	0	980392	39216	1961	95%	196078	49020	15686	392	5882	0	0	0	58824	0	0
10-MPB-014	0	288462	19231	58	10%	192308	4808	769	0	57692	0	0	0	57692	0	0
10-MPB-018	0	0	0	0	75	0	0	0	980	2	0	0	0	0	0	0
10-MPB-020	105	15789	263	3	20%	4211	158	26	0	8421	0	0	0	5	0	0
10-MPB-021	105	42105	105	14	20%	3158	632	27	40%	15789	0	0	0	21	0	0
10-MPB-022	0	3	2	0	100	2	0	1	0	0	0	0	0	0	0	0
10-MPB-023	0	0	0	0	6	0	0	0	164	0	0	0	0	0	0	0
10-MPB-024	0	4	0	0	0	0	0	0	25	4	0	0	0	0	0	0
10-MPB-025	0	0	0	0	2	0	0	0	48	0	0	0	0	0	0	0
10-MPB-026	40	159	198	7	40%	397	952	0	20%	952	0	0	0	6	0	0
10-MPB-027	0	38	5	0	75	11	1	0	189	152	0	0	0	0	0	0
10-MPB-028	40	3226	32	0	50%	8065	242	23	0	1613	0	0	0	40	0	0
10-MPB-029	0	19	13	1	200	13	8	6	0	1	0	0	0	0	0	0
10-MPB-030	0	114	5	1	5%	45	38	11	0	7576	0	0	0	0	0	0
10-MPB-031	0	38	0	0	500	30	30	12	152	1136	0	0	0	0	0	0
10-MPB-032	0	40	2	0	2000	28	5	0	77	462	0	0	0	0	0	0
10-MPB-033	0	3	0	0	50	3	1	0	2	19	0	0	0	0	0	0
10-MPB-034	0	0	0	0	1	0	0	0	10	29	0	0	0	0	0	0
10-MPB-036	0	47	4	0	1000	16	1	0	76	379	0	0	0	0	0	0
10-MPB-037	0	3	0	0	10000	75	8	0	0	113	0	0	0	0	0	0
10-MPB-038	0	0	0	0	3	0	0	0	10	192	0	0	0	0	0	0
10-MPB-039	0	63	3	0	1000	236	43	2	39	1181	0	0	0	0	0	0
10-MPB-040	0	2	0	0	0	0	0	0	0	9	0	0	0	0	0	0
10-MPB-041	0	4	0	0	5	3	0	0	96	58	0	0	0	0	0	0
11-MPB-001	0	0	0	0	0	0	0	0	0		0	0	0	0	0	0
11-MPB-002	0	0	0	0	0	0	0	0	223	18	0	0	0	0	0	0
11-MPB-003	0	0	0	0	9	0	0	0	89	1	0	0	0	0	0	0
11-MPB-004	0	5	0	0	0	0	0	0	1	9	0	0	0	0	0	0
11-MPB-005	0	9	0	0	304	23	8	2	174	130	0	0	0	0	0	0
11-MPB-006	0	63	13	0	394	15	2	1	31	2	0	0	0	0	0	0
11-MPB-007	0	7	0	0	1695	102	8	1	169	4	0	0	0	0	0	0
11-MPB-008	0	42	1	0	840	15	3	1	42	1681	0	0	0	0	0	0
11-MPB-009	0	2308	46	1	76923	62	15	0	385	615	0	0	0	0	0	0
11-MPB-010	0	0	0	0	1	0	0	0	132	3	0	0	0	0	0	0
11-MPB-011	0	0	0	0	2	0	0	0	83	21	0	0	0	0	0	0
11-MPB-012	0	6	0	0	9	0	0	0	172	172	0	0	0	0	0	0
11-MPB-013	0	2	0	0	3968	63	5	2	40	8	0	0	0	0	0	0
11-MPB-014	0	0	0	0	16	0	0	0	4	3	0	0	0	0	0	0
11-MPB-015	0	0	0	0	0	0	0	0	0	0	0	0	0	0	0	0
11-MPB-016	0	2	0	0	23	1	0	0	153	2	0	0	0	0	0	0
11-MPB-017	0	3	1	0	80	0	0	0	0	6	0	0	0	0	0	0

Table 4 continued.

Sample	Sphalerite				Galena				Pyrite				Smithsonite			
	No. grains pan	No. grains 0.25-0.5 mm	No. grains 0.5-1.0 mm	No. grains 1.0-2.0 mm	No. grains pan	No. grains 0.25-0.5 mm	No. grains 0.5-1.0 mm	No. grains 1.0-2.0 mm	No. grains pan	No. grains 0.25-0.5 mm	No. grains 0.5-1.0 mm	No. grains 1.0-2.0 mm	No. grains pan	No. grains 0.25-0.5 mm	No. grains 0.5-1.0 mm	No. grains 1.0-2.0 mm
11-MPB-018	0	2	0	1	403	13	4	0	16	8	0	0	0	0	0	0
11-MPB-019	0	13	4	0	74	7	5	0	7	7	0	0	0	0	0	0
11-MPB-020	0	0	0	0	4	0	0	0	16	4	0	0	0	0	0	0
11-MPB-021	0	1	0	0	0	0	1	0	16	8	0	0	0	0	0	0
11-MPB-022	0	0	0	0	407	26	6	0	16	8	0	0	0	0	0	0
11-MPB-023	0	3	0	0	1695	68	11	5	169	254	0	0	0	0	0	0
11-MPB-024	0	0	0	0	11	0	0	0	15	15	0	0	0	0	0	0
11-MPB-025	0	1	0	0	0	0	0	0	156	2	0	0	0	0	0	0
11-MPB-026	0	5	1	0	0	0	0	0	77	4	0	0	0	0	0	0
11-MPB-027	0	0	0	0	0	0	0	0	23	8	0	0	0	0	0	0
11-MPB-028	0	0	0	0	75	8	1	1	376	5	0	0	0	0	0	0
11-MPB-029	0	7	0	0	153	6	2	0	76	5	0	0	0	0	0	0
11-MPB-030	0	31	5	0	233	31	2	0	78	12	0	0	0	0	0	0
11-MPB-031	0	2	0	0	0	1	0	0	152	2	0	0	0	0	0	0
11-MPB-032	0	22	1	0	3704	13	7	1	148	22	0	0	0	0	0	0
11-MPB-033	0	3	2	0	41	0	0	0	25	41	0	0	0	0	0	0
11-MPB-034	0	0	0	0	159	4	3	0	16	1	0	0	0	0	0	0
11-MPB-035	0	0	0	0	0	0	0	0	4	4	0	0	0	0	0	0
11-MPB-036	0	81	10	0	2823	242	40	11	0	8	0	0	0	0	0	0
11-MPB-037	0	0	0	0	0	2	0	0	122	6	0	0	0	0	0	0
11-MPB-038	0	0	0	0	16	6	2	1	16	8	0	0	0	0	0	0
11-MPB-039	0	2	0	0	8	0	0	0	0	8	0	0	0	0	0	0
11-MPB-040	0	36	5	0	39	1	1	2	78	3	0	0	0	0	0	0
11-MPB-041	0	3	0	0	388	23	4	2	39	2	0	0	0	0	0	0
11-MPB-042	0	0	0	0	0	2	0	0	21	5	0	0	0	0	0	0
11-MPB-043	0	31	1	0	0	0	0	0	16	2	0	0	0	0	0	0
11-MPB-044	0	0	0	0	0	0	0	0	0	0	0	0	0	0	0	0
11-MPB-045	0	7	2	1	787	31	9	2	24	8	0	0	0	0	0	0
11-MPB-046	0	0	0	0	0	2	5	0	0	0	0	0	0	0	0	0
11-MPB-047	0	2	0	0	2	0	0	0	8	4	0	0	0	0	0	0
11-MPB-048	0	9	1	0	12	0	0	0	62	15	0	0	0	0	0	0
11-MPB-049	0	0	0	0	0	1	0	0	39	1	0	0	0	0	0	0
11-MPB-050	0	1	0	0	1563	78	23	6	16	1	0	0	0	0	0	0
11-MPB-051	0	2	0	0	4	1	1	0	16	0	0	0	0	0	0	0
11-MPB-052	0	0	0	0	7692	8	2	0	38	4	0	0	0	0	0	0
11-MPB-053	0	2	0	1	385	31	5	0	115	9	0	0	0	0	0	0
11-MPB-054	0	20	3	0	8	5	0	0	197	31	0	0	0	0	0	0
11-MPB-055	0	152	38	8	379	76	9	2	0	2273	0	0	0	0	0	0
11-MPB-056	0	15	0	0	40	0	0	0	81	48	0	0	0	0	0	0
11-MPB-057	0	6	0	0	379	17	0	0	152	61	0	0	0	0	0	0
11-MPB-058	0	0	0	0	3	0	0	0	38	8	0	0	0	0	0	0
11-MPB-059	0	0	0	0	0	1	1	1	20	5	0	0	0	0	0	0
11-MPB-060	0	6	0	0	2	6	1	0	125	33	0	0	0	0	0	0
11-MPB-061	0	459	46	5	18349	28	7	0	4587	2752	0	0	0	0	0	0
11-MPB-062	0	0	0	0	0	0	0	0	15	31	0	0	0	0	0	0
11-MPB-063	0	0	0	0	0	0	0	0	0	0	0	0	0	0	0	0
11-PTA-037	0	4	0	0	84	6	0	0	168	8	0	0	0	0	0	0
11-PTA-042	0	0	0	0	5	0	0	0	13	18	0	0	0	0	0	0

Table 5. Listing of the indicator minerals in the 0.25–0.5 mm fraction, geochemistry of till samples, and relative distances from the O-28 ore zone subcrop that is located on the west side of the open pit (see Fig. 8) normalized to 10 kg sample weight

Sample	Surface till sample ?	Distance from ore zone (m)	Sample depth top (m)	Sample depth bottom (m)	Relative to ore zone	No. sphalerite grains/10 kg	No. galena grains/10 kg	No. smithsonite grains/10 kg	No. pyrite grains/10 kg	Pb (ppm)	Zn (ppm)	Cd (ppm)	Fe (%)	Tl (ppm)	S (%)	Se (ppm)
11-MPB-058		-15000	1.3	1.6	up-ice	0	0	0	8	10.55	36.5	0.07	1.71	0.046	0.01	0.1
11-MPB-055	yes	-280	7.8	8.0	up-ice	152	76	0	2273	33.22	88.3	0.16	0.93	0.027	0.10	0.2
11-MPB-056		-280	3.5	3.7	up-ice	15	0	0	48	25.86	88.9	0.24	0.73	0.019	0.01	0.1
11-MPB-057		-280	1.0	1.3	up-ice	6	17	0	61	23.45	66.0	0.17	0.88	0.025	0.01	0.1
10-MPB-023		-250	4.0	5.0	up-ice	2	0	0	205	37.40	109.1	0.28	0.77	0.020	0.01	0.2
10-MPB-024		-200	4.0	4.5	up-ice	4	0	0	4	35.30	97.6	0.26	0.80	0.024	0.01	0.1
10-MPB-025		-200	2.5	3.0	up-ice	0	0	0	0	29.97	84.5	0.21	0.86	0.024	0.01	0.2
10-MPB-004		7	5.4	5.9	overlying	35398	53097	133	26549	2015.41	3497.4	11.37	1.15	0.016	0.27	0.3
10-MPB-005		19	5.4	5.9	overlying	4839	2419	65	3226	383.43	911.0	2.08	0.78	0.020	0.08	0.2
10-MPB-030		20	5.8	5.9	overlying	114	45	0	7576	877.72	2215.5	3.18	1.67	0.018	0.06	0.3
10-MPB-026		23	5.8	5.9	overlying	159	397	0	952	1018.36	1620.4	5.91	1.11	0.017	0.10	0.2
10-MPB-031		24	5.8	5.9	down-ice	38	30	0	1136	410.96	1772.2	2.07	1.00	0.020	0.05	0.3
10-MPB-039		40	3.5	4.0	down-ice	63	236	0	1181	145.22	322.7	0.72	0.95	0.017	0.01	0.2
10-MPB-040		40	2.0	2.5	down-ice	2	0	0	9	30.79	86.3	0.19	1.08	0.028	0.01	0.3
10-MPB-041	yes	40	0.8	1.0	down-ice	4	3	0	58	26.87	82.1	0.21	0.95	0.024	0.01	0.3
11-MPB-008		50	5.8	5.9	down-ice	42	15	0	1681	33.90	92.4	0.22	0.80	0.017	0.01	0.1
10-MPB-027		50	3.8	3.9	down-ice	38	11	0	152	64.67	122.9	0.25	0.86	0.022	0.02	0.2
10-MPB-028		51	3.7	3.9	down-ice	3226	8065	40	1613	610.97	679.5	2.98	0.96	0.019	0.03	0.2
10-MPB-032		54	5.0	5.5	down-ice	40	28	0	462	128.50	291.1	0.47	0.86	0.018	0.01	0.2
10-MPB-033		54	2.0	2.5	down-ice	3	3	0	19	53.60	183.6	0.35	1.03	0.027	0.01	0.1
10-MPB-034	yes	54	1.0	1.5	down-ice	0	0	0	29	130.87	332.1	0.72	0.92	0.023	0.01	0.1
10-MPB-036		60	2.5	3.0	down-ice	47	16	0	379	85.95	255.1	0.46	0.78	0.018	0.02	0.2
10-MPB-037		60	1.5	2.0	down-ice	3	75	0	113	48.40	113.3	0.27	0.72	0.021	0.01	0.1
10-MPB-038	yes	60	0.9	1.1	down-ice	0	0	0	192	35.94	74.5	0.16	0.82	0.022	0.01	0.1
11-MPB-009		65	5.0	5.3	down-ice	2308	62	0	615	15.41	41.4	0.11	0.80	0.022	0.01	0.1
11-MPB-010		65	3.0	3.3	down-ice	0	0	0	3	29.99	114.7	0.26	0.86	0.024	0.01	0.1
11-MPB-011	yes	65	0.8	1.2	down-ice	0	0	0	21	594.62	589.1	1.39	1.35	0.022	0.01	0.1
11-MPB-002	yes	75	2.5	2.7	down-ice	0	0	0	18	21.40	64.0	0.14	0.84	0.024	0.01	0.1
11-MPB-003		75	1.2	1.3	down-ice	0	0	0	1	16.52	47.4	0.16	0.88	0.028	0.01	0.1
11-MPB-004		75	0.5	0.6	down-ice	5	0	0	9	35.21	118.6	0.33	0.81	0.023	0.01	0.2
11-MPB-005	yes	80	0.8	1.0	down-ice	9	23	0	130	206.55	603.5	1.19	1.07	0.024	0.01	0.2
11-MPB-006		80	1.5	1.6	down-ice	63	15	0	2	136.29	404.2	0.88	1.03	0.025	0.01	0.2
11-MPB-007		80	2.8	2.9	down-ice	7	102	0	4	25.82	86.3	0.27	0.86	0.027	0.01	0.2
11-MPB-012	yes	90	1.1	1.2	down-ice	6	0	0	172	33.42	155.0	0.48	0.84	0.024	0.01	0.1
11-MPB-013		90	2.5	2.7	down-ice	2	63	0	8	66.03	233.7	0.56	0.86	0.027	0.01	0.1
11-MPB-014		90	1.9	2.1	down-ice	0	0	0	3	32.78	137.2	0.39	0.85	0.027	0.01	0.2
11-MPB-030	yes	90	1.3	1.5	down-ice	31	31	0	12	117.11	310.2	0.63	0.84	0.021	0.01	0.2
11-MPB-031		90	2.2	2.4	down-ice	2	1	0	2	20.23	70.2	0.20	0.78	0.025	0.01	0.3

Table 5 continued.

Sample	Surface till sample ?	Distance from ore zone (m)	Sample depth top (m)	Sample depth bottom (m)	Relative to ore zone	No. sphalerite grains/10 kg	No. galena grains/10 kg	No. smithsonite grains/10 kg	No. pyrite grains/10 kg	Pb (ppm)	Zn (ppm)	Cd (ppm)	Fe (%)	Tl (ppm)	S (%)	Se (ppm)
11-MPB-032		90	2.7	2.9	down-ice	22	13	0	22	26.26	83.8	0.22	0.78	0.025	0.01	0.1
11-MPB-024	yes	100	0.6	0.9	down-ice	0	0	0	15	15.36	50.3	0.14	0.78	0.021	0.01	0.1
11-MPB-025		100	1.7	1.8	down-ice	1	0	0	2	23.08	68.6	0.19	0.81	0.028	0.01	0.1
11-MPB-026		100	2.5	2.8	down-ice	5	0	0	4	28.91	75.4	0.21	0.83	0.025	0.01	0.2
11-MPB-027	yes	120	1.0	1.4	down-ice	0	0	0	8	17.03	54.4	0.12	0.80	0.021	0.01	0.1
11-MPB-028		120	2.4	2.6	down-ice	0	8	0	5	25.16	90.1	0.24	0.83	0.027	0.01	0.2
11-MPB-029		120	2.9	3.1	down-ice	7	6	0	5	20.02	80.7	0.17	0.82	0.027	0.01	0.2
11-MPB-037	yes	140	0.8	1.0	down-ice	0	2	0	6	85.10	272.1	0.65	0.92	0.023	0.01	0.1
11-MPB-038		140	2.0	2.2	down-ice	0	6	0	8	77.43	280.4	0.63	0.83	0.021	0.01	0.1
11-MPB-039		140	2.6	2.8	down-ice	2	0	0	8	87.70	363.6	0.68	0.88	0.024	0.01	0.2
11-MPB-033	yes	150	1.2	1.4	down-ice	3	0	0	41	59.10	228.6	0.55	0.95	0.025	0.01	0.1
11-MPB-035		150	1.6	1.8	down-ice	0	0	0	4	60.24	224.7	0.55	0.88	0.023	0.01	0.1
11-MPB-036		150	2.7	2.8	down-ice	81	242	0	8	185.00	475.2	1.13	0.94	0.027	0.01	0.2
11-MPB-017	yes	160	0.7	0.9	down-ice	3	0	0	6	65.68	234.0	0.55	0.78	0.020	0.01	0.2
11-MPB-018		160	1.6	1.7	down-ice	2	13	0	8	91.12	311.4	0.67	0.89	0.022	0.01	0.1
11-MPB-019		160	2.2	2.3	down-ice	13	7	0	7	97.03	360.7	0.73	0.67	0.016	0.01	0.2
11-MPB-020		160	3.1	3.3	down-ice	0	0	0	4	74.67	282.4	0.66	0.80	0.022	0.01	0.1
11-MPB-021	yes	160	0.8	1.0	down-ice	1	0	0	8	80.95	241.4	0.70	0.84	0.026	0.01	0.1
11-MPB-022		170	1.6	1.9	down-ice	0	26	0	8	77.26	278.1	0.62	0.86	0.022	0.01	0.2
11-MPB-023		170	2.7	2.9	down-ice	3	68	0	254	82.91	414.3	0.85	0.89	0.022	0.01	0.1
11-MPB-043	yes	350	0.9	1.0	down-ice	31	0	0	2	36.10	115.6	0.38	0.75	0.023	0.01	0.2
11-MPB-048	yes	400	0.8	0.9	down-ice	9	0	0	15	46.11	142.0	0.40	0.73	0.023	0.01	0.2
11-MPB-052	yes	400	1.0	1.2	down-ice	0	8	0	4	46.62	153.5	0.42	0.75	0.024	0.01	0.2
11-MPB-053		400	2.0	2.1	down-ice	2	31	0	9	48.63	189.1	0.53	0.80	0.026	0.01	0.3
11-MPB-054		400	2.9	3.0	down-ice	20	5	0	31	31.05	108.2	0.32	0.82	0.027	0.01	0.3
11-MPB-049	yes	450	0.8	1.0	down-ice	0	1	0	1	64.28	211.9	0.60	0.85	0.026	0.01	0.3
11-MPB-050		450	1.8	2.0	down-ice	1	78	0	1	79.34	250.1	0.62	0.86	0.027	0.01	0.2
11-MPB-051		450	2.5	2.6	down-ice	2	1	0	0	56.63	218.6	0.65	0.81	0.026	0.01	0.2
11-MPB-045	yes	600	2.0	2.1	down-ice	7	31	0	8	70.64	214.3	0.60	0.76	0.023	0.01	0.1
11-MPB-046		600	1.0	1.2	down-ice	0	2	0	0	95.50	248.8	0.72	0.80	0.023	0.01	0.2
11-MPB-047		600	2.9	3.0	down-ice	2	0	0	4	67.71	235.1	0.62	0.80	0.025	0.01	0.2
11-MPB-040	yes	700	1.2	1.3	down-ice	36	1	0	3	38.45	166.8	0.52	0.80	0.025	0.01	0.2
11-MPB-041		700	1.8	2.0	down-ice	3	23	0	2	41.30	166.5	0.56	0.82	0.026	0.01	0.2
11-MPB-042		700	2.4	2.6	down-ice	0	2	0	5	19.36	59.8	0.13	0.87	0.026	0.01	0.1

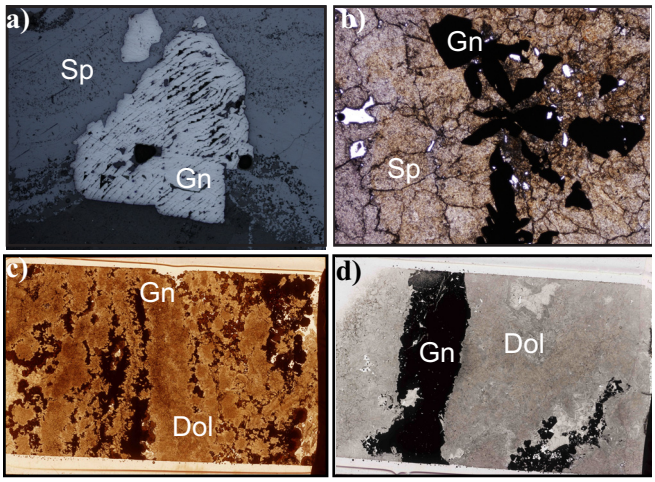

Figure 18. Photomicrographs of types and textures of galena grains in bedrock samples. **a)** A galena crystal with curved crystal faces, indicating that bedrock sample 10-MPB-R63 underwent tectonic deformation. **b)** Skeletal galena in bedrock sample 10-MPB-R35. **c)** Banded galena and sphalerite in bedrock sample 10-MPB-R55. **d)** Banded galena in bedrock sample 10-MPB-R50. Dol = dolomite, Gn = galena, Sp = sphalerite.

18). Cubic grains range from 50 to 5000 µm and dimensions for skeletal grains range from 50 to 1500 µm. As with sphalerite grains, fragments of each of these types of galena occur in brecciated samples. A summary of modal abundances of galena in PTS is listed in Table 6.

Galena grains were recovered from heavy mineral concentrates of bedrock samples from pan concentrate (<0.25 mm) to 2 mm in size, though most grains were recovered from the pan concentrate fraction (Table 2). More galena grains were recovered from the pan concentrates than sphalerite grains. The highest concentration was recovered from sample 10-MPB-R57, which contained approximately 80% galena.

EMP analysis was conducted on 58 grains of cubic and skeletal varieties of galena, as well as each texture observed in PTS (Appendix C3). The concentration of Pb in galena ranges from 83.87 to 89.27 wt.%. Sulphur concentrations in galena range from 12.53 to 13.93 wt.% and have a bimodal distribution (Fig. 19a). Low S concentrations range from 12.5 to 13.25 wt.% and

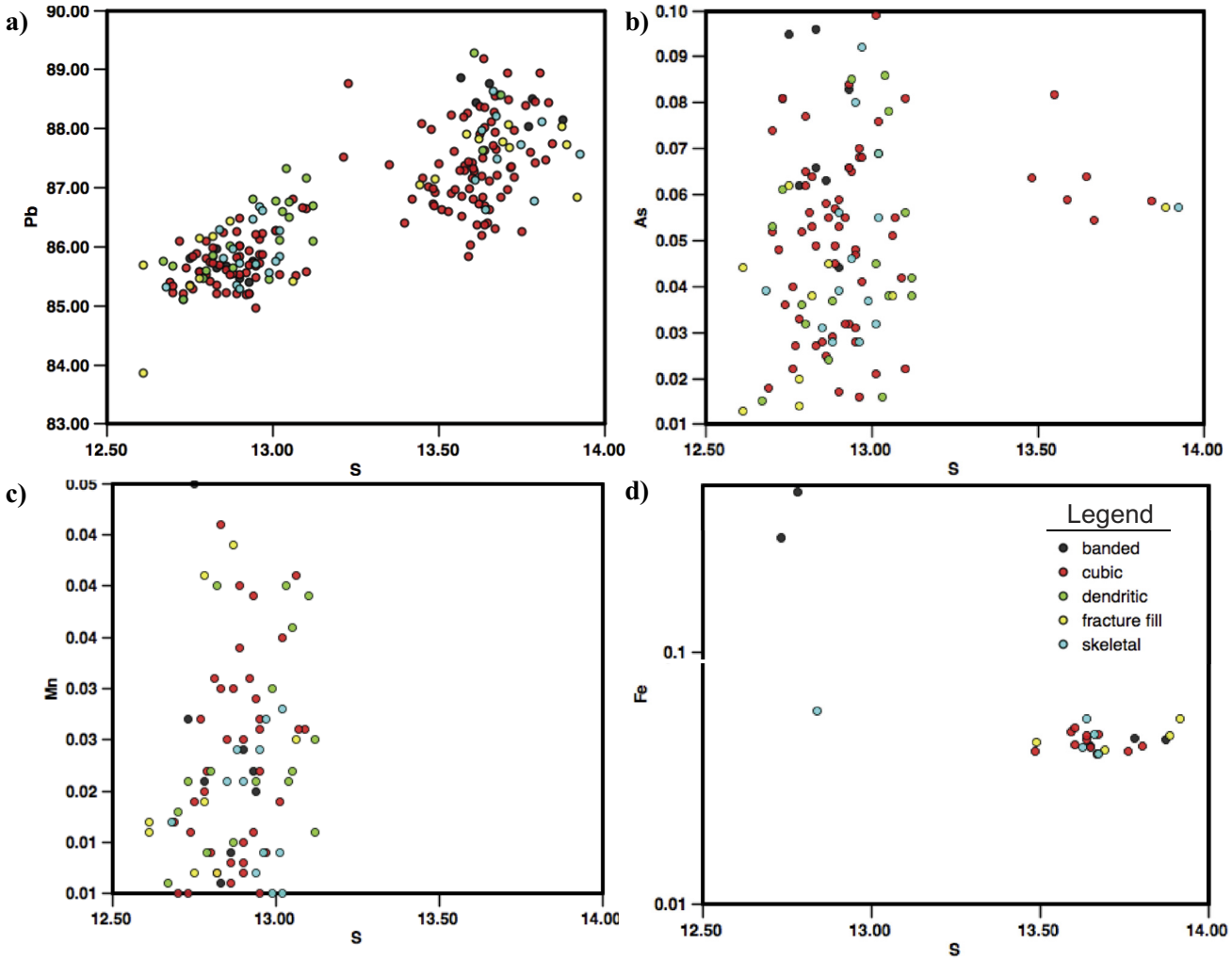

Figure 19. Concentrations of **(a)** Pb, **(b)** As, **(c)** Mn, and **(d)** Fe versus S determined by EMP analysis on several varieties of galena grains from bedrock samples.

Table 6. Modal abundances of minerals identified in polished thin sections of bedrock samples from this study.

Sample #	Sphalerite (%)				Galena (%)					Pyrite (%)		Sulphur (%)	Gangue (%)
	Honey brown	Colloform	Cleiophane	Blackjack	Cubic	Fracture fill	Banded	Dendritic	Skeletal	Cubic	Colloform		
10-MPB-R01	35	0	0	0	40	0	0	0	0	tr	0	0	25
10-MPB-R02	50	0	0	0	35	0	0	0	0	tr	0	0	15
10-MPB-R03	20	35	0	20	3	4	0	0	3	tr	0	0	15
10-MPB-R04	35	40	0	0	2	8	0	0	0	5	0	10	0
10-MPB-R06	60	10	0	10	5	5	0	0	0	tr	0	5	5
10-MPB-R07	20	0	0	5	tr	0	0	0	0	tr	0	20	55
10-MPB-R08	10	0	0	0	tr	0	0	0	0	tr	0	0	90
10-MPB-R09	5	0	0	0	15	0	0	0	0	tr	0	0	80
10-MPB-R11	20	5	0	0	5	0	0	0	0	0	0	0	70
10-MPB-R15	50	0	0	0	5	0	0	0	0	25	0	0	20
10-MPB-R17	15	10	5	10	5	0	0	0	0	40	5	0	10
10-MPB-R19	15	0	0	0	20	0	0	0	0	tr	0	0	65
10-MPB-R20	10	0	0	5	0	0	0	0	0	5	0	0	80
10-MPB-R24	20	0	0	0	20	0	0	0	0	10	0	0	50
10-MPB-R25	10	0	0	10	0	0	0	0	0	5	0	0	75
10-MPB-R26	25	0	0	0	0	0	0	0	0	5	0	0	70
10-MPB-R27	10	5	0	40	tr	0	0	0	0	tr	0	0	50
10-MPB-R28	10	5	0	5	tr	0	0	0	0	tr	0	0	80
10-MPB-R30	10	50	0	0	2	0	0	0	8	tr	0	0	30
10-MPB-R31	0	40	15	0	10	0	0	0	5	0	0	0	30
10-MPB-R32	0	25	0	0	0	0	0	0	10	tr	0	0	65
10-MPB-R35	0	0	0	50	20	0	0	0	0	tr	0	0	30
10-MPB-R37	0	0	0	0	0	0	0	0	0	60	0	0	40
10-MPB-R38	tr	0	0	0	0	0	0	0	0	60	0	0	40
10-MPB-R40	60	0	0	5	0	5	0	0	0	tr	0	0	30
10-MPB-R41	10	15	0	10	10	0	0	0	tr	tr	0	0	55
10-MPB-R42	10	30	0	10	0	0	0	0	5	tr	0	0	45
10-MPB-R44	0	5	0	30	10	0	0	0	5	5	0	0	45
10-MPB-R46A	15	45	0	0	35	0	0	0	0	0	0	0	5
10-MPB-R46B	40	0	0	0	55	0	0	0	0	0	0	0	5
10-MPB-R47	0	0	0	0	0	0	0	0	0	40	0	0	60
10-MPB-R50	5	0	0	0	5	0	20	0	0	tr	0	0	70
10-MPB-R51	75	0	0	0	0	5	0	0	0	0	0	0	20
10-MPB-R52	10	0	0	5	5	0	0	0	0	tr	0	0	80
10-MPB-R53	20	0	0	0	5	0	0	0	0	10	0	0	65
10-MPB-R55	15	25	0	0	5	0	0	0	0	20	0	0	35
10-MPB-R56	10	0	0	0	25	0	0	0	0	tr	0	0	65
10-MPB-R62	0	0	15	10	20	0	0	0	5	tr	0	0	50
10-MPB-R63	20	30	0	10	25	0	0	0	0	tr	0	10	5
10-MPB-R64	tr	0	0	0	0	0	0	0	0	30	15	0	55
10-MPB-R65	0	0	0	0	40	0	0	0	0	tr	0	0	60
10-MPB-R66	15	0	0	5	10	0	0	0	0	5	0	0	65
10-MPB-R67	20	15	0	0	0	0	0	20	10	tr	0	0	35
10-MPB-R68	65	0	0	0	20	0	0	0	0	0	0	0	15
10-MPB-R69	15	0	0	0	55	0	0	0	0	tr	0	0	30
10-MPB-R70	15	10	0	15	10	0	0	0	0	tr	0	0	50
10-MPB-R71	tr	0	0	0	2	0	0	0	0	3	0	0	95
10-MPB-R72	5	35	0	25	15	5	0	0	0	5	0	0	10
10-MPB-R73	5	20	0	10	0	0	0	0	5	tr	0	0	60
10-MPB-R74	0	0	0	30	0	5	0	10	0	5	0	0	50
10-MPB-R75	20	10	10	5	5	0	0	0	5	tr	0	0	45
10-MPB-R76	0	0	0	25	10	0	0	0	5	0	0	0	60
10-MPB-R77	tr	0	0	0	tr	0	0	0	0	tr	0	0	100

high S concentrations range from 13.75 to 14.00 wt.%. Galena grains with lower S concentrations have higher As (Fig. 19b) and Mn contents (Fig. 19c) than grains with higher S concentrations. Galena grains with high concentrations of S have low concentrations of Fe (Fig. 19d). Deposit R190 (Pb=86.69–89.18 wt.%) and HZ (Pb=83.87–89.27 wt.%) have the highest Pb concentrations in galena. All five deposits have similar concentrations of S, As, Ag, Cd, Pb, and Se in galena. The differences in composition of bedrock galena grains occur in elements Mn, Fe, Zn, Ge, In, Sb, and Hg. Deposit O-28 has the highest concentration of Mn (0.01–0.05 wt.%) and the lowest concentration of Zn (0.02–2.12 wt.%). Deposit O-28 also has an elevated concentration

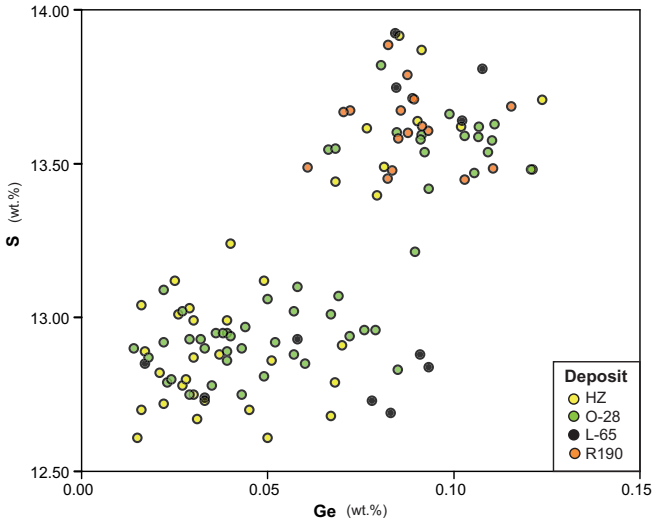

Figure 20. Concentrations of S versus Ge in galena grains in bedrock samples from different deposits; values were determined by EMP analysis. Grains from deposit M-67 are absent because their Ge values were reported as less than detection limit (109 ppm).

of In (0.02–0.07 wt.%) and Sb (0.02–0.04 wt.%). Deposits R190 and M-67 have concentrations of In, Sb, and Hg that are below detection limit. Deposit M-67 has concentrations of Ge, As, Ag, Cd, In, Sb, Cu, and Hg that are below detection limit, as well as a low concentration of Fe (0.04–0.05 wt.%). Deposits O-28 and HZ have the highest concentrations of Ge (0.01–0.12 wt.% and 0.02–0.12 wt.%, respectively; Fig. 20).

Cubic and skeletal galena grains have varying Zn, In, Sb, and Hg concentrations. Skeletal galena has a higher concentration of Zn (0.02–0.91 wt.%) and lower concentrations of In (0.02–0.04 wt.%), Sb and Hg (below detection limit) than cubic galena. Dendritic and banded galena contain approximately the same concentrations of analyzed elements, excluding Fe and In. Iron concentration in dendritic galena is below detection limit, though banded galena has a concentrations ranging from 0.043 to 0.47 wt.% Fe. Banded galena has below detection limit concentrations of In, though dendritic galena contains from 0.026 to 0.043 wt.% In. Fracture-filling galena is compositionally very similar to skeletal galena.

Till

Galena grains were recovered from all size fractions (pan concentrate, 0.25–0.5, 0.5–1.0, and 1.0–2.0 mm) in 27% of the till samples (Table 4). The coarsest grains (1.0–2.0 mm) were recovered from samples closest to the deposit. Most grains were recovered from the pan concentrate of till. Till sample 10-MPB-004 contains 53,097 grains (normalized to 10 kg) in the 0.25 to 0.5 mm fraction, till sample 10-MPB-005 contains 2,419 grains, and till sample 10-MPB-028 contains 8065 grains. These till samples are all immediately down-ice of the ore zone of deposit O-28 (Fig. 21). Background concentration for galena is 0 grains, defined in the same manner as for the sphalerite grains background.

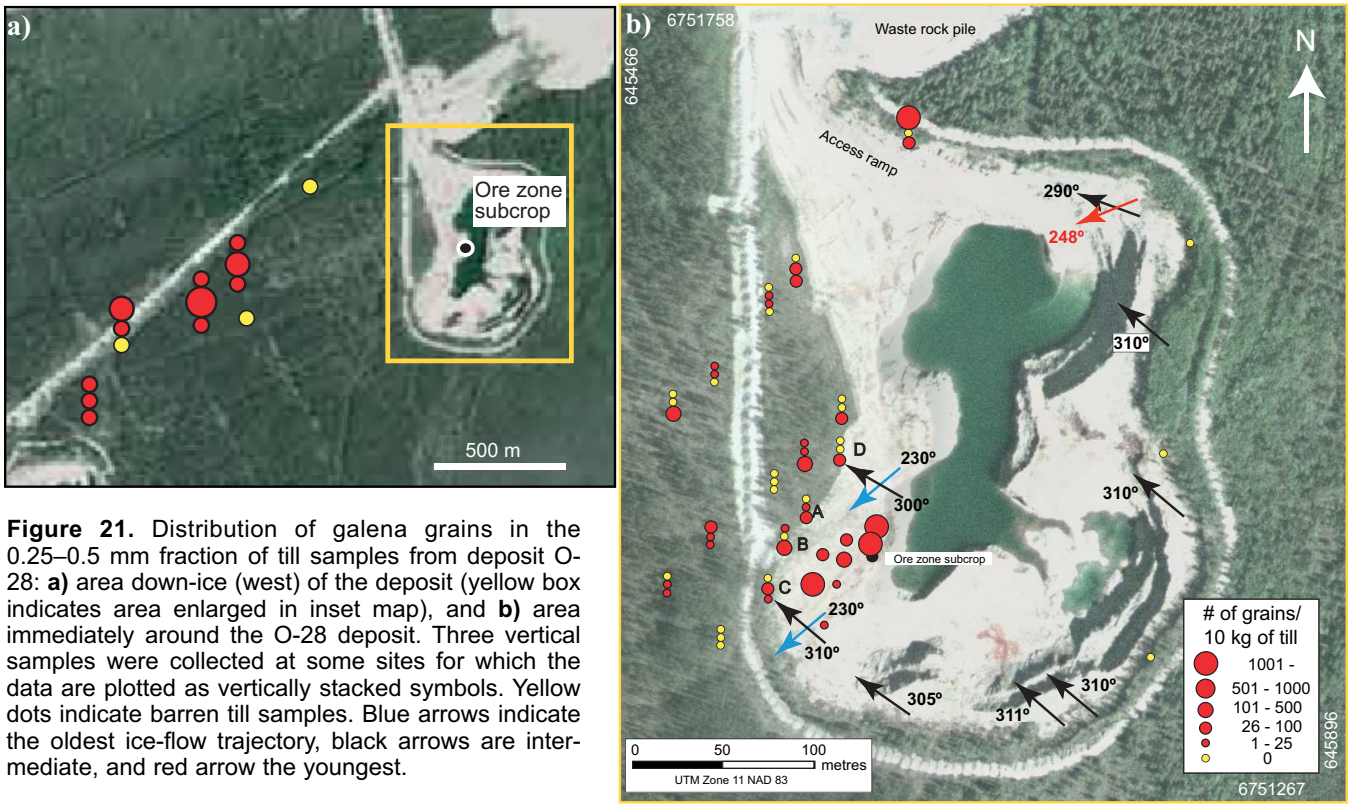

Figure 21. Distribution of galena grains in the 0.25–0.5 mm fraction of till samples from deposit O-28: **a)** area down-ice (west) of the deposit (yellow box indicates area enlarged in inset map), and **b)** area immediately around the O-28 deposit. Three vertical samples were collected at some sites for which the data are plotted as vertically stacked symbols. Yellow dots indicate barren till samples. Blue arrows indicate the oldest ice-flow trajectory, black arrows are intermediate, and red arrow the youngest.

Figure 22. Galena grains from the 1.0–2.0 mm fraction of till sample 11-MPB-029 showing grain morphology, which includes cubic grains, some with sharp crystal edges and some with rounded edges that are a result of white anglesite coatings.

Metal-rich till samples from deposit P-24 (samples 10-MPB-013 and -014) each contain 192,308 and 196,078 grains, and samples 10-MPB-020 and -021 from deposit N42 contain 4,211 and 3,158 galena grains, respectively. Buffalo River till samples (11-MPB-059, -060, and 085B-2010-1008) contain between 0 and 6 grains of galena. Regional till sample 11-MPB-061, collected at deposit K-77, contains 28 grains and sample 11-MPB-062, collected at deposit S-65, contains 0 grains of galena (Table 4).

Grain morphology of galena in till is typically cubic, though some grains have a coating of anglesite that makes the grains appear subrounded to rounded (Fig. 22). EMP analysis conducted on galena grains recovered from till samples indicate that grains in till contain similar concentrations of Pb, S, and Se to those recovered from bedrock samples (Appendix C3). Concentrations of Fe, Zn, Ge, As, In, Sb, Cu, and Hg are much lower in grains recovered from till samples than those recovered from bedrock samples. Cadmium concentration ranges from 0.008 to 0.093 wt.% in galena grains recovered from till samples.

Pyrite

Bedrock

Pyrite in PTS occurs as cubic crystals, botryoidal fans, or needles and fine-grained masses (Fig. 23). Disseminated euhedral grains also occur throughout most samples (Fig. 24). Pyrite grains typically range in size from <50 to 500 µm, though some larger grains (~2500 µm) do occur. In hand sample, pyrite cubes were observed to be 2 cm across (Fig. 25).

Pyrite grains in bedrock HMC were observed in the pan concentrate and the 0.25 to 0.5 mm fraction, from

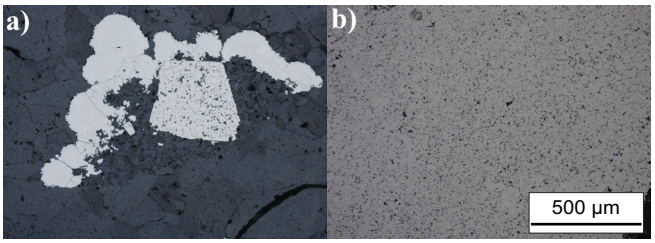

Figure 23. Photomicrographs of pyrite textures in bedrock samples: **a)** botryoidal pyrite in sample 10-MPB-64, and **b)** very fine aggregates of botryoids of pyrite in sample 10-MPB-R38.

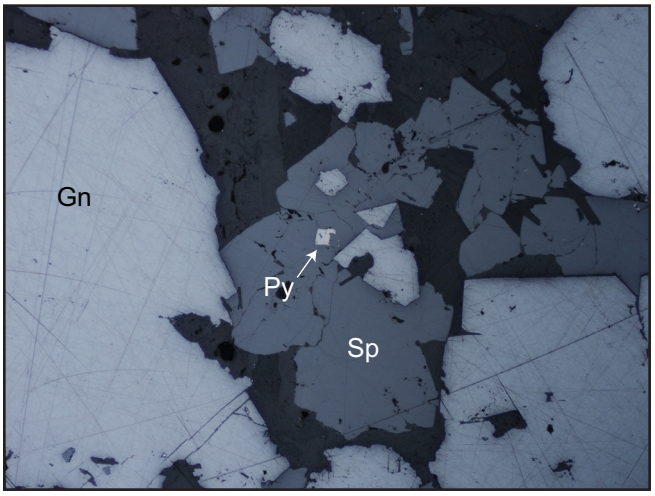

Figure 24. Photomicrograph of a cubic pyrite (Py) grain encased in a honey-brown sphalerite (Sp) grain from bedrock sample 10-MPB-R69. The sphalerite grain also contains fragments of galena (Gn).

Figure 25. Cubic pyrite in a bedrock grab sample from deposit S-65.

which the majority of grains were recovered. Samples 10-MPB-R37 and -R38 contain 100% pyrite, with an estimated 730,689 and 527,241 grains/1 kg, respectively. Sample 10-MPB-R17 contains >1,000,000 grains/1 kg.

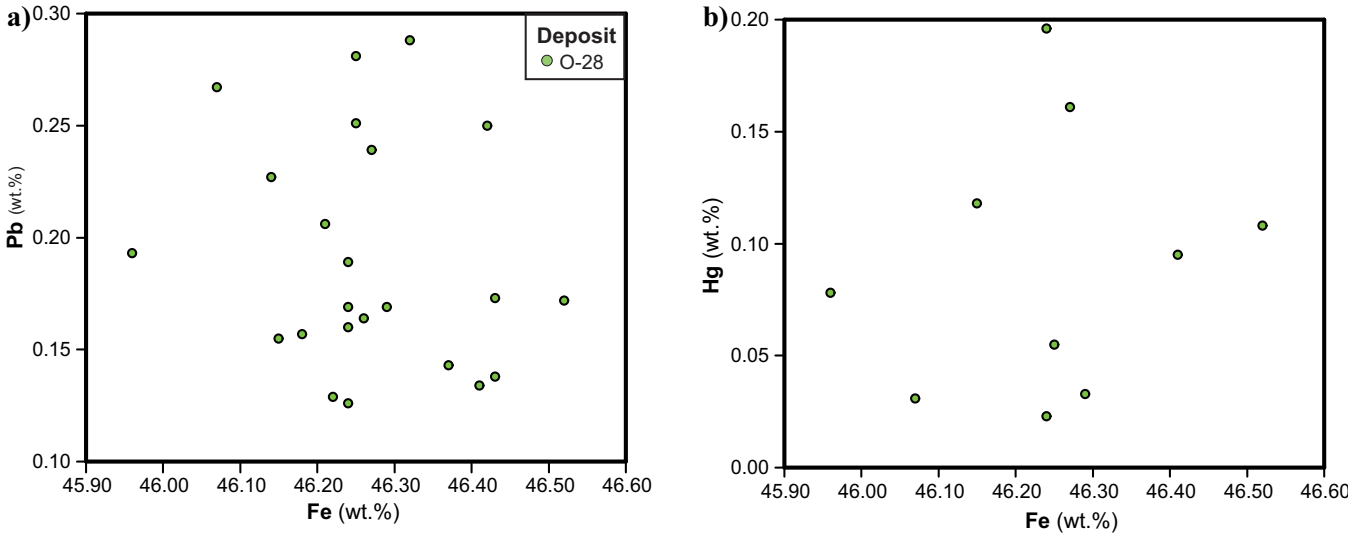

Figure 26. Concentrations of **(a)** Pb and **(b)** Hg versus Fe (determined by EMP analysis) in pyrite grains from bedrock samples from deposit O-28. Deposit O-28 is the only deposit for which Pb and Hg values were reported as greater than the lower detection limits.

EMP data (Appendix C3) indicate that the concentrations of major elements Fe and S range from 41.98 to 47.25 wt.% and 51.70 to 54.37 wt.%, respectively. Minor elements include Zn (0.012–7.03 wt.%), As (less than detection to 0.22 wt.%), and Pb (less than detection to 0.29 wt.%). Selenium (0.012–0.07 wt.%) occurs in all five deposits excluding R190. Deposit O-28 shows enrichment in Ge, In, Sb, Pb (Fig. 26a), and Hg (Fig. 26b) in pyrite, though pyrite concentrations in the other four deposits were below detection limits of these elements. In Deposit O-28, Ge and Hg concentrations range from less than detection to 0.05 wt.% and 0.20 wt.%, respectively. Indium concentration ranges from less than detection to 0.04 wt.% and Sb concentration ranges from less than detection to 0.03 wt.%. Pyrite in deposit L-65 contains more Mn (0.03–0.24 wt.%) and As (0.05–0.22 wt.%) than other deposits. Deposit HZ contains the highest concentration of Zn (0.48–7.03 wt.%) in pyrite, and deposit R190 contains a higher concentrations of Cu (0.06–0.70 wt.%) in pyrite than the other deposits. Inclusion pyrite and botryoidal pyrite have near identical concentrations of all elements analyzed using EMP except that botryoidal pyrite contains 0.03 to 0.24 wt.% Mn and inclusion pyrite contains 0.05 to 0.22 wt.% As. Fine-grained massive pyrite aggregates contain the highest concentrations of Zn (0.02–7.03 wt.%) as well as Cu (0.01–0.46 wt.%).

Till

Pyrite grains were recovered from the pan concentrate and 0.25–0.5 mm fractions of till. From deposit O-28, till sample 10-MPB-004 contains 26,549 grains of pyrite, sample 10-MPB-030 contains 7,576 grains, and till sample 10-MPB-005 contains 3,226 grains (Fig. 27). These till samples were collected overlying and immediately down-ice in the oldest ice-flow direction from the orebody. Till samples 10-MPB-020 and 10-MPB-021, collected from deposit N-32, contain 15,789 and 8,421 grains of pyrite, respectively. Till samples collected from deposit P-24 (samples 10-MPB-013 and

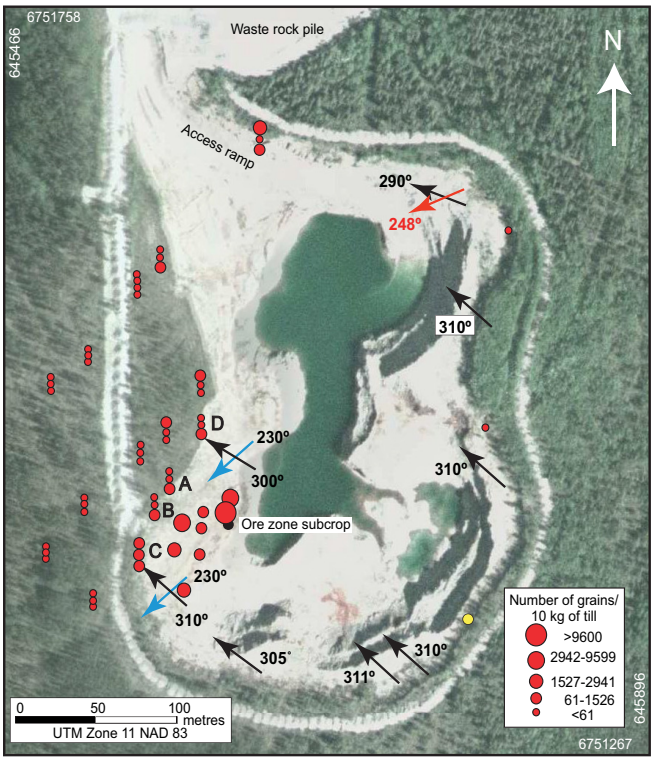

Figure 27. Distribution of pyrite grains in the 0.25–0.5 mm fraction of till samples collected around deposit O-28. Three vertical samples were collected at several sites, which are shown as vertically stacked symbols. Yellow dot indicates a barren sample. Blue arrows indicate the oldest ice-flow trajectory, black arrows are intermediate, and red arrows are youngest.

Figure 28. Smithsonite grains from the 1–2 mm heavy mineral fraction of till sample 10-MPB-014.

-014) contain 5,882 and 57,692 grains. Buffalo River till samples (samples 11-MPB-059, -060 and 085B-2010-1008) contain between 6 and 33 grains of pyrite. Regional till sample 11-MPB-061, collected at deposit K-77, contains 2,752 grains and sample 11-MPB-062, collected at deposit S-65, contains 31 grains.

Smithsonite ($ZnCO_3$)

Bedrock

No smithsonite grains were identified in PTS or bedrock HMC.

Till

Smithsonite (Fig. 28) was identified in till heavy mineral concentrates by its white colour and botryoidal habit. Smithsonite was recovered from till samples 10-MPB-004, -005, -20, -021, -026, and -028. All of these till samples, excluding samples 10-MPB-020 and -021, were collected from the shoulder of pit O-28 (Fig. 29). Till samples 10-MPB-020 and -021 were collected on the west shoulder of pit N-32. Smithsonite concentrations range from 0 to 133 grains and the background concentration is 0 grains. Most smithsonite grains were recovered from the 0.25 to 0.5 mm fraction of till. Till samples 10-MPB-013 and -014 (from deposit P-24) contain 58,824 and 57,692 smithsonite grains, respectively.

Cerussite ($PbCO_3$)

Bedrock

No cerussite grains were identified in PTS or bedrock HMC.

Till

Cerussite (Fig. 30) was identified in till HMC by its white colour. It was recovered from the 0.25 to 1 mm fraction of till samples 11-MPB-036 and 11-MPB-021, down-ice of pit O-28. Till sample 11-MPB-036 contains 27 grains of cerussite and sample 11-MPB-021 contains 1 grain.

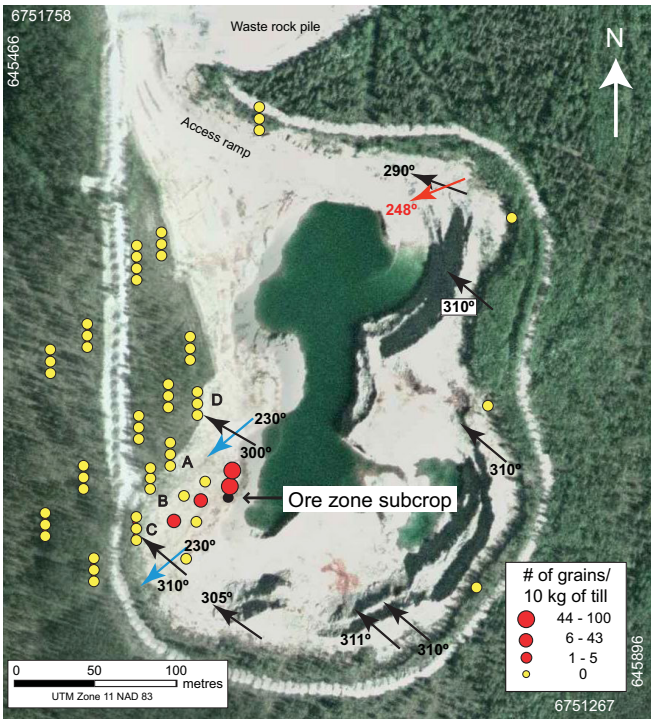

Figure 29. Distribution of smithsonite grains in the 0.25 to 0.5 mm fraction of till around deposit O-28. Three vertical samples were collected at some sites, which are shown as vertically stacked symbols. Yellow dots indicate barren samples. Blue arrows indicate the oldest ice-flow trajectory, black are intermediate, and red are youngest.

DISCUSSION

Indicator Mineral Compositions

Cleiophane and colloform sphalerite in bedrock contain higher concentrations of Pb than the other sphalerite varieties. These two varieties of sphalerite commonly occur with skeletal galena, which could account for the high concentrations of Pb. Deposits R190 and O-28 have the highest Zn concentration in sphalerite grains in bedrock, which could indicate the presence of more cleiophane and colloform sphalerite than in the other deposits. Cadmium and Fe both substitute for Zn

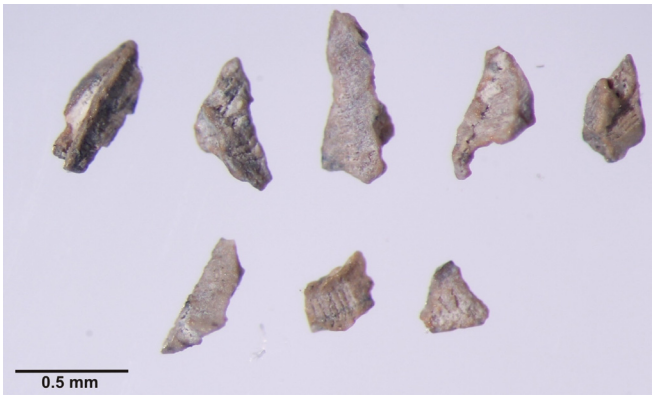

Figure 30. Photograph of cerussite grains from the 0.25–0.5 mm heavy mineral fraction of till sample 11-MPB-036.

in sphalerite's crystal structure, which could account for the decreased concentrations of Cd in blackjack sphalerite.

Deposit M-67 contains lower concentrations of Ge, Ag, In, Sb, Pb, Cu, and Hg in bedrock samples than other deposits. Acicular sphalerite in bedrock also has lower concentrations of these elements. which could indicate that the sphalerite in deposit M-67 may contain more of this texture of sphalerite.

The bimodal distribution of S (low and high) in galena grains in bedrock as determined by EMP could be due the differences in geochemistry among the different varieties of galena. The majority of skeletal grains are in the low S group; this could be due to the presence of more Zn in the crystal structure than in cubic galena. Deposits R190 and M-67 have lower concentrations of In, Sb, and Hg in bedrock, which could indicate that these deposits contain more of the fracture-filling and skeletal galena than the other deposits.

EMP data shows some differences in trace element content of pyrite in bedrock samples among deposits and among varieties of pyrite. Botryoidal pyrite and inclusions of pyrite in other minerals have essentially the same geochemical signature. This could indicate that the botryoidal pyrite is an early-stage mineralization or that the mineralizing fluids for each of these varieties of pyrite were the same. Pyrite in deposit L-65 has higher concentrations of As and Mn than the other deposits, which could indicate the presence of more botryoidal pyrite in this deposit. Deposits R190 and HZ contain the highest concentrations of Zn and Cu in pyrite grains from bedrock samples, indicating that these deposits may contain more massive pyrite than the other deposits.

Comparison of Pine Point Grain Compositions with Other Deposits

Table 7 compares EMP data for selected elements for bedrock grains of galena and sphalerite from this study versus other MVT deposits in Canada. Data for sphalerite grains in this study are similar to data from previous studies done at Pine Point (Kyle, 1981), with the exception of Cd concentrations in sphalerite. This study detected, on average, a higher Cd concentration (0.17 wt.% higher) than has previously been reported for Pine Point. This could be due to the larger sample set of this study (n=418) compared to the previous study (n=69), which captured a larger range in compositions of Cd in sphalerite.

Pine Point sphalerite has higher Zn and lower Fe, Mn, and Cu concentrations on average compared to the Nanisivik MVT deposit on Baffin Island. This MVT deposit has different general chemical characteristics, such as a higher Ag content and higher formation temperatures, than Pine Point (Arne et al., 1990). Nanisivik also has three vertical and four horizontal ore zones that are texturally and mineralogically distinct (Arne et al., 1990). Wurtzite ((Zn, Fe)S) is also documented to occur at Nanisivik (Olson, 1977), which could account for the higher Fe concentrations in sphalerite than at Pine Point.

Table 7. Comparison of electron microprobe data for sphalerite, galena, and pyrite in samples from this study compared to those found in till from the Pine Point, Nanisivik MVT deposit (Nunavut), and in a similarly Great Slave Lake shear zone-derived but an unknown bedrock source in northwest Alberta.

Sphalerite		Zn wt.%	S wt.%	Pb wt.%	Fe wt.%	Mn wt.%	Cu wt.%	Cd wt.%
This study	Mean (n=418)	64.15	33.10	0.29	2.04	0.02	0.02	0.23
	Minimum	44	32	0.03	0.04	0.01	0.01	0.03
	Maximum	67.48	39.2	0.87	16.9	0.04	0.12	0.51
Pine Point	Mean (n=69)	64.2	33.4	0.21	2.23	0.01	0.02	0.05
(Kyle, 1981)	Minimum	55.5	31.5	0.00	0.15	0.00	0.00	0.00
	Maximum	66.6	33.6	1.05	10.30	0.02	0.16	0.32
Nanisivik	Mean (n=52)	63.87	33.19	N/A	4.54	0.41	0.24	0.30
(Arne et al., 1990)	Minimum	59.5	32.80	N/A	0.12	0.12	0.18	0.27
	Maximum	68.7	34	N/A	15.00	1.15	0.53	0.32
Northwestern Alberta	Mean (n=180)	65.45	33.39	0.00	0.71	0.00	0.01	0.43
(Plouffe et al., 2007)	Minimum	63.30	32.47	0.00	0.10	0.00	0.00	0.00
	Maximum	66.7	34.22	0.11	3.13	0.02	0.08	1.56

Galena		Zn wt.%	S wt.%	Pb wt.%	Fe wt.%	Mn wt.%	Cu wt.%	Cd wt.%
This study	Mean (n=232)	0.27	13.25	86.66	0.12	0.02	0.02	N/A
	Minimum	0.01	12.6	83.9	0.04	0.01	0.01	N/A
	Maximum	3.32	13.92	89.27	1.33	0.05	0.03	N/A
Pine Point	Mean (n=24)	0.23	13.3	85.8	0.01	N/A	0.08	N/A
(Kyle, 1981)	Minimum	0.00	13.1	84.5	0.00	N/A	0.00	N/A
	Maximum	1.30	13.7	86.60	0.15	N/A	0.24	N/A

Pyrite		Zn wt.%	S wt.%	Pb wt.%	Fe wt.%	Mn wt.%	Cu wt.%	Cd wt.%
This study	Mean (n=87)	1.96	53.06	0.19	45.95	0.04	0.22	0.00
	Minimum	0.01	51.70	0.13	41.98	0.01	0.01	0.00
	Maximum	7.03	54.37	0.29	47.25	0.24	0.70	0.00
Pine Point	Mean (n=31)	N/A	53.3	N/A	46.10	N/A	0.16	N/A
(Kyle, 1981)	Minimum	N/A	52	N/A	45.00	N/A	0.00	N/A
	Maximum	N/A	54	N/A	46.8	N/A	1.27	N/A

Pb and Zn-rich till without a known bedrock source, yet fingerprinted to the same basement structure (GSLSZ), has been reported in northwestern Alberta (Plouffe et al., 2006; Paulen et al., 2011), ~330 km to the southwest of Pine Point. Concentrations of Pb and Fe in sphalerite grains from northwestern Alberta are lower, and concentrations of Cd (on average) are higher than sphalerite from Pine Point bedrock in this study.

Concentrations of selected elements in galena grains from this study are similar to those previously studied at Pine Point (Kyle, 1981), with the exception of Fe and Cu concentrations. On average, Fe concentrations are higher and Cu concentrations are lower in galena grains than those determined by Kyle (1981).

Concentrations of elements in pyrite grains from this study are similar to those determined by previous studies (Kyle, 1981).

Indicator Mineral Abundances

Sphalerite and galena abundances in till around the O-28 deposit vary from 0 to 17 grains in till samples up-ice, to tens of thousands of grains in till directly overlying mineralization. Till samples at the till/bedrock interface up to 120 m down-ice contain 1000s of grains of sphalerite and galena. Contents decrease with increasing distance above the bedrock surface and with increasing distance down-ice. At surface, till samples 700 m down-ice contain 10s of grains of sphalerite.

Smithsonite was detectable immediately down-ice (to the southwest) from the O-28 deposit for approximately 50 m. Smithsonite is a secondary Zn-carbonate mineral that forms from the oxidation of Zn sulphides (e.g. sphalerite). Smithsonite has a hardness of 4.5 and would likely survive glacial transport. Its presence in till just down-ice of the deposit may reflect (1) incorporation of a preglacial oxidized cap on the deposit that contained smithsonite, or (2) post-glacial weathering of Zn-rich carbonate till that has formed smithsonite in situ.

Cerussite is a secondary Pb-carbonate mineral that forms from the oxidation of Pb sulphides (e.g. galena). It was detected in two till samples down-ice of the O-28 deposit. No cerussite was observed in bedrock samples from deposit O-28 or any other deposit in this study. Cerussite has a hardness of 3 to 3.5. Its presence in till just down-ice of the deposit may reflect (1) incorporation of a pre-glacial oxidized cap on the deposit that contained cerussite, or (2) post-glacial weathering of Pb-rich carbonate till that has formed cerussite in situ.

Till samples that had high concentrations of Zn in the silt + clay fraction (<0.063 mm) did not necessarily have large quantities of sphalerite grains in the sand-sized fraction of till. For example, till sample 11-MPB-009 contains 2308 sphalerite grains in the 0.25–0.5 mm fraction and only 41 ppm Zn in the <0.063 mm fraction. This till sample was collected approximately 30 m down-ice from the ore zone. The likely explanation for this is that the sphalerite grains were not yet glacially crushed to the <0.063 mm size fraction, analogous to the sphalerite grain anomaly in northwest Alberta (Paulen et al., 2011). Conversely, some till samples (10-MPB-034, 11-MPB-011, and 11-MPB-005) contain high concentrations of Zn (332–604 ppm) in the till matrix and contain little to no visible sphalerite grains; these three till samples were collected at surface. Till in these locations would have been subjected to all three phases of ice-flow and thus it is possible that any sphalerite grains in the till were comminuted to the silt size, resulting in the high Zn content in the <0.063 mm fraction and the relatively barren sand-sized fraction.

Abundance of galena grains recovered from the 0.25 to 0.5 mm fraction of till have a stronger correlation with Pb concentrations in the silt + clay fraction of till. This correlation is that the result of galena being a softer mineral (hardness: 2.5) than sphalerite (hardness: 3.5–4), and therefore would be more susceptible to glacial comminution than sphalerite. Coarse (1.0–2.0 mm) sphalerite grains were mainly detected in till samples on the bedrock bench surrounding deposit O-28, though galena grains of this size were detected at larger distances from the ore body. This could be due to the larger initial grain size of the galena crystals and massive patches of galena ore compared to the smaller sphalerite grain size.

Galena grains coated in anglesite ($PbSO_4$) were recovered from till samples 10-MPB-021, -026, -030, -032, 11-MPB-005, -007, -008, -013, -016, -019, -021, -033, -036, -038, -045, and -046. Anglesite is a secondary Pb sulphate mineral that forms from the oxidation of Pb sulphides, primarily galena. Its presence on galena grains in till just down-ice of the deposit may reflect (1) incorporation of a partially pre-glacial oxidized cap on the deposit in which galena grains have started to oxidize; or (2) post-glacial weathering of Pb-rich carbonate till that has formed anglesite on the outside of galena grains in situ. Anglesite coatings on galena grains usually only covers a small area, indicating likely only minor weathering of galena grains or that the anglesite coating has been scraped off during glacial transport. Anglesite has a hardness of 2 to 2.5 and could easily be scoured off during glacial transport. Galena grains coated with anglesite were recovered from till samples that were considered to be low to moderately oxidized. There was no anglesite identified in PTS or recovered from bedrock HMCs.

Till samples 10-MPB-020 and -021 had some of the highest concentrations of sphalerite, galena, and pyrite grains of the samples in this study, as well as high concentrations of Zn, Pb, Fe, and Se in the till matrix. These till samples were collected from deposit N-32, which had a total tonnage of 2.1 Mt with an average grade of 3.4% Pb and 8.4% Zn. These values are nearly double the recorded grades for deposit O-28 (Holroyd et al., 1988), which could account for the higher concentrations in these samples than those collected at deposit O-28.

Till samples collected along the banks of the Buffalo River do not contain any sphalerite grains and have only slightly elevated concentrations of galena and pyrite. These till sample sites are located approximately 9 km west from the western-most known orebody in the district. It is not known if this orebody subcrops or where the nearest subcropping orebody is to Buffalo River, so these values may be a reflection of the region or they could indicate that the transport dis-

tance of these grains are possibly upwards of 9 km. Further work would be required to establish the dispersal train associated with the Pine Point deposits. Till samples that were collected further west (>150 km west) during Northwest Territories Protected Area assessments (Watson, 2010, 2011) do contain in excess of 100 grains of sphalerite with minor galena grains. It is unknown at this time if those sulphide minerals were derived from deposits of the Pine Point district.

Indicator Minerals Recovered from Till Samples Compared to Bedrock Grains

Sphalerite and galena grains recovered from till samples have a composition similar to the grains recovered from bedrock samples. Sphalerite grains recovered from till samples have lower concentrations of As, Ag, Cd, In, Sb, Pb, Cu, and Hg than those from bedrock samples. Galena grains recovered from till samples were depleted in Fe, Zn, Ge, As, In, Sb, Cu, and Hg, and enriched in Cd in comparison to galena grains from bedrock samples. Some of these elements show an enrichment in the till matrix geochemistry, possibly from matrix/grain interaction.

CONCLUSIONS

Minerals indicative of the presence of Pb-Zn mineralization in the Pine Point mining district include sphalerite, galena, pyrite, cerussite, and smithsonite. These indicator minerals, with the exception of cerussite and smithsonite, are detectable in surface till samples at least 700 m down-ice, to the west and northwest, of the O-28 deposit. This pattern suggests that sampling surface till in the eastern part of the district can be useful for detecting buried Pb-Zn mineralization. Collecting till samples at depth would be even more useful to detect the more proximal parts of glacial dispersal trains.

EMP data for sphalerite and galena in bedrock suggests a difference in trace element geochemistry across the five deposits in this study. Further investigation using LA-ICPMS is recommended to quantify these differences and to determine their validity.

The relationship between till matrix geochemistry and indicator minerals recovered from till is less obvious between Zn content and sphalerite grains than that of Pb content and galena grains. This difference is likely due to the differences in mineral hardness and the original size of the grains in the bedrock. The softness (H=2.5) and brittle cubic cleavage of galena, compared to sphalerite (H=3.5–4), means galena is more susceptible to crushing by glacial transport, allowing for galena grains to contribute to both indicator mineral counts (sand-sized grains) and till matrix geochemistry (silt+clay fraction). Sphalerite is more physically robust than galena; therefore the morphology of sphalerite grains may be useful for indicating relative glacial transport distances.

Till matrix geochemistry and indicator mineral concentrates recovered from till are both useful tools when exploring for MVT deposits in glaciated terrain. Indicator minerals were detectable in regional till samples that had above background concentrations of pathfinder elements, indicating that both indicator minerals and till geochemistry are measurable at a regional scale. Indicator mineral and till geochemical methods used to explore for MVT deposits each have their strengths and weaknesses. Using one in conjunction with the other will yield the best results.

AKNOWLEDGEMENTS

GSC funding for this project was provided under the Geo-mapping for Energy and Minerals Program (GEM 2008-2013), as part of the Tri-Territorial Indicator Mineral Project. Tamerlane Ventures Incorporated is thanked for providing access to confidential information and bedrock samples. Wolf Schliess (Tamerlane Ventures) provided aerial photographs and borehole information, and helped with till and bedrock sampling in 2010. Teck Resources Limited provided access to confidential geological information and financial support as part of a GEM NSERC-CRD. M. McCurdy and R. McNeil (GSC) are thanked for assisting with till sampling in 2010, J. Rice (Brock University) is thanked for field assistance in 2011. M. McCurdy (GSC) is acknowledged for a thorough editorial review of an earlier version of this report.

REFERENCES

Arne, D.C., Curtis, L.W., and Kissin, S.A., 1990. Internal zonation in a carbonate-hosted Zn-Pb-Ag deposit, Nanisivik, Baffin Island, Canada; Economic Geology, v. 86, p. 699–717.

Averill, S.A., 2001. The application of heavy indicator minerals in mineral exploration. *In* Drift Exploration in Glaciated Terrain, (eds.) M.B. McClenaghan, P.T. Bobrowsky, G.E.M. Hall, and S.J. Cook; Geological Society of London, Special Publication 185, p. 69–82.

Brabec, D., 1983. Evaluation of soil anomalies by discriminant analysis in geochemical exploration for carbonate-hosted lead-zinc deposits; Economic Geology, v. 78, p. 333–339.

Campbell, N., 1966. The lead-zinc deposits of Pine Point; Canadian Mining and Metallurgical Bulletin, v. 59, p. 953–960.

Dyke, A.S., 2004. An outline of North American deglaciation with emphasis on central and northern Canada, *In* Quaternary Glaciations - Extent and Chronology, Part II. North America, (eds.) J. Ehlers and P.L. Gibbard; Elsevier, Amsterdam, Development in Quaternary Science Series, v. 2, p. 373–424.

Dyke, A.S. and Prest, V.K., 1987. Late Wisconsin and Holocene history of the Laurentide Ice Sheet; Géographie physique et Quaternaire, v. 41, p. 237–263.

Eaton, D.W. and Hope, J., 2003. Structure of the crust and upper mantle of the Great Slave Lake shear zone, northwestern Canada, from teleseismic analysis and gravity modeling; Canadian Journal of Earth Sciences, v. 40, p. 1203–1218.

Hannigan, P.K., 2006. Introduction, *In* Potential for Carbonate-hosted Lead-zinc Mississippi Valley-type Mineralization in Northern Alberta and Southern Northwest Territories: Geoscience Contributions, Targeted Geoscience Initiative, (ed.) P.K. Hannigan; Geological Survey of Canada, Bulletin 591, p. 9–39.

Hannigan, P., 2007. Metallogeny of the Pine Point Mississippi Valley-type zinc-lead district, southern Northwest Territories, *In* Mineral Deposits of Canada: A Synthesis of Major Deposit Types, District Metallogeny, the Evolution of Geological Provinces, and Exploration Methods, (ed.) W.D. Goodfellow; Geological Association of Canada, Mineral Deposits Division, Special Publication No. 5, p. 609–632.

Hannon, P.J., Roy, W.D., Flint, I.M., and Ernst, B.E., 2012. Technical report on the R190, X-25, P-499, O-556, Z-155 and G-03 deposits of the Pine Point project for Tamerlane Ventures Incorporated; MineTech International Limited, Halifax, 160 p.

Holroyd, R.W., Hodson, T.W., and Carter, K.M., 1988. Unpublished termination report; Pine Point Mines Ltd., June 28, 1988.

Kyle, J.R., 1977. Development of sulphide hosting structures and mineralization, Pine Point, Northwest Territories; Ph.D. thesis, University of Western Ontario, London, Ontario, 226 p.

Kyle, J.R., 1981. Geology of the Pine Point lead-zinc district, *In* Handbook of Strata-bound and Stratiform Ore Deposits, (ed.) K.H. Wolf; Elsevier Publishing Company, New York, v. 9, p. 643–741.

Lemmen, D.S., 1990. Surficial materials associated with glacial Lake McConnell, southern District of Mackenzie, *In* Current Research, Part D; Geological Survey of Canada, Paper 90-1D, p. 79–83.

Lemmen, D.S., 1998a. Surficial geology, Klewi River, District of Mackenzie; Northwest Territories; Geological Survey of Canada, "A" Series Map 1905, scale 1: 250 000.

Lemmen, D.S., 1998b. Surficial geology, Buffalo Lake, District of Mackenzie; Northwest Territories; Geological Survey of Canada, "A" Series Map 1906, scale 1:250 000.

Lemmen, D.S., Duk-Rodkin, A., and Bednarski, J.M., 1994. Late glacial drainage systems along the northwestern margin of the Laurentide Ice Sheet; Quaternary Science Reviews, v. 13, p. 805–828.

Macqueen, R.W. and Ghent, E.D., 1975. Occurrence of zinc in Devonian metalliferous shales, Pine Point region, District of Mackenzie; Geological Survey of Canada, Paper 75-1B, p. 53–57.

McClenaghan, M.B., 2005. Indicator mineral methods in mineral exploration; Geochemistry: Exploration, Environment, Analysis, v. 5, p. 233–245.

McClenaghan, M.B., Oviatt, N.M., Averill, S.A., Paulen, R.C., Gleeson, S.A., McNeil, R.J., McCurdy, M.W., Paradis, S., and Rice, J.M., 2012a. Indicator mineral abundance data for bedrock, till and stream sediment samples from the Pine Point Mississippi Valley-Type Zn-Pb deposits, Northwest Territories; Geological Survey of Canada, Open File 7267. doi:10.4095/292121

McClenaghan, M.B., Budulan, G., Averill, S.A., Layton-Matthews, D., and Parkhill, M.A., 2012b. Indicator mineral abundance data for bedrock and till samples from the Halfmile Lake Zn-Pb-Cu volcanogenic massive sulphide deposit, Bathurst Mining Camp, New Brunswick; Geological Survey of Canada, Open File 7076. doi:10.4095/291437

Morrow, D.W., MacLean, B.C., Miles, W.F., Tzeng, P., and Pana, D., 2006. Subsurface structures in southern Northwest Territories and northern Alberta: implications for mineral and petroleum potential, *In* Potential for Carbonate-Hosted Lead-Zinc Mississippi Valley Type Mineralization in Northern Alberta and Southern Northwest Territories, (ed.) P.K. Hannigan; Geoscience Contributions, Targeted Geoscience Initiative, Geological Survey of Canada, Bulletin 591 p. 41–59.

Nelson, J., Paradis, S., Christensen, J., and Gabites, J., 2002. Canadian Cordilleran Mississippi Valley-type deposits: A case for Devonian-Mississippian back-arc hydrothermal origin; Economic Geology, v. 97, p. 1013–1036.

Okulitch, A.V. (compiler), 2006. Phanerozoic bedrock geology, Slave River, District of Mackenzie, Northwest Territories; Geological Survey of Canada, Open File 5281.

Olson, R.A., 1977. Geology and genesis of zinc-lead deposits within a late Proterozoic dolomite, northern Baffin Island, N.W.T.; Ph.D. thesis, University of British Columbia, Vancouver, British Columbia.

Oviatt, N.M. and Paulen, R.C. 2013. Surficial geology, Breynat Point NTS 85-B/15, Northwest Territories; Geological Survey of Canada, Canadian Geoscience Map 114 (preliminary), scale 1:50,000.

Oviatt, N.M., McClenaghan, M.B., Paulen, R.C., and Gleeson, S.A., 2013. Till geochemical signatures of the Pine Point Pb-Zn Mississippi Valley type district, Northwest Territories; Geological Survey of Canada, Open File 7320.

Paradis, S., Turner, W.A., Coniglio, M., Wilson, N., and Nelson, J.L., 2006. Stable and Radiogenic isotopic signatures of mineralized Devonian carbonate rocks of the northern Rocky Mountain and WCSB, *In* Potential for Carbonate-Hosted Lead-Zinc Mississippi Valley-Type Mineralization in Northern Alberta and Southern Northwest Territories, (ed.) P.K. Hannigan; Geoscience Contributions, Targeted Geoscience Initiative, Geological Survey of Canada, Bulletin 591, p. 75–103.

Paulen, R.C., Paradis, S., Plouffe, A., and Smith, I.R., 2009. Base metal exploration with indicator minerals in glacial sediments of northwest Alberta, Canada, *In* Proceedings of the 24th International Applied Geochemistry Symposium (IAGS), (eds.) D.R. Lentz, K.G. Thorne, and K.L. Beal; Fredericton, New Brunswick, v. 2, p. 557–560.

Paulen, R.C., Paradis, S., Plouffe, A., and Smith, I.R., 2011. Pb and S isotopic composition of indicator minerals in glacial sediments from NW Alberta, Canada: implications for Zn-Pb base metal exploration; Geochemistry: Exploration, Environment, Analysis, v. 11, p. 309–320.

Plouffe, A., Paulen, R.C., and Smith, I.R., 2006. Indicator mineral content and geochemistry of glacial sediments from northwest Alberta (NTS 84L, M): new opportunities for mineral exploration; Geological Survey of Canada, Open File 5121.

Plouffe, A., Paulen, R.C., Smith, I.R., and Kjarsgaard, I.M. 2007. Chemistry of kimberlite indicator minerals and sphalerite derived from glacial sediments of northwest Alberta. Alberta Energy and Utilities Board, Alberta Geological Survey, Special Report 87, Geological Survey of Canada, Open File 5545.

Plouffe, A., McClenaghan, M.B., Paulen, R.C., McMartin, I., Campbell, J.E., and Spirito, W.A., in press. Processing of unconsolidated glacial sediments for the recovery of indicator minerals: protocols used at the Geological Survey of Canada; Geochemistry: Exploration, Environment, Analysis.

Prest, V.K., Grant, D.R., and Rampton, V.N., 1968. Glacial map of Canada; Geological Survey of Canada, "A" Series Map 1253.

Rice, J.M., Paulen, R.C., Menzies, J.M., McClenaghan, M.B., and Oviatt, N.M., 2013. Glacial stratigraphy of the Pine Point Pb-Zn mine site, Northwest Territories; Geological Survey of Canada, Current Research 2013-5, 14 p. doi:104095/292184

Rhodes, D., Lantos, E.A., Lantos, J.A., Webb, R.J., and Owens, D.C., 1984. Pine Point orebodies and their relationship to the stratigraphy, structure, dolomitization, and karstification of the middle Devonian Barrier complex; Economic Geology, v. 79, p. 991–1055.

Sangster, D.F., 2002. MVT deposits of the world; database documentation of the World Minerals Geoscience Database Project, http://www.nrcan.gc.ca/gsc/mrd/wmgdb/index_e.php

Skall, H., 1975. The paleoenvironment of the Pine Point lead-zinc district.;Economic Geology, v. 70, p. 22–47.

Skall, H., 1977. The geology of the Pine Point barrier reef complex, *In* The Geology of Selected Carbonate Oil, Gas and Lead-zinc Reservoirs in Western Canada, (eds.) I.A. McIlreath and R.D. Harrison; Canadian Society of Petroleum Geologists, Core Conference, no. 5, p. 19–38.

Smith, D.G., 1994. Glacial Lake McConnell: paleogeography, age, duration and associated river deltas, Mackenzie River basin, western Canada; Quaternary Science Reviews, v. 13, p. 829–843.

Stothart, P., 2011. "The Mining Association of Canada." 2011 Facts and Figures. http://www.miningnorth.com/wp-content/uploads/2012/04/MAC-FactsFigures-2011-English-small.pdf, accessed 15 March 2013.

Watson, D.M., 2010. Sambaa K'e Candidate Protected Area Phase II non-renewable resource assessment – Minerals, Northwest Territories, Parts of NTS 085D, 095A, B, H; Northwest Territories Geoscience Office, Open File 2010-08.

Watson, D.M., 2011. Ka'a'gee Te Area of Interest, Phase II Non-renewable Resource Assessment – Minerals, Northwest Territories, Parts of NTS 85C, 85D, 85E and 85F; Northwest Territories Geoscience Office, NWT Open File 2011-01.

Wilson, R.A., 2007. Bedrock geology of the Nepisiguit Lakes area (NTS 21O/7), Restigouche and Northumberland counties, New Brunswick.;New Brunswick Department of Natural Resources, Minerals, Policy and Planning Division, Plate 2007-32.

Wolfe, S.A., Huntley, D.J., and Ollerhead, J., 2005. Relict Late Wisconsinan dune fields of the northern Great Plains, Canada; Géographie physique et Quaternaire, v. 58, p. 323–336.

Wolfe, S.A., Paulen, R.C., Smith, I.R., and Lamothe, M., 2007. Age and paleoenvironmental significance of Late Wisconsinan dune fields in the Mount Watt (84-K) and Fontas River (94-I) map sheets, northern Alberta and British Columbia; Geological Survey of Canada, Current Research 2007-B4, 10 p.

Appendix A2. Colour photographs of hand specimens and petrographic descriptions of bedrock samples used in this study.

Sample 10-MPB-R01

Deposit: R190

Hand Sample

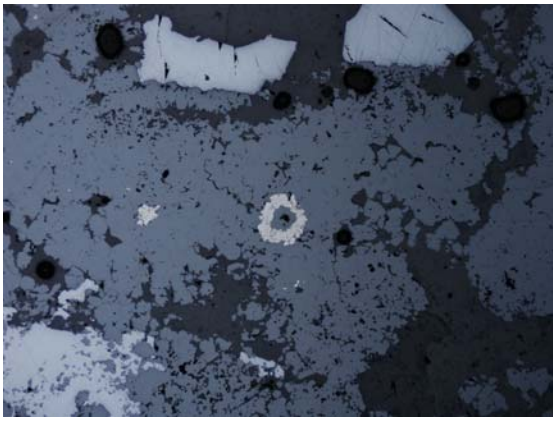

Thin Section: Pyrite ring in sphalerite host. Field of view is 4 mm.

Galena and sphalerite dissolution boundary. Sphalerite has been replaced by galena. Field of view is 4 mm.

Hand Sample:
Galena cubes (0.3 cm) are replacing calcite (0.3 cm); galena also replaces brown carbonaceous materal. Native sulphur occurs in calcite unit.

Thin Section:
Sphalerite and galena are interfingering. Large galena grains are up to 1 cm and subhedral. Sphalerite grains are light coloured, subhedral, and are up to 250 µm. Dolomite grains are sub- to anhedral and range in size from 250 to 500 µm; boundaries of these grains have been dissolved by sulphides. Some galena grains have curved faces. Pyrite occurs between sphalerite grains 100 µm. Sphalerite grains range from 50 to 500 µm. Honey brown sphalerite average 750 µm and have Fe-rich core. Late-stage calcite has filled remaining voids.

Modal Distribution:
Sphalerite: 35%
Galena: 40%
Pyrite: trace
Gangue: 25%

Appendix A2 continued.

Sample 10-MPB-R02

Deposit: R190

Hand Sample

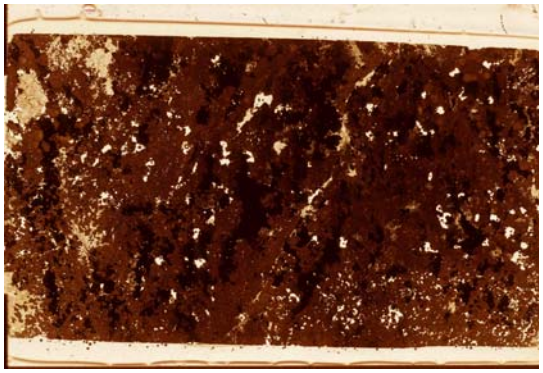

Thin Section: Red has been enhanced to define sphalerite.

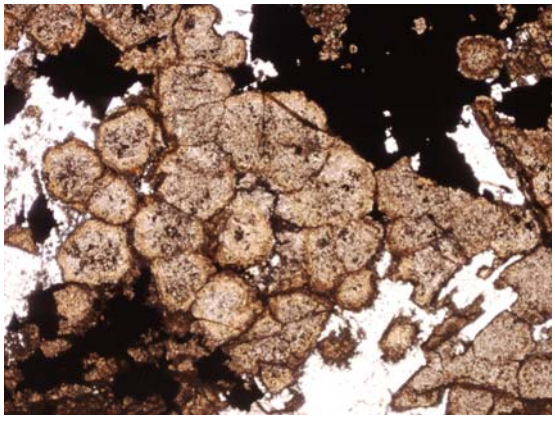

Honey-brown sphalerite crystals.

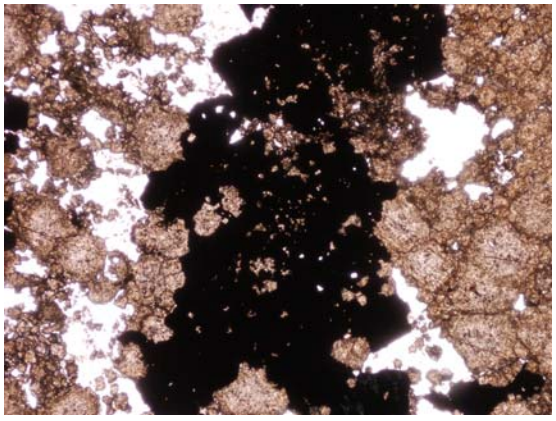

Honey-brown sphalerite crystals contained in galena crystal.

Hand Sample:
This sample was collected in the massive sulphide zone. Sphalerite is abundant, occurring as honey brown and botryodial. Galena occurs throughout the sample as 0.1 cm crystals. Sulphur occurs as small anhedral crystals. Calcite occurs as isolated, approximately 0.2 cm, vug-filling crystals.

Thin Section:
Sphalerite (50%) occurs as dodecahedron crystals that are 100–500 μm across. These grains are smaller in the vicinity of galena crystals. Some grains are zoned and occur together in all sizes. Galena (35%) is anhedral, and occurs in patches of 2 mm or less. Some galena has sphalerite inclusions. Galena and sphalerite both have voids (unfilled). Calcite (15%) is almost completely replaced; a few isolated grains, approximately 500 μm in size, occur throughout the sample. Pyrite occurs in trace amounts.

Modal Distribution:
Sphalerite: 50%
Galena: 35%
Pyrite: trace
Gangue: 15%

Appendix A2 continued.

Sample 10-MPB-R03

Deposit: R190

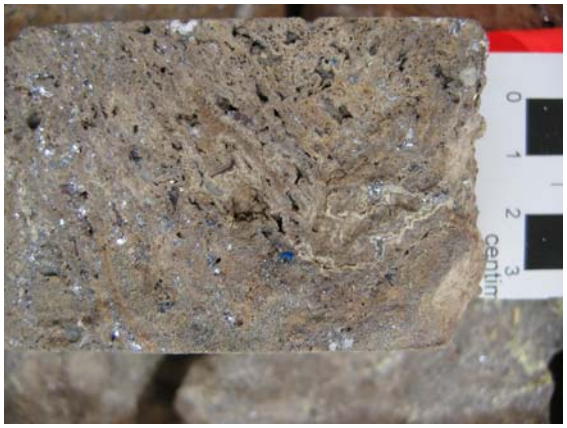

Hand Sample

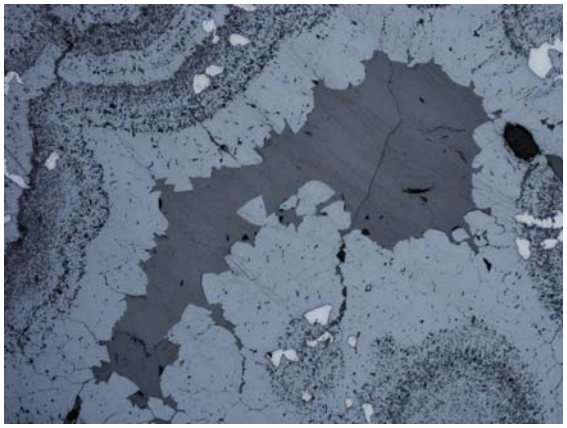

Thin Section: Galena fragments within sphalerite botryoids.

Hand Sample:
Blackjack sphalerite (<0.1 cm) rims vugs. Sulphur crystals (0.3 cm) comprises approximately 5% of the rock, galena approximately 20%, and sphalerite approximately 75%. Sphalerite occurs as dark brown and bulbous (0.2 cm) lined with small blackjack crystals. Galena content may be higher than 20%. Minor traces (approximately 5%) of host dolomite.

Thin Section:
There is almost complete replacement by sulphides. Galena fills void space that is lined with sphalerite. Some sphalerite crystals are zoned. Botryodial sphalerite is controlling galena. Skeletal galena crystals are up to 400 µm. The vugs are filled with euhedral calcite crystals 500 by 1000 µm. Galena is anhedral. Heavily dissolved calcite crystals (100–500 µm) with sphalerite. Well defined vugs (clasts?), which are only slightly altered on some edges, are filled with calcite crystals that range in size from 250 to 1000 µm. Sphalerite grows outwards from these. Some vugs are filled with galena, some calcite only, some are void, and some are a combination of all. Galena fragments (100 µm) are located in both botryoidal and blackjack sphalerite. Blackjack crystals range from 25 to 250 µm, depending on the size of the vug and form an isopachous crust. Galena fill has curved faces and sphalerite is penetrating along planes of weakness. Trace of pyrite cubes (100 µm).

Modal Distribution:
Sphalerite: 75%
Galena: 10%
Pyrite: trace
Gangue: 15%

Appendix A2 continued.

Sample 10-MPB-R04

Deposit: R190

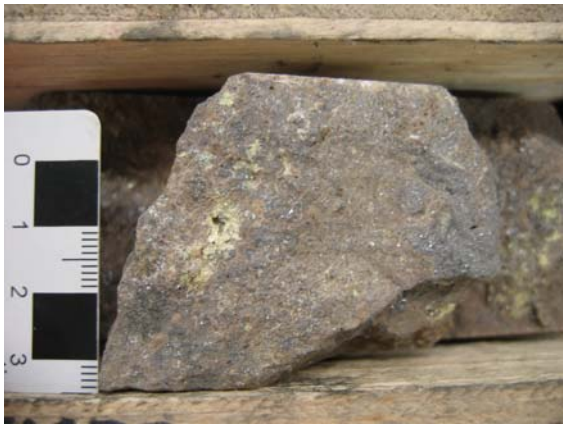

Hand Sample

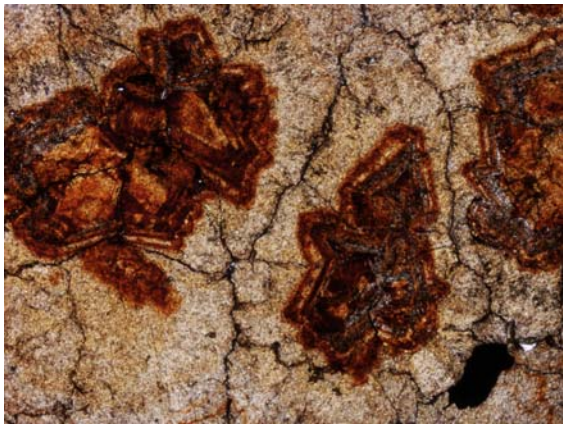

Thin Section: Zoned sphalerite crystals.

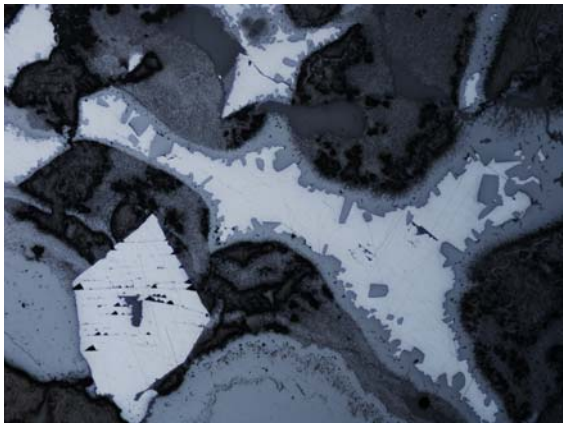

Vug filled with galena and lined with sphalerite crystals.

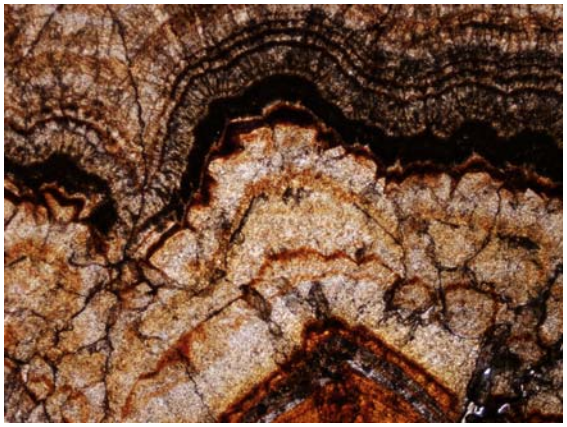

Zoned sphalerite crystals intersecting with colloform sphalerite.

Hand Sample:
Total replacement by sulphides, native sulphur fills vugs, and pores. Sulphides are galena (0.2 cm), mostly sphalerite (blackjack (0.1 cm)) and botryoidal (finely banded 0.1 cm).

Thin Section:
Sulphur fills cracks and voids; vugs are lined with fine-grained sphalerite (100 μm) and filled with galena. Colloform sphalerite has Fe-rich layers, which are up 1000 μm thick; transverse sphalerite is 1000 by 1500 μm. Colloform sphalerite with interstitial galena and sulphur. Some skeletal galena occurs within colloform sphalerite.

Modal Distribution:
Sphalerite: 75%
Galena: 10%
Pyrite: 5%
Sulphur: 10%

Appendix A2 continued.

Sample 10-MPB-R06

Deposit: R190

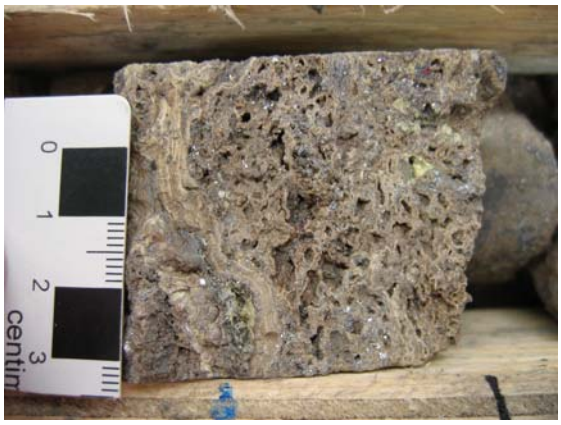

Hand Sample

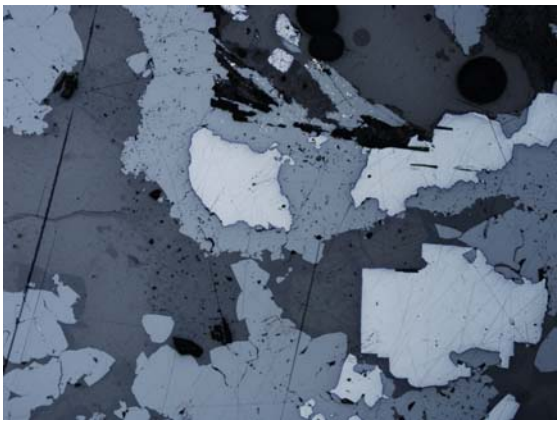

Thin Section: Botryoidal sphalerite crystals have replaced galena.

Chalcopyrite grain in sphalerite crystals.

Hand Sample:
Total replacement by sulphides. Sulphur and blackjack sphalerite (<0.1 cm) line vugs. Galena is 0.1 cm or less. Thin layers of botryoidal sphalerite. Sucrosic and very vuggy.

Thin Section:
Galena has been dissolved by pyrite and unknown (pyrite). Isolated patches of pyrite (10 μm) occur in sphalerite grains. Galena occurs as anhedral to subhedral crystals of up to 1000 μm. Sulphur crystals are void-filling and range in size from 1500 to 5000 μm. Some voids are filled with dolomite/calcite, with sweeping extinction. Fe-rich layers snake through the sample; isopachous crust is formed from 100 μm crystals. Galena is also void-filling (2500–1000 μm). Sulphur grains are 500 to 1000 μm. Colloform sphalerite layers are up to 100 μm but usually less than 50 μm. Isolated sphalerite grains occur throughout and are 500 μm. Traces of possible chalcopyrite

Modal Distribution:
Sphalerite: 80%
Galena: 10%
Pyrite: trace
Sulphur: 5%
Gangue: 5%

Appendix A2 continued.

Sample 10-MPB-R07

Deposit: R190

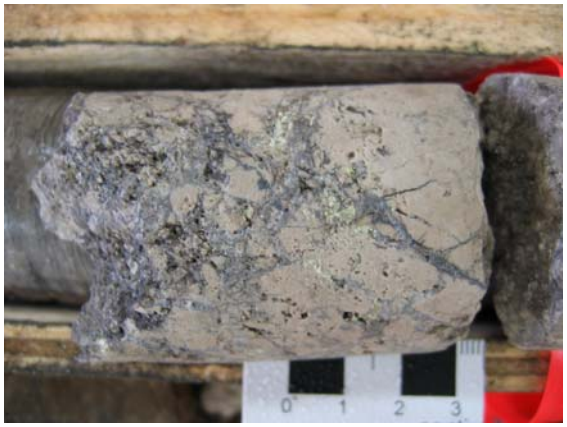

Hand Sample

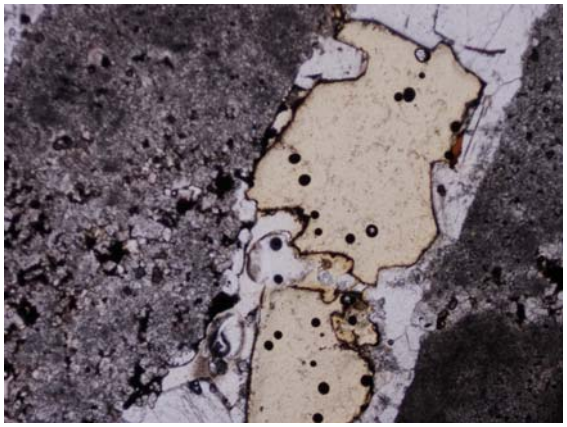

Thin Section: Native sulphur crystal in calcite vein.

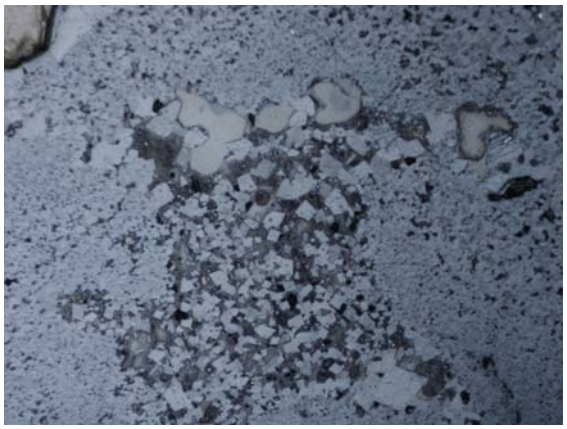

Rhombic dolomite crystals.

Hand Sample:
Brecciated cracks and fractures filled with sulphur and dark sphalerite. Clasts are buff-brown dolomite.

Thin Section:
Dolomite rhombs are 25 μm, occur within sphalerite and are surrounded by sulphur. Calcite veins contain sulphur (500 μm). Calcite crystals are 750 μm. Small amounts of sphalerite are fine grained (50–100 μm). Possible trace amounts of galena and pyrite. Dirty dolomite contains sphalerite, which are equigranular. Some Fe-rich sphalerite has filled voids and fractures that are associated with rhombic dolomite. Trace pyrite (10 μm) occurs in sphalerite.

Modal Distribution:
Sphalerite: 25%
Galena: trace
Pyrite: trace
Sulphur: 20%
Gangue: 55%

Appendix A2 continued.

Sample 10-MPB-R08

Deposit: R190

Hand Sample

Thin Section: Bitumen (?) in thin section. Field of view is 4 mm.

Sphalerite being replaced by saddle dolomite. Field of view is 4 mm.

Hand Sample:
Bitumen is present (20%). 'Dirty' calcite crystals are 0.2 to 0.3 cm. Very fine-grained mud (crystalline) may be a clay seam. Some vugs are filled with calcite spar. The whole sample appears to be brecciated.

Thin Section:
Mostly dolomite, rhombs are 750 µm. Saddle dolomite crystals are 3000 to 5000 µm. Isolated sphalerite crystals are 400 µm. A patch of very fine dolomite (50–100 µm) contains fragments of pyrite and sphalerite (50 µm). Unknown grain (bitumen?) is 1000 µm across.

Modal Distribution:
Sphalerite: 10%
Galena: trace
Pyrite: trace
Gangue: 90%

Appendix A2 continued.

Sample 10-MPB-R09

Deposit: R190

Hand Sample

Thin Section: Sphalerite fragments in a large galena crystal. Field of view is 4 mm.

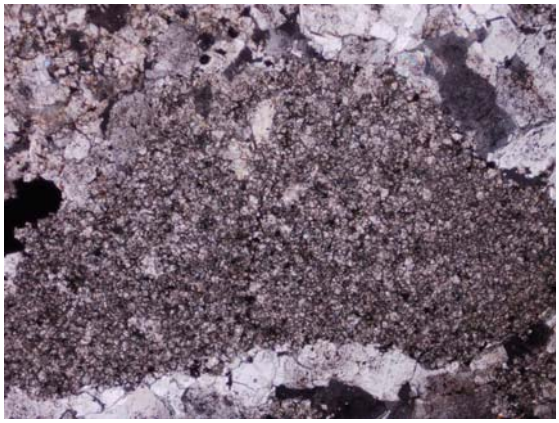

Dolomite rhombs filling a void. Possibly filling a mould left by a fossil. Field of view is 4 mm.

Hand Sample:
Galena crystals are very fine-grained (size cannot be determined with a hand lens), honey brown sphalerite crystals (0.1 cm) occur within galena and light grey dolomite; darker muddy unit is separated from grey/white dolomite by a fracture filled with galena. Possible fossils.

Thin Section:
Anhedral to subhedral galena grains (up to 1 cm), have dissolution pits that are filled with sphalerite. Isolated patches of fine-grained calcite (fossils ?) 2 mm across. These fragments occur within dirty dolomite of 150 to 300 μm. All dolomite has a reddish tinge (weathering of pyrite?), may be traces of sphalerite. Fragments of sphalerite (500 μm) and pyrite (10-25 μm) occur throughout dolomite; these fragments are all anhedral.

Modal Distribution:
Sphalerite: 5%
Galena: 15%
Pyrite: trace
Gangue: 80%

Appendix A2 continued.

Sample 10-MPSB-R11

Deposit: R190

Hand Sample

Thin Section: Galena precipitating along a fracture. Field of view is 4 mm.

Galena filling a vug. Field of view is 4 mm.

Hand Sample:
Sulphur (<0.1 cm), dark grey-blue dolomite, and vugs and fractures filled with sparry dolomite. This sample may contain bitumen.

Thin Section:
Anhedral galena grains (500 μm) occur in saddle dolomite, anhedral sphalerite grains, and possible presence of bitumen.

Modal Distribution:
Sphalerite: 25%
Galena: 5%
Gangue: 70%

Appendix A2 continued.

Sample 10-MPB-R15

Deposit: R190

Hand Sample

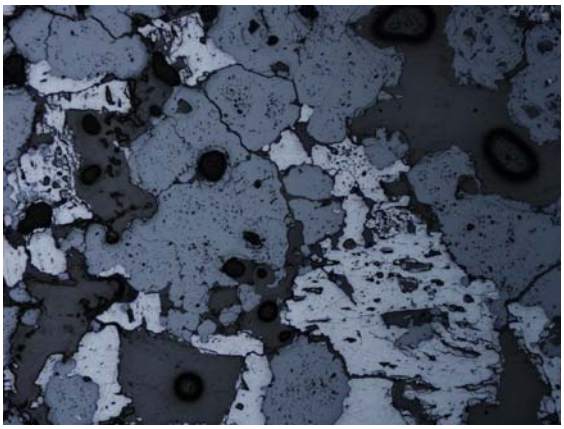

Thin Section: Anhedral sphalerite and galena. Field of view is 4 mm.

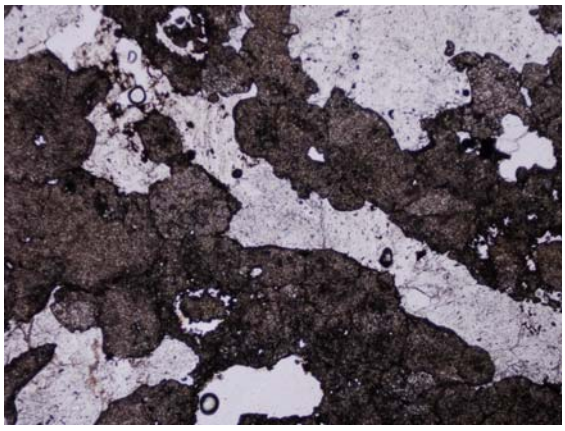

Calcite vein cross-cutting sphalerite. Field of view is 4 mm.

Hand Sample:
Sulphur crystals (~0.2 cm), galena (~0.1 cm avg), and sphalerite (average size <0.1 cm) occur in a dolomite matrix.

Thin Section:
Anhedral sphalerite and pyrite grains (50–100 μm) with trace amounts of subhedral galena (500 μm cubes). Sulphur lines and has filled some ~500 μm vugs. Sphalerite grains average 500 μm and are anhedral. These grains are cut by later calcite. Galena is heavily pitted and has filled the interstitial space between sphalerite grains. There is no pyrite where galena and sphalerite occur together.

Modal Distribution:
Sphalerite: 50%
Galena: 5%
Pyrite: 25%
Gangue: 20%

Appendix A2 continued.

Sample 10-MPB-R17

Deposit: R190

Hand Sample

Thin Section: Galena and sphalerite occuring together. Field of view is 4 mm.

Brecciated ore grains. Pyrite is replacing sphalerite and galena. Field of view is 4 mm.

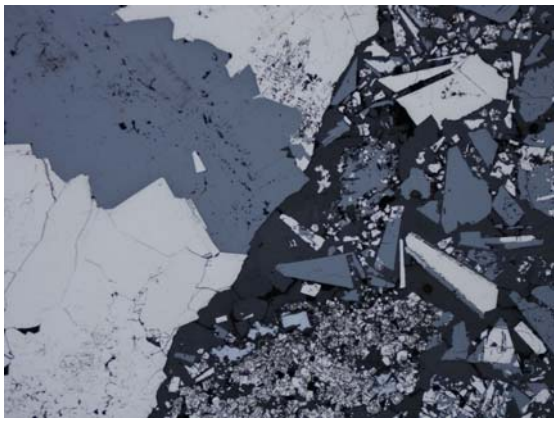

Brecciated ore grains. Field of view is 4 mm.

Hand Sample:
This sample is almost completely replaced by sulphides. Pyrite crystals are approximately 0.1 cm. Botryodial sphalerite and galena occur throughout sample.

Thin Section:
Brecciated pyrite, sphalerite, and galena. Pyrite crystals are approximately 1000 µm. Sphalerite crystals average 1500 µm, though some micro grains (10 µm) occur in patches that also contain 200 µm pyrite cubes. Most sphalerite grains are euhedral, contain pyrite crystals, and show zoning. Botryoidal sphalerite occurs throughout. Isolated crystals of sphalerite are approximately 0.5 cm. Pyrite is coated with botryodial sphalerite. Isolated patches of very fine-grained pyrite (~100 µm) occurs throughout sample. Trace amounts of galena occur as interfingering with pyrite on edge of large pyrite crystal. Pyrite has possibly replaced galena.

Modal Distribution:
Sphalerite: 40%
Galena: 5%
Pyrite: 45%
Gangue: 10%

Appendix A2 continued.

Sample 10-MPB-R19

Deposit: L65

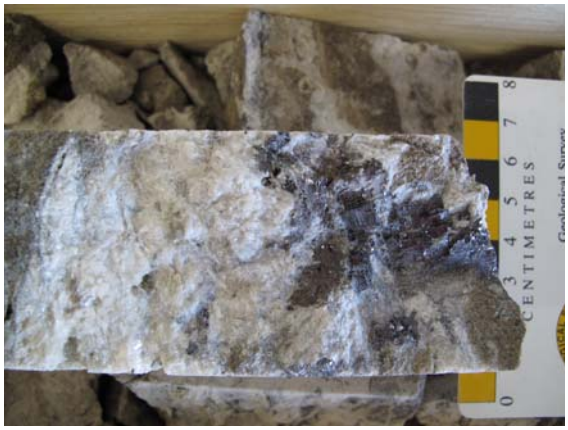

Hand Sample

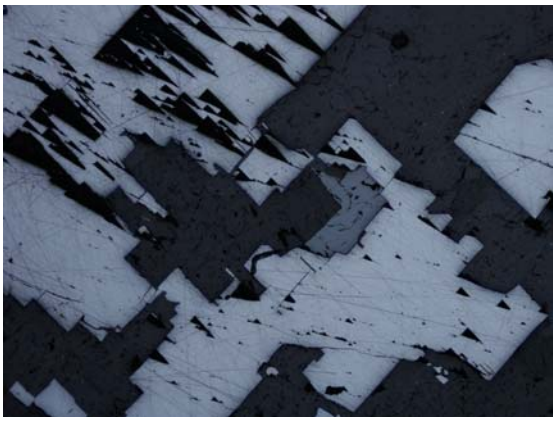

Thin Section: Cubic galena. Field of view is 4 mm.

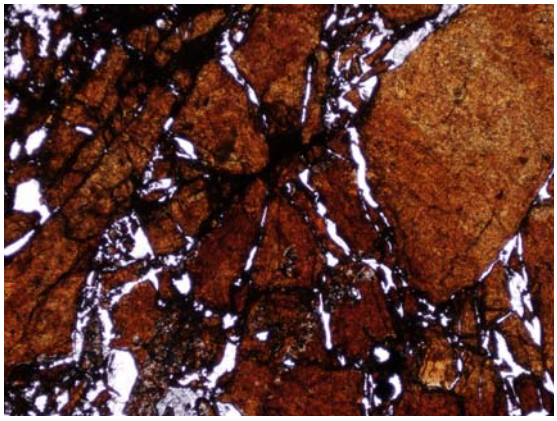

Brecciated sphalerite grains. Field of view is 4 mm.

Hand Sample:
Cubic galena (up to 1 cm) is concentrated in one area of the sample. A white dolomite encloses galena and sphalerite (0.2–0.3 cm). Grey dolomite reacts vigorously with HCl. A brown-buff coloured sandy matrix has a moderate reaction with HCl. These are possibly bioclasts. Blackjack sphalerite lines pore and vug spaces. Galena appears to fill some of the sphalerite-lined pores.

Thin Section:
Brecciated sphalerite (17%) occurs as angular, subhedral grains (250–500 μm). The interstitial space of these fragments is filled with gangue minerals. Galena (20%) occurs as 1 cm cubes, though some areas show brecciated fragments that are 250 μm. Fractures within galena are filled with calcite. Saddle dolomite penetrates sphalerite in some cases and crystals range from 500–3000 μm. Trace amounts of pyrite occur in gangue dolomite.

Modal Distribution:
Sphalerite: 15%
Galena: 20%
Pyrite: trace
Gangue: 65%

Appendix A2 continued.

Sample 10-MPB-R20

Deposit: L65

Hand Sample

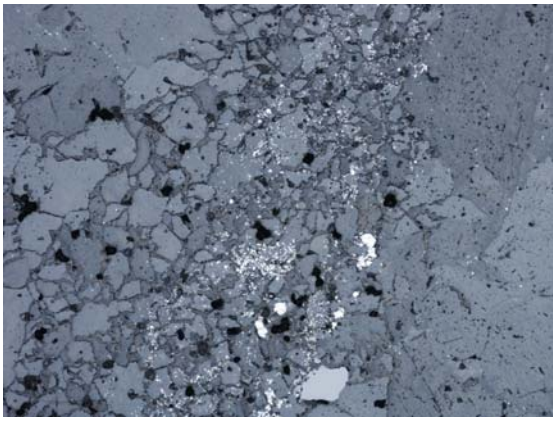

Thin Section: Disseminated pyrite grains in dolomite host. Fragments of galena and sphalerite also occur within interstitial matrix. Field of view is 4 mm.

Hand Sample:
White to grey limestone; isolated patches of sphalerite with white grey limestone intermixed. Sphalerite is hosted mostly in grey dolomite. Vugs filled with coarse calcite (0.3–0.4 cm). Sphalerite is 0.1 cm to finer. Paragenesis: grey dolomite, white dolomite, sphalerite, and calcite.

Thin Section:
Fine-grained pyrite (<10–100 μm) associated with brecciated sphalerite. Chalcopyrite disease in some sphalerite. Trace amounts of pyrite throughout dolomite (<10 μm). Minor fragments of interstitial galena. Some sphalerite crystals are zoned. Pyrite grains (<50 μm) occur in patches of fine-grained dolomite. Sphalerite grains occur in anhedral to subhedral forms, 1000 to 2000 μm.

Modal Distribution:
Sphalerite: 15%
Pyrite: 5%
Gangue: 80%

Appendix A2 continued.

Sample 10-MPB-R24

Deposit: L65

Hand Sample

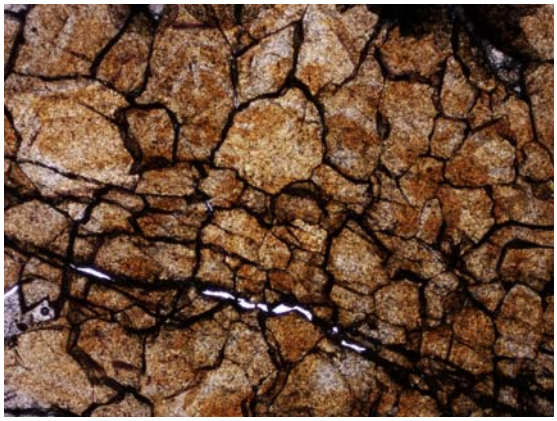

Thin Section: Crystals of honey-brown sphalerite with Fe zoning. Field of view is 4 mm.

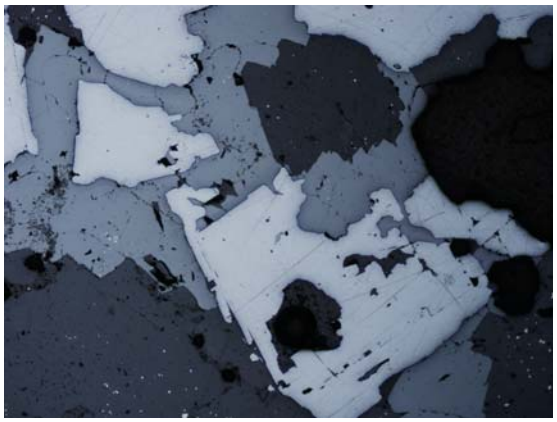

Cubic galena being replaced by sphalerite. Field of view is 4 mm.

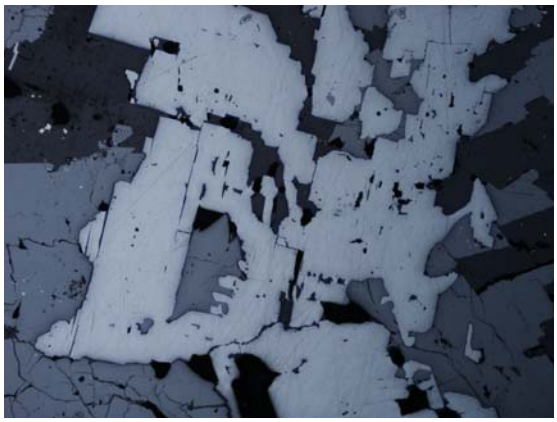

Cubic galena replacing sphalerite. Field of view is 4 mm.

Hand Sample:
Galena (0.1–0.2 cm), some sphalerite (honey-brown), blue-grey dolomite, disseminated galena, sphalerite occurs in a vein.

Thin Section:
Galena cubes, some exhibit curved faces and dissolved boundaries. Pyrite (10–25 μm) anhedral forms occur in finer grained dolomite. No pyrite occurs within the saddle dolomite. 'Dirty' dolomite that abuts sulphide layer contains abundant pyrite. This dirty dolomite also fills vugs that are within the sulphide layer. Honey-brown subhedral grains of sphalerite are 400 μm.

Modal Distribution:
Sphalerite: 20%
Galena: 20%
Pyrite: 10%
Gangue: 50%

Appendix A2 continued.

Sample 10-MPB-R25

Deposit: L65

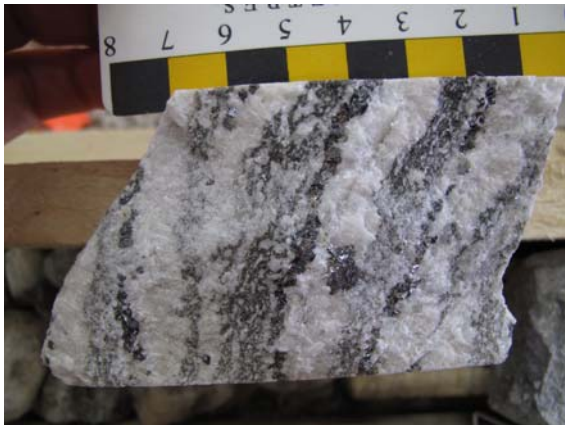

Hand Sample

Thin Section: Sphalerite fragments being replaced by dolomite. Field of view is 4 mm.

Hand Sample:
White dolomite, sparry, interbedded with fine-grained Watt Mountain Formation (?), alternating with coarser 0.1 to 0.2 cm sphalerite. Dolomite crystals are ~0.1 cm.

Thin Section:
Euhedral sphalerite grains, 2500 μm across, form two chains (discontinuous). Patches of sphalerite and pyrite (fragments are 50 μm) in dolomite. Coarser dolomite is 0.1 cm and does not contain sulphides. Euhedral grains are in clean dolomite. Some sphalerite grains (500 μm) are almost completely dissolved. Alternating layers of 'dirty' sphalerite and pyrite.

Modal Distribution:
Sphalerite: 20%
Pyrite: 5%
Gangue: 75%

Appendix A2 continued.

Sample 10-MPB-R26

Deposit: L65

Hand Sample

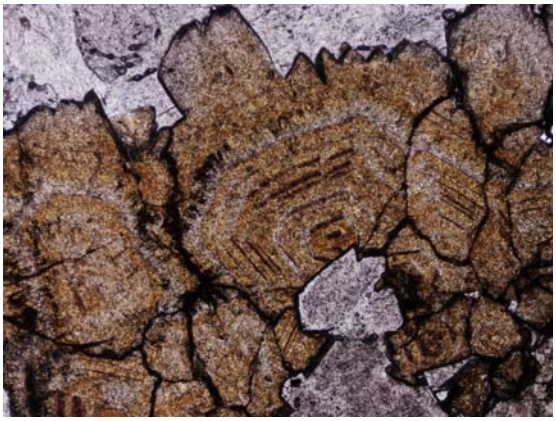

Thin Section: Honey-brown sphalerite crystals. Field of view is 4 mm.

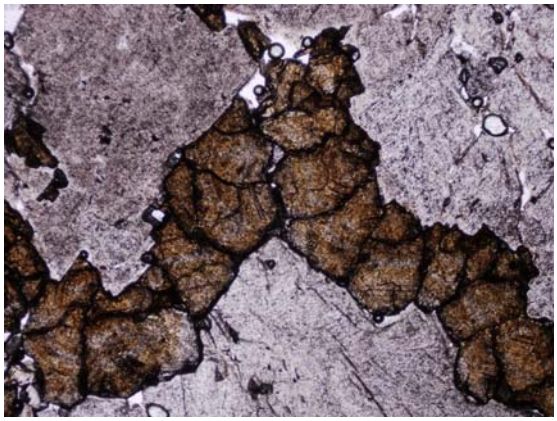

Honey-brown sphalerite crystals crosscutting saddle dolomite. Field of view is 4 mm.

Hand Sample:
Similar to 10-MPB-R25 with no colloform sphalerite. White dolomite, sparry, interbedded with fine-grained Watt Mountain Formation (?), alternating with coarser, 0.1 to 0.2 cm sphalerite. Dolomite crystals are approximately 0.1 cm.

Thin Section:
Honey-brown sphalerite forms lining on vugs that are cross-cut by a calcite vein. Very fine-grained (<10 μm) pyrite occurs within and surrounding sphalerite. Sub- to euhedral sphalerite grains fill voids (grains are up to 500 μm). Pyrite does not occur in saddle dolomite or late-stage calcite. Some sphalerite grains are zoned and are up to 1000 μm. Isolated clusters of sphalerite grains occur.

Modal Distribution:
Sphalerite: 25%
Pyrite: 5%
Gangue: 70%

Appendix A2 continued.

Sample 10-MPB-R27

Deposit: L65

Hand Sample

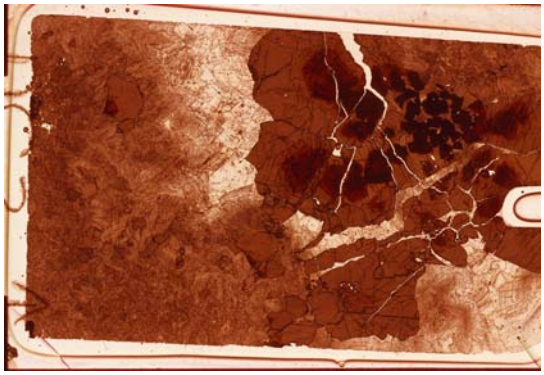

Thin section: Honey-brown sphalerite with dark Fe-rich cores. Red colour has been enhanced to define sphalerite cores. Field of view is 4 mm.

Hand Sample:
Zoned, honey-brown , 0.2 to 0.3 cm sphalerite crystals; very fine-grained white drusy calcite, and coarse (0.5 cm) calcite crystals. Buff-brown sandy material present in isolated patches; sparry white dolomite that includes light blue-grey dolomite. Sphalerite is contained in blue-grey dolomite

Thin Section:
Sphalerite: isolated grains (500+ μm) occur in calcite, subhedral grains, which are brown-red in plain polarized light. The largest grain is 7 mm; grains occur in clusters up to 1 cm across. Some isolated crystals are euhedral. Fe-rich sphalerite (dark red) has very ragged edges, and occurs as grains up to 2 mm. Trace amounts of galena are associated with darker sphalerite grains, as well as trace amounts of pyrite (25 μm). Gangue minerals are coarse calcite, saddle dolomite, and dolomite.

Modal Distribution:
Sphalerite: 50%
Galena: trace
Pyrite: trace
Gangue: 50%

Appendix A2 continued.

Sample 10-MPB-R28

Deposit: L65

Hand Sample

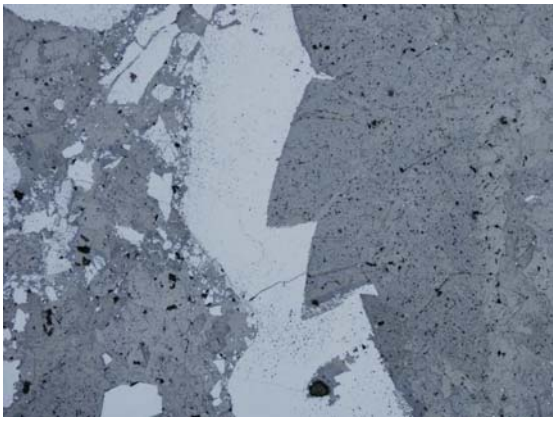

Thin Section: Saddle dolomite crystals cutting into botryoidal sphalerite. Field of view is 4 mm.

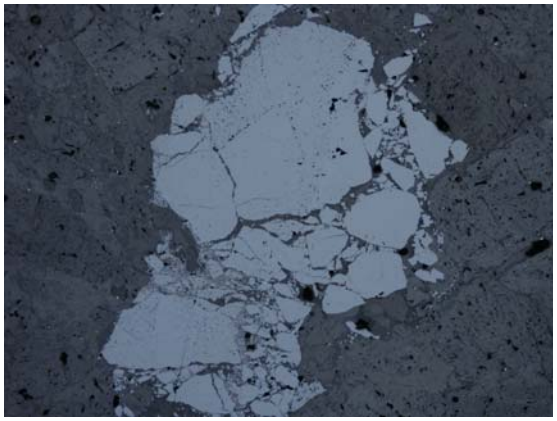

Brecciated sphalerite crystals. Field of view is 4 mm.

Hand Sample:
Sucrosic dolomite, and dark grey dolomite occur throughout sample. Vugs are lined with calcite crystals (0.2–0.5 cm), thin botryoidal (1–2 mm) layers of sphalerite. Sphalerite is contained in blue-grey dolomite.

Thin Section:
Saddle dolomite cuts into cleiophane sphalerite. Three types of sphalerite are contained in this sample: blackjack, cleiophane, and dark brown. Galena occurs as tiny blebs (20 μm). Some sphalerite is brecciated and ragged. Some sphalerite is zoned: very dark to light yellow crystals. Dolomite grains range from 100 to 1000 μm. Trace amounts of pyrite are associated with dolomite grains.

Modal Distribution:
Sphalerite: 20%
Galena: trace
Pyrite: trace
Gangue: 80%

Appendix A2 continued.

Sample 10-MPB-R30

Deposit: L65

Hand Sample

Thin Section: Calcite filled fracture cross-cutting colloform sphalerite. Field of view is 4 mm.

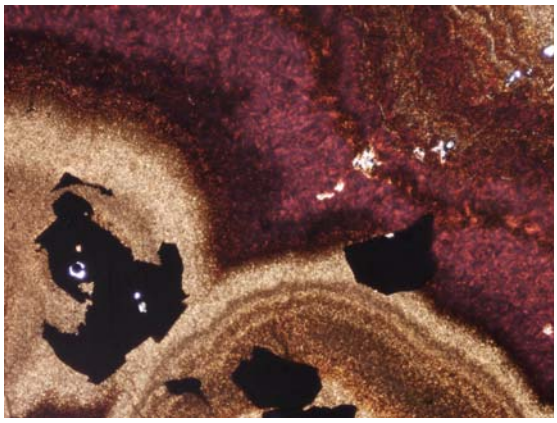

Galena crystals cross-cutting botryoidal sphalerite. Field of view is 4 mm.

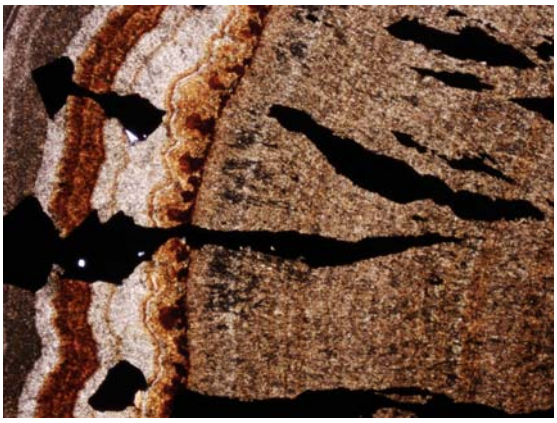

Skeletal galena crystals cross-cutting botryoidal sphalerite. Field of view is 4 mm.

Hand Sample:
Sphalerite is botryoidal with light and dark bands coating massive (2–3 cm) blackjack masses. Coarse calcite fills fractures between sphalerite. Sphalerite has very fine laminations.

Thin Section:
Sphalerite occurs as vug-filling colloform bands that are heavily zoned. The vugs range is size up to 3 cm. Sphalerite grains in the large vugs are fractured into 3000 µm bits. Layered sphalerite occurs as colloform bands that are continuous around a point. The layers range from 750 to 1000 µm thick and terminate in very light-coloured sphalerite. Skeletal galena occurs within in the zoned sphalerite, radiating outward from the centre but is void in the outer rims. The galena grains are sub- to anhedral and range from 100 to 50 µm. Dolomite occurs as large (3000 µm), subhedral, uniform extinction grains.

Modal Distribution:
Sphalerite: 60%
Galena: 10%
Pyrite: trace
Gangue: 30%

Appendix A2 continued.

Sample 10-MPB-R31

Deposit: L65

Hand Sample

Thin Section: Skeletal galena within sphalerite crystals. Field of view is 4 mm.

Hand Sample:
Galena cubes (0.2 cm) with botryoidal sphalerite (fans up to 2 cm across). Fine-grained calcite (dolomite?) cuts sphalerite. Galena occurs on edges of the fans with fine fingers protruding into the sphalerite. Coarse calcite fills 0.3–0.4 cmvugs.

Thin Section:
Two phases of galena: cubic and skeletal. Cubic galena crystals are 3000 μm. Cleiophane sphalerite occurs within colloform bands. Skeletal galena is 500 μm across. Coarse calcite (3000 μm) fills interstitial space.

Modal Distribution:
Sphalerite: 55%
Galena: 15%
Gangue: 30%

Appendix A2 continued.

Sample 10-MPB-R32

Deposit: L65

Hand Sample

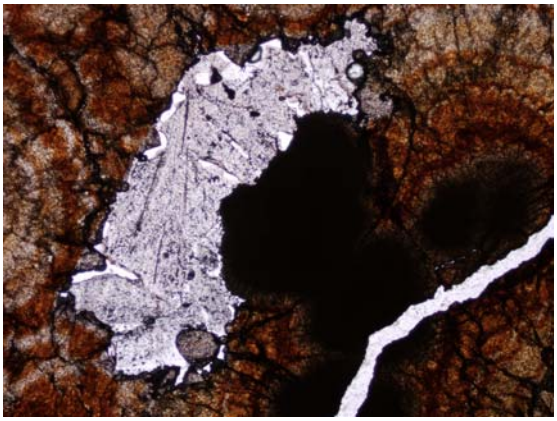

Thin Section: Calcite partially replacing the core of botryoidal sphalerite. Field of view is 4 mm.

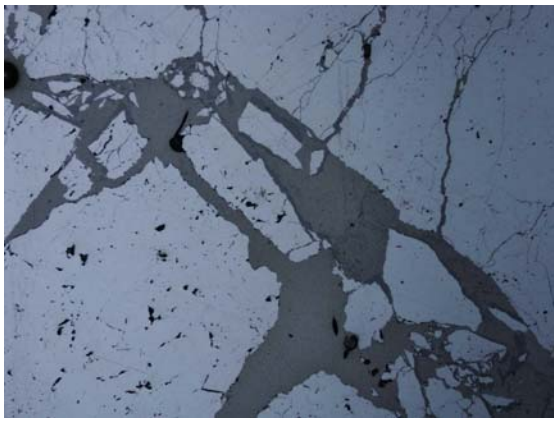

Brecciated fragments of sphalerite in calcite. Field of view is 4 mm.

Hand Sample:
Calcite replacing sphalerite; average grain size for both is 0.1 cm. Vugs are filled with coarse calcite (0.3 cm crystals). Trace amounts of galena are present.

Thin Section:
Colloform sphalerite forms transverse sections that are 0.75 cm across. Brecciated sphalerite fragments fill space between the colloform sphalerite; the fragments range in size from 25 to 500 µm. Isolated patches of subhedral grains occur that are 1000 µm across. Colloform sphalerite has dark red (Fe-rich) cores. Colloform sphalerite occurs in clusters and is cut by late-stage calcite/dolomite.

Modal Distribution:
Sphalerite: 25%
Galena: 10%
Pyrite: trace
Gangue: 65%

Appendix A2 continued.

Sample 10-MPB-R35

Deposit: HZ

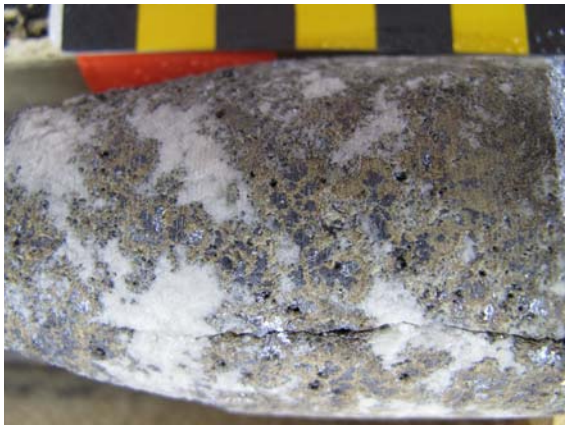

Hand Sample

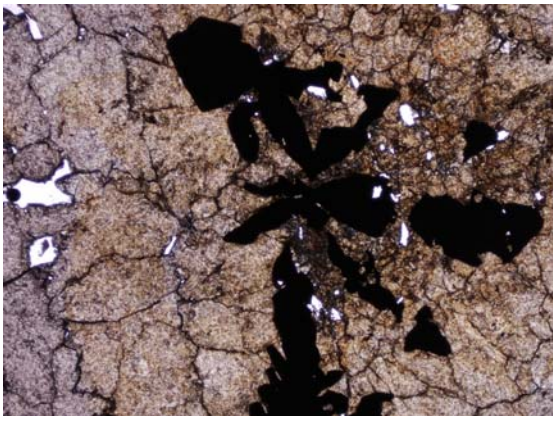

Thin Section: Sphalerite crystals containing dendritic galena. Field of view is 4 mm.

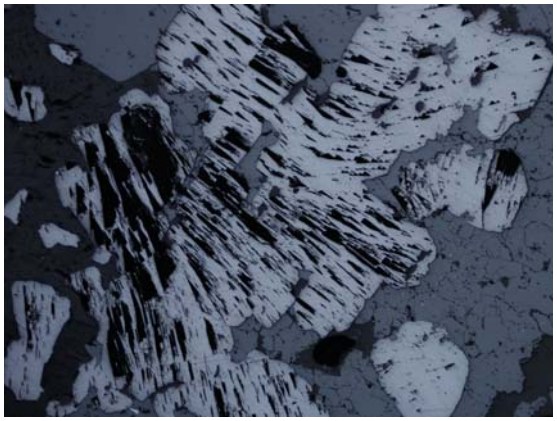

Galena crystal with some curved crystal faces. Field of view is 4 mm.

Hand Sample:
Sphalerite occurs as fine honey-brown crystals to blackjack (~1 mm) crystals. Galena crystals range from 0.1 to 0.3 cm. Mineralization appears to have replaced dolomite.

Thin Section:
Skeletal galena (20%) occurs in and around fine-grained sphalerite (100 μm). The sphalerite grains grade into euhedral, larger (500–1000 μm) blackjack sphalerite grains. Sphalerite appears to have replaced or co-precipitated with galena. Sphalerite (50%) exhibits chalcopyrite disease. Galena crystals range from 100-1000 μm and some have curved faces, indicating deformation.

Modal Distribution:
Sphalerite: 50%
Galena: 20%
Pyrite: trace
Gangue: 30%

Appendix A2 continued.

Sample 10-MPB-R37

Deposit: M67

Hand Sample

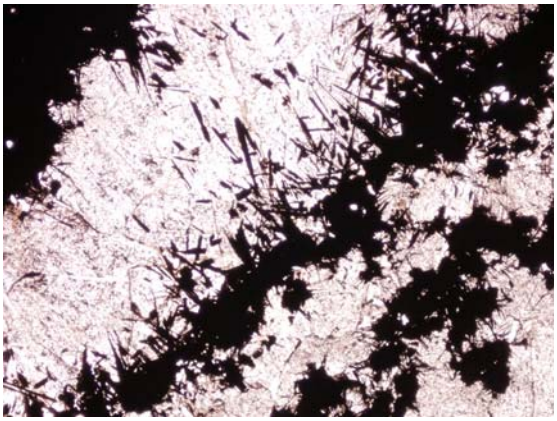

Thin Section: Needle-like pyrite crystals in calcite. Field of view is 4 mm.

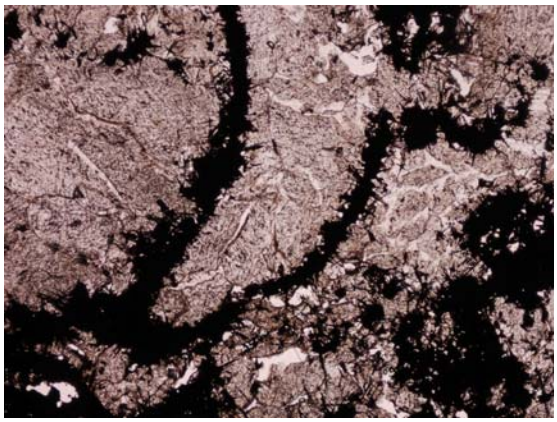

Pyrite has precipitated along fractures, possible fossil moulds. Field of view is 4 mm.

Hand Sample:
Disseminated fine-grained pyrite, too small to distinguish with the naked eye. Calcite crystals (0.2 cm) occur in vugs. Pyrite contains isolated patches of calcite.

Thin Section:
Pyrite (65%), calcite and dolomite (25%), and sphalerite (10%). Pyrite is massive, individual grains cannot be determined with microscope, and appears to have replaced Ca along cleavage and grain boundaries. Calcite grains show sweeping extinction; subhedral crystals that range in size from 100 to 1500 µm. Some dolomite rhombs are preserved, though most grains are subhedral. The grains average 500 to 1000 µm and the grain boundaries are very ragged (dissolution?).

Modal Distribution:
Pyrite: 60%
Gangue: 40%

Appendix A2 continued.

Sample 10-MPB-R38

Deposit: M67

Hand Sample

Thin Section: Massive fine-grained pyrite. Field of view is 4 mm.

Hand Sample:
Very fine-grained crystalline pyrite (too small for hand lens). Calcite veins have cut through the pyrite. Very clean calcite crosscuts a larger vein consisting of calcite and pyrite.

Thin Section:
Most sulphide minerals in this sample occur as very fine-grained (10–50 μm) patches that are 500 μm across. A fine dark grain is 2000 μm (possibly sphalerite). Some dolomite has been replaced by pyrite and some pyrite was crosscut by later dolomite. 'Dirty' dolomite also contains abundant pyrite. Clean dolomite contains some pyrite and possible sphalerite (100–200 μm).

Modal Distribution:
Sphalerite: trace?
Pyrite: 60%
Gangue: 40%

Appendix A2 continued.

Sample 10-MPB-R40

Deposit: M67

Hand Sample

Thin Section: Curved galena crystal face. Field of view is 4 mm.

Hand Sample:
Galena cubes are 0.5 cm and occur within and around dark brown fine-grained sphalerite. Dark grey dolomite occurs within sulphides. White clean dolomite crosscuts the sulphide minerals.

Thin Section:
Dolomite grains (500–1000 μm) all show dissolution features along grain boundaries. Interstitial space is filled with anhedral clean dolomite. Sphalerite is heavily zoned and grains range from 1500 to 3000 μm. Dolomite not completely cut off by sphalerite is saddle dolomite, which crosscuts sphalerite grains. Galena is heavily deformed; grains are 5 to 7.5 mm. Possible trace amounts of pyrite occur in dolomite. Galena fragments are subrounded (<50 μm) and faces are curved.

Modal Distribution:
Sphalerite: 65%
Galena: 5%
Pyrite: trace
Gangue: 30%

Appendix A2 continued.

Sample 10-MPB-R41

Deposit: M67

Hand Sample

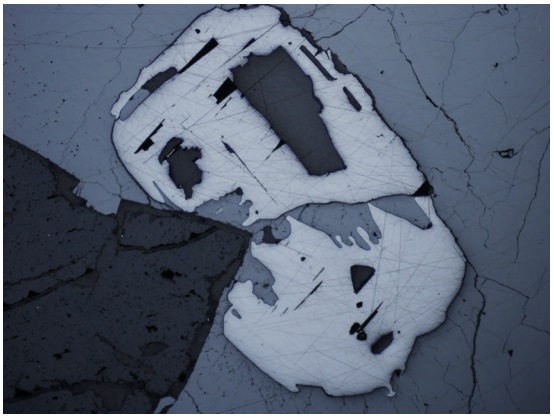

Thin Section: Galena crystal encased in sphalerite and partly dissolved by saddle dolomite. Field of view is 4 mm.

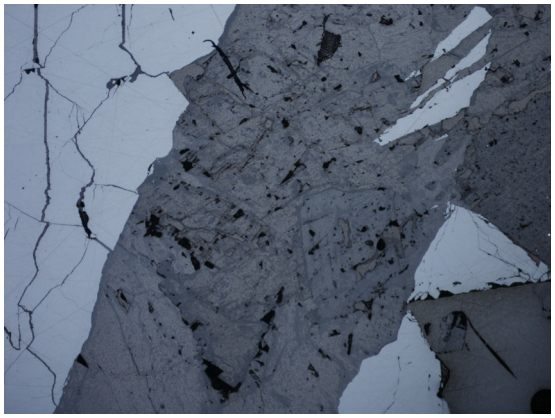

Dolomite vein crosscuts sphalerite. Field of view is 4 mm.

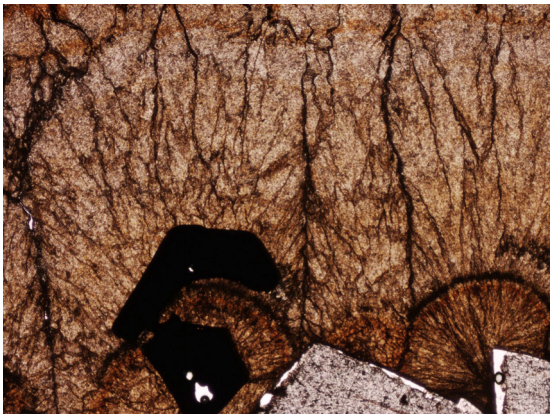

Acicular sphalerite crystals radiate outward from a Fe-rich core. A galena crystal is encased within the core. Field of view is 4 mm.

Hand Sample:
Coarse calcite (0.5 cm) fills vugs and voids. White, fine-grained (0.1 cm) dolomite crosscuts mineralization as well as other dolomite and calcite. Sphalerite occurs as blackjack and honey-brown.

Thin Section:
Sphalerite (35%) grains are zoned and occur as blackjack and honey-brown, and both types average size is 500 to 1000 µm. Botryoidal sphalerite fans have Fe-rich (dark red) cores. Galena (10%) appears to be heavily altered; it has ragged grain boundaries and is perforated. These grains range from 500 to 2000 µm. Pyrite (tr) occurs as isolated patches of very fine grains (10–500 µm) and is associated with saddle dolomite and sphalerite. Calcite and dolomite (55%) have completely replaced galena in some cases. Isolated patches of fine-grained (25–50 µm) crystals occur next to saddle dolomite (3000 µm). Well defined euhedral crystals cut through saddle dolomite in fine veins that are 25 µm across. Some clear calcite crystals occur within dirty dolomite grains, perhaps indicating only partial dolomitization has occurred.

Modal Distribution:
Sphalerite: 35%
Galena: 10%
Pyrite: trace
Gangue: 55%

Appendix A2 continued.

Sample 10-MPB-R42

Deposit: M67

Hand Sample

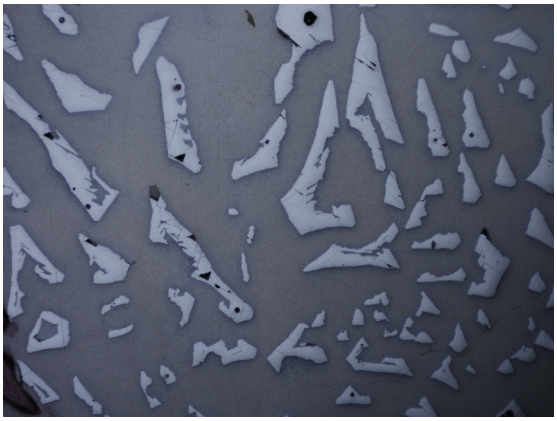

Thin Section: Skeletal galena in cleiophane sphalerite. Field of view is 4 mm.

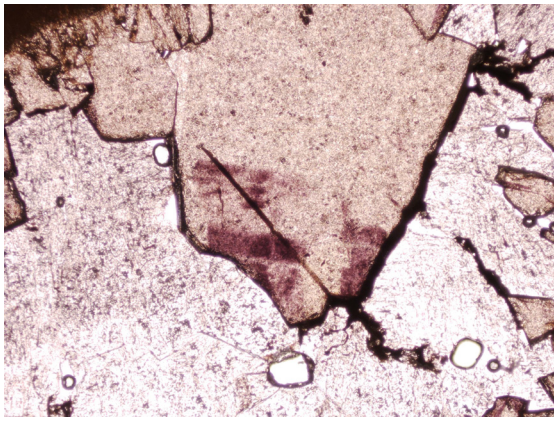

Large honey-brown sphalerite grain radiating from botryoidal sphalerite. Field of view is 4 mm.

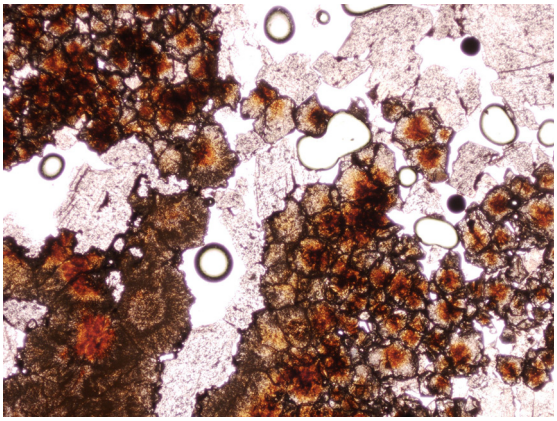

Blackjack and honey-brown sphalerite grains with dolomite. Field of view is 4 mm.

Hand Sample:
Sphalerite, (cleiophane-rimmed with blackjack sphalerite), Blackjack sphalerite (isolated crystals, 0.1 cm), very fine-grained (<0.1 cm) skeletal galena within cleiophane, Honey-brown sphalerite (<0.1 cm) associated with both blackjack and cleiophane, All sphalerite is hosted by blue-grey dolomite, sharp contact between white and grey dolomite.

Thin Section:
Dolomite is dominant gangue mineral with minor calcite. Galena occurs as skeletal grains within cleiophane sphalerite. Cleiophane sphalerite occurs with botryoidal sphalerite. Fine-grained (<100 µm) pyrite occurs throughout the sample though not within cleiophane sphalerite. Blackjack sphalerite occurs as vug fillings, grains (50–100 µm) are along dolomite boundaries that get larger towards the centre, most sphalerite grains are <500 µm; some are as large as 1500 µm. Euhedral honey-brown sphalerite also occurs in the sample.

Modal Distribution:
Sphalerite: 50%
Galena: 5%
Pyrite: trace
Gangue: 45%

Appendix A2 continued.

Sample 10-MPB-R44

Deposit: HZ

Hand Sample

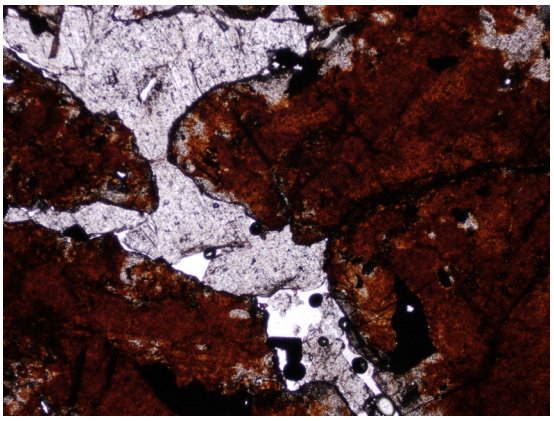

Thin Section: Blackjack sphalerite. Field of view is 4 mm.

Hand Sample:
Dendritic sphalerite grains (0.2 cm) occur within dark grey-blue sphalerite; white calcite and dolomite has filled fractures.

Thin Section:
Dark red (Fe-rich) sphalerite occurs in isolated patches approximately 0.5 to 1 cm across; individual subhedral grains within patches are 500 to 1500 µm. Galena (250 µm) is associated with this sphalerite. Some isolated fragments of anhedral sphalerite (150 µm) occur within saddle dolomite. Galena occurs as subhedral, 400 µm grains that are associated with or without sphalerite. Pyrite cubes (50 µm) occur within dolomite. Skeletal dolomite (500 µm) occurs within sphalerite (cleiophane). Some isolated cubes of galena (500 µm) occur within dolomite.

Modal Distribution:
Sphalerite: 35%
Galena: 15%
Pyrite: 5%
Gangue: 45%

Appendix A2 continued.

Sample 10-MPB-R46

Deposit: O28

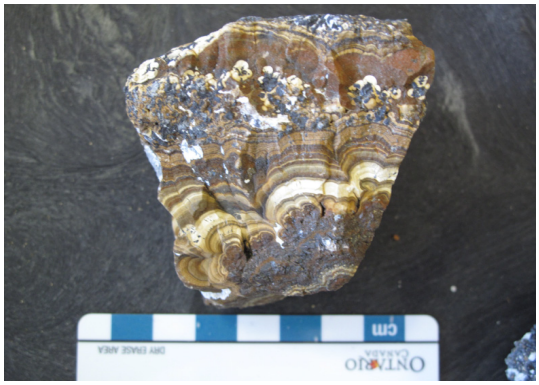

Hand Sample:
Near total replacement by sulphides (honey-brown sphalerite, botryoidal sphalerite, and galena). There are very fine (<1 mm) white veins that crosscut mineralization. Botryoidal sphalerite grows on galena core. Honey-brown sphalerite fills void spaces. Botryoidals are up to 5 mm across with one large 2 cm botryoid.

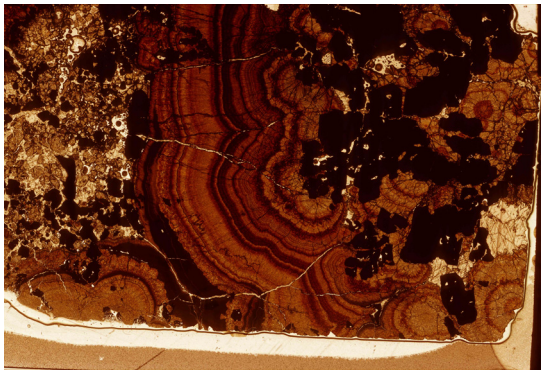

Thin Section R46A

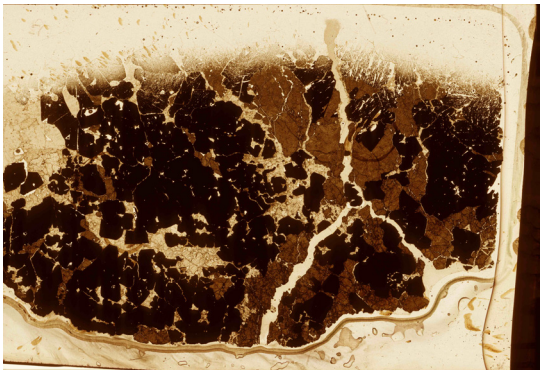

Thin Section R46B

Thin Sections:
R46A: Calcite (<0.3 mm) fill interstitial space. Botryoidal sphalerite is replaced by galena and honey-brown sphalerite. Layers within the botryoidal sphalerite are iron-rich and range from 0.005 to 0.1 mm. Honey-brown sphalerite grains average ~0.06 mm and galena fragments average ~0.2 mm. Galena fragments occur in within honey-brown sphalerite crystals. There is no pyrite in this section.

R46B: Thin section appears to be all galena and sphalerite. Galena exhibits curved crystal faces indicative of burial diagenesis. Calcite veins crosscut sphalerite and galena. Average size of cubic galena is 0.2 mm. Honey-brown sphalerite has iron zoning. Cubic galena is crosscut by sphalerite grains, which are subhedral to anhedral and average 0.1 mm. Possible earlier galena occurs as fragments of cubes that range from 0.01 to 0.33 mm.

Modal Distribution:

Thin Section R46A
- Sphalerite (botryoidal): 45%
- Sphalerite (honey-brown): 15%
- Galena: 35%
- Pyrite: 0%
- Gangue: 5%

Thin Section R46B
- Sphalerite: 40%
- Galena: 55%
- Pyrite: 0%
- Gangue: 5%

Appendix A2 continued.

Sample 10-MPB-R47

Deposit: O28

Hand Sample

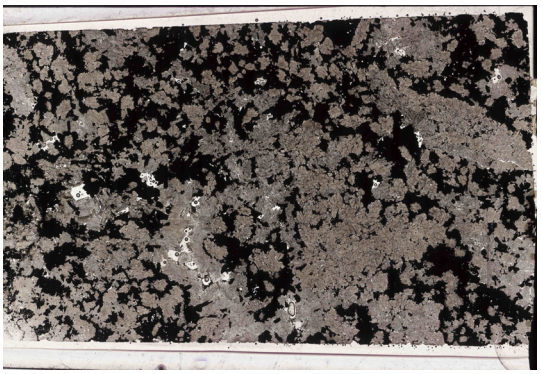

Thin Section

Hand Sample:
Sample has pyrite that has replaced dolomite and later stage sparry dolomite lines vugs and voids. Subhedral pyrite grains are ≤1. Some pyrite is heavily weathered to a reddish-rusty colour. Earlier dolomite appears to be a dark blue-grey variety.

Thin Section:
Thin section appears to contain mostly pyrite and gangue minerals. There are no fragments or grains of sphalerite or galena. Pyrite is cubic to subhedral and grains range from 0.001 mm fragments to 0.08 mm cubes. Saddle dolomite is the main gangue mineral and grain boundaries are stylolitic. Pyrite appears to have replaced saddle dolomite along grain boundaries.

Modal Distribution:
Sphalerite: 0%
Galena: 0%
Pyrite: 40%
Gangue: 60%

Appendix A2 continued.

Sample 10-MPB-R50

Deposit: O28

Hand Sample

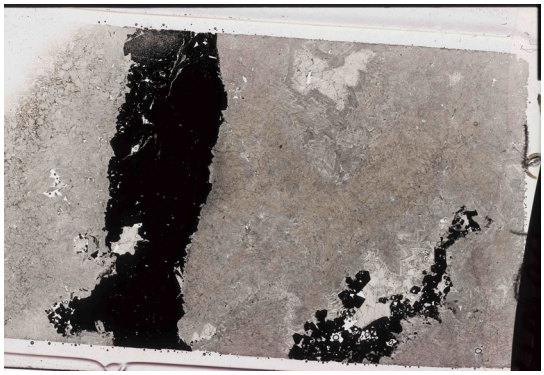

Thin Section

Hand Sample:
Sample is mainly dolomite (white and dark grey-blue); coarse calcite fills vugs. A thick galena vein cuts through the sample. Sparry white dolomite is not crosscut by the galena vein. Galena cubes within the veins are approximately 1 mm. Some traces of sphalerite occur within galena.

Thin Section:
The galena vein that cuts through this sample is 1 cm wide. It appears to be continuously crystalline. Dolomite grains have stylolitic grain boundaries. Saddle dolomite cuts the galena vein. Calcite crystals fill the void space between saddle dolomite crystals. Sphalerite crystals also cut into the galena vein. There are pyrite and sphalerite fragments (0.002–0.02 mm) throughout the saddle dolomite. Cubic galena (0.2 mm) occurs after botryoidal sphalerite. Botryoidal sphalerite occurs in small sections; grains are no more than 0.01 mm.

Modal Distribution:
Sphalerite: 5%
Galena: 25%
Pyrite: trace
Gangue: 70%

Appendix A2 continued.

Sample 10-MPB-R51

Deposit: O28

Hand Sample

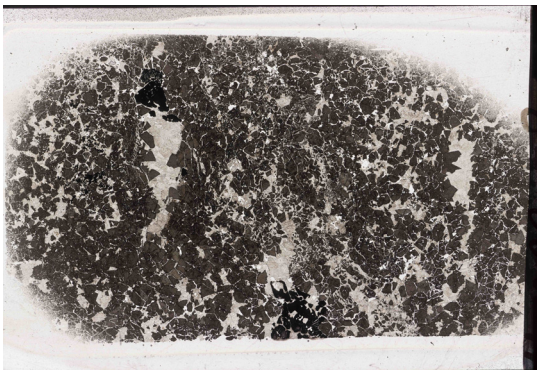

Thin Section

Hand Sample:
Sample is heavily weathered with abundant iron staining. It contains galena veins that are associated with clear white dolomite. Galena cubes are up to 2 mm but most are smaller. Sphalerite is scattered throughout and has replaced dolomite. Sphalerite grains are too small to distinguish individually with a hand lens.

Thin Section:
Sample appears to mainly consist of honey-brown sphalerite with galena-filled fractures and voids. Crackle breccia of honey-brown sphalerite grains range from 0.0005 to 0.12 mm. Interstitial space is filled with calcite and rounded dolomite grains (0.08 mm). There are no pyrite or iron-rich sphalerite grains. The paragenesis appears to be honey-brown sphalerite, galena, then calcite.

Modal Distribution:
Sphalerite: 75%
Galena: 5%
Pyrite:
Gangue: 20%

Appendix A2 continued.

Sample 10-MPB-R52

Deposit: O28

Hand Sample

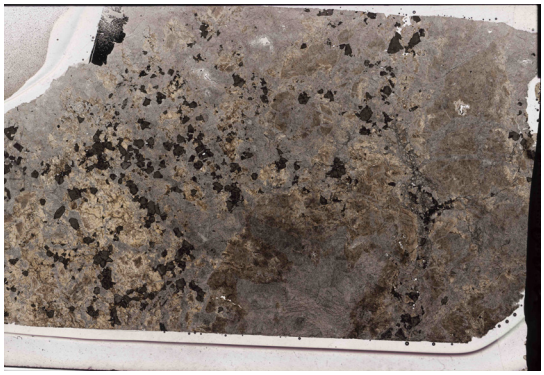

Thin Section

Hand Sample:
Sample contains mainly honey-brown sphalerite with isolated patches of blackjack sphalerite. Galena cubes are ≤5 mm and occur within honey-brown sphalerite and late, white sparry dolomite. Sphalerite grains are too small to determine with a hand lens.

Thin Section:
Thin section consists mainly of sphalerite fragments that average 0.06 mm. Galena occurs as small (0.02 mm) fragments. Saddle dolomite contains fragments of pyrite and sphalerite and is coated with bitumen.

Modal Distribution:
Sphalerite: 15%
Galena: 5%
Pyrite: trace
Gangue: 80%

Appendix A2 continued.

Sample 10-MPB-R53

Deposit: O28

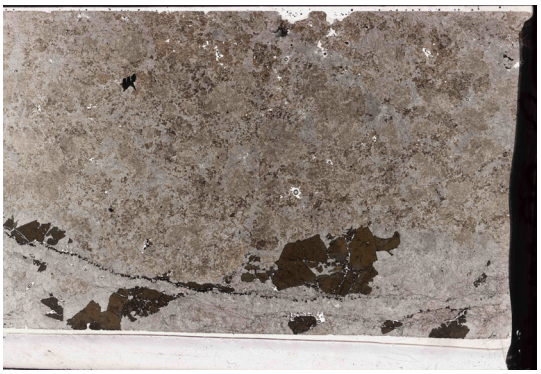

Thin Section

Hand Sample:
Sample is mostly dolomite with isolated grains of honey-brown sphalerite. Sphalerite occurs throughout sample (in all types of dolomite) with the exception of white sparry dolomite. Some blackjack sphalerite also occurs but mostly within dark grey-blue dolomite and sparry white dolomite. Sphalerite grains are ≤5 mm.

Thin Section:
Saddle dolomite in thin section has ragged edges (indicating diagenesis) and contains isolated fragments of Presqu'ile dolomite. Galena preferentially precipitated along fractures. Galena occurs after honey-brown sphalerite. Sphalerite grains range occur as fragments that are 0.02 to ≤0.5 mm. Dolomite contains pyrite (<0.01 mm) and sphalerite (<0.01 mm) fragments. Pyrite occur as <0.1 mm fragments.

Modal Distribution:
Sphalerite: 20%
Galena: 5%
Pyrite: 10%
Gangue: 65%

Appendix A2 continued.

Sample 10-MPB-R54

Deposit: O28

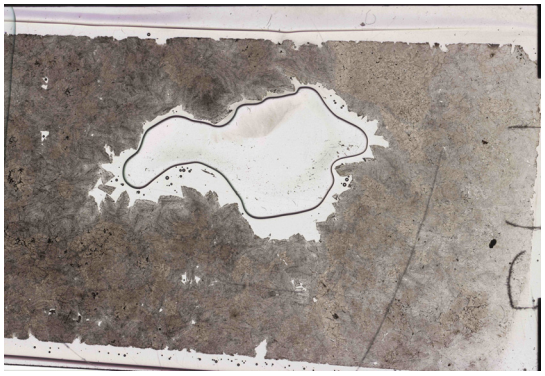

Thin Section

Hand Sample:
Blackjack sphalerite with iron staining; sphalerite grains are ≤5 mm. Calcite veins (≤2 mm) cut sphalerite and fill voids within sphalerite. Dirty dolomite (pyrite-rich variety) has replaced finer white dolomite.

Thin Section:
Thin section consists of mixed dolomite with fragments of galena and sphalerite, of undetermined paragenesis. Dolomite occurs mainly as the saddle variety in large (3 mm) crystals. Smaller (0.01 mm) subhedral dolomite grains occur in patches. Some of these dolomite grains still exhibit a rhomb shape. Fragments of galena (0.06 mm) and heavily dissolved and pitted sphalerite grains (0.04 mm) occur within dolomite.

Modal Distribution:
Sphalerite: 5%
Galena: 10%
Gangue: 85%

Appendix A2 continued.

Sample 10-MPB-R55

Deposit: O28

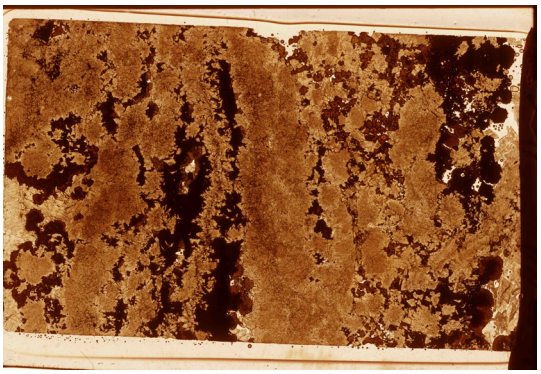

Thin Section

Hand Sample:
Sulphide minerals are concentrated in bands. Where space was available, sphalerite grew as botryoidal variety (≤2 mm across). Galena (<1 mm) occurs fills voids within the botryoidal sphalerite. Calcite has filled the larger voids.

Thin Section:
Thin section contains honey-brown sphalerite, botryoidal sphalerite, and galena fragments. Pyrite appears to have replaced sphalerite. Anhedral galena grains contain pyrite fragments. Pyrite and botryoidal sphalerite appear to have co-precipitated. Galena (≤0.04 mm) has dissolved grain boundaries. Honey-brown sphalerite crystals (0.06 mm) are zoned, sub- to euhedral, and have Fe-rich cores. Void spaces within mineralization are filled with cloudy dolomite and grain boundaries are difficult to see. There are many collapse features, which makes paragenesis difficult to determine.

Modal Distribution:
Sphalerite (botryoidal): 25%
Sphalerite (Honey-brown): 15%
Galena: 5%
Pyrite: 20%
Gangue: 35%

Appendix A2 continued.

Sample 10-MPB-R56

Deposit: O28

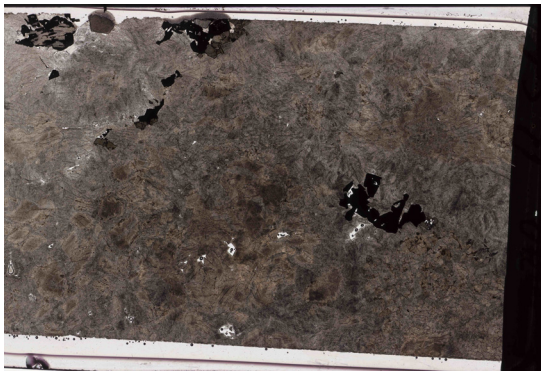

Thin Section

Hand Sample:
Galena and sphalerite occur together in hand sample. Galena crystals are up to 2 mm. Sphalerite is honey-brown variety and ≤1 mm. Gangue appears to be pre-mineralized collapse with fragments of dirty dolomite. Creamy and white sparry dolomite formed after mineralization and collapse.

Thin Section:
Dolomite is very dirty in plain polarized light, likely coated by bitumen. Saddle dolomite throughout the sample is subhedral. Within this saddle dolomite, isolated patches of rounded dolomite occur. Fragments of sphalerite, pyrite, and galena occur throughout the saddle dolomite (≤0.06 mm, most are much smaller). Stylolitic, cloudy dolomite is free of sulphide fragments. Sphalerite occurs after galena. Galena grains are subhedral and are ≤0.2 mm. Sphalerite grains are also subhedral with dissolution features and are ≤0.1 mm. Pyrite occurs as 0.01 mm cubes and as smaller fragments within saddle dolomite.

Modal Distribution:
Sphalerite: 10%
Galena: 25%
Pyrite: trace
Gangue: 65%

Appendix A2 continued.

Sample 10-MPB-R62

Deposit: L65

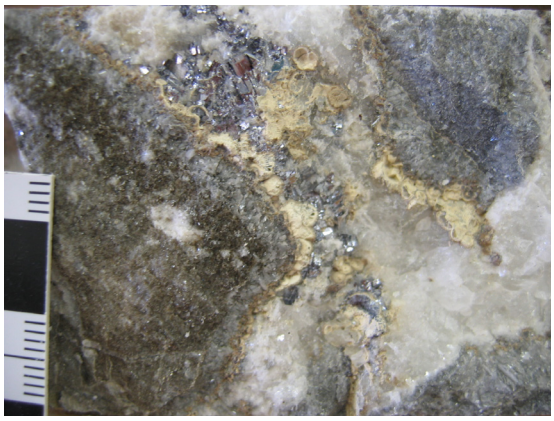

Hand Sample

Thin Section: Cubic galena replacing botryoidal sphalerite containing skeletal galena. Field of view is 4 mm.

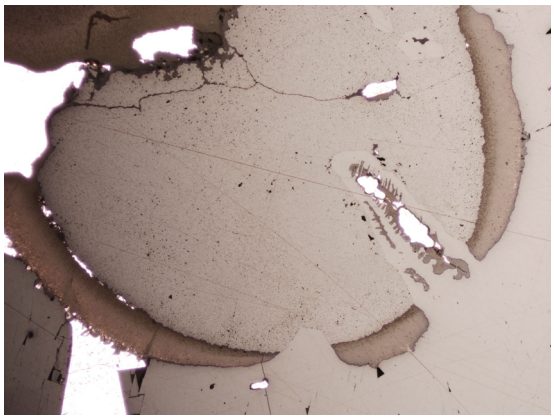

Galena cutting into botryoidal sphalerite.
Field of view is 4 mm.

Hand Sample:
Sulphide mineralization occurs along fractures; large vugs are filled with coarse (0.2–0.3 cm) calcite rhombs. Brown-green sandy matrix contains shell fragments (?) that are rimmed with uniform 2 mm thick blue-grey dolomite. Cleiophane sphalerite coats blue-grey dolomite and galena coats sphalerite. Brown-grey sandy material forms clasts. Galena cubes fill the centre of interstitial space.

Thin Section:
Cleiophane sphalerite shows zoning to brown sphalerite crust. Galena fragments occur along fractures. Boundaries between sphalerite and galena are sharp, some with stylolitic features. Small galena crystals (50 μm) occur within sphalerite. Galena cubes range from <50 μm to 5 mm. Skeletal galena occurs in cleiophane. Dolomite crystal faces are curved (saddle), and show dissolution features along boundaries with sphalerite that exibits what is possibly snow-on-roof texture.

Modal Distribution:
Sphalerite: 25%
Galena: 25%
Pyrite: trace
Gangue: 50%

Appendix A2 continued.

Sample 10-MPB-R63

Deposit: R190

Hand Sample

Thin Section: Galena with curved crystal faces.

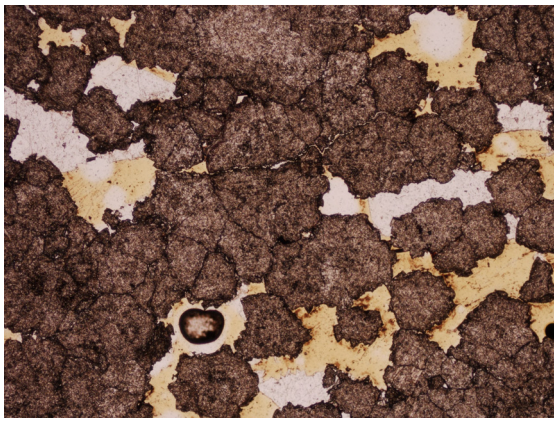

Honey-brown sphalerite crystals with interstital sulphur.

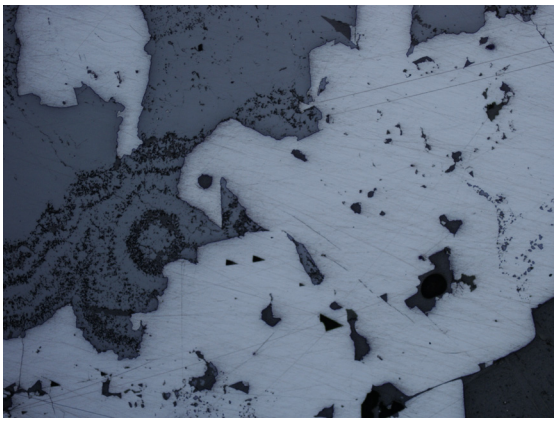

Cubic galena crosscutting botryoidal sphalerite.

Hand Sample:
Native sulphur occurs as 0.2 to 1 cm crystals. Sphalerite occurs as honey-brown and as small-scale botryoidal fans. Cubic galena occurs as 0.3 to 0.5 cm grains. Sucrosic calcite occurs in isolated patches, though most has been totally replaced.

Thin Section:
Saddle dolomite (5%) occurs as isolated patches no more that 5 mm across. These grains were replaced by sulphur (10%). Sphalerite (60%) occurs as botryoidal fans (2 mm across), isolated euhedral crystals (500 µm), or as small patches of euhedral crystals (100 µm across). Galena (25%) occurs as subhedral to cubic crystals (1.5–5 mm). Most of the galena grains are heavily pitted. Sphalerite and galena occur intergrown, indicating co-precipitation. Trace amounts of pyrite occur and is approximately 500 µm in size.

Modal Distribution:
Sphalerite: 60%
Galena: 25%
Gangue: 5%
Sulphur: 10%
Pyrite: trace

Appendix A2 continued.

Sample 10-MPB-R64

Deposit: L65

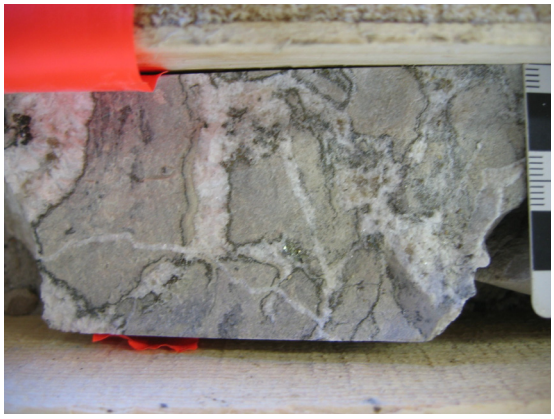

Hand Sample

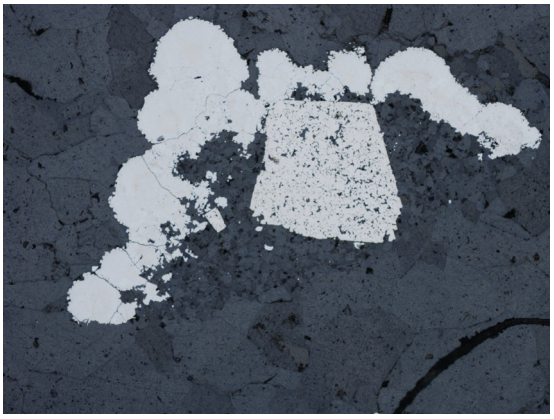

Thin Section: Botryoidal pyrite, with subhedral pyrite cube. Field of view is 4 mm.

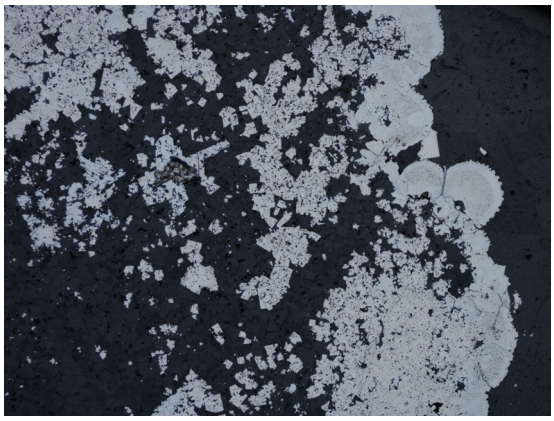

Botryoidal pyrite radiating from anhedral cubes of pyrite. Field of view is 4 mm.

Hand Sample:
Very fine-grained (Watt Mountain Formation?), bioclasts are rimmed with pyrite and sphalerite grains that are too small to identify with a hand lens. Calcite has filled large vugs (crystals 0.3 cm), while dolomite (grains to small to see) fill interstitial space between clasts, and in some cases, crosscut them. In some places, this dolomite has crosscut the pyrite rims.

Thin Section:
Pyrite (45%) has ragged, semi-dissolved grain boundaries, though a few cubes still remain. The grains range from 10 to 500 μm. These grains line clasts or colloform fractures. Some pyrite occurs as needles that are up to 250 μm long. Within the fine-grained dolomite, buckshot pyrite occurs. Dolomite (55%) occurs in a range of sizes (10–1500 μm). The finest grains are associated with pyrite; the larger grains have crosscut the sample and filled void space.

Modal Distribution:
Sphalerite: trace?
Pyrite: 45%
Gangue: 55%

Appendix A2 continued.

Sample 10-MPB-R66

Deposit: HZ

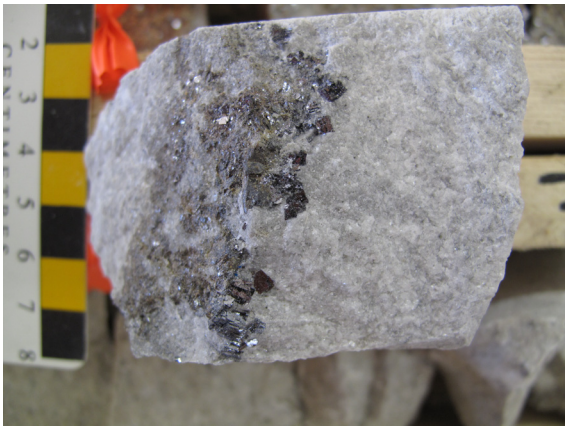

Hand Sample

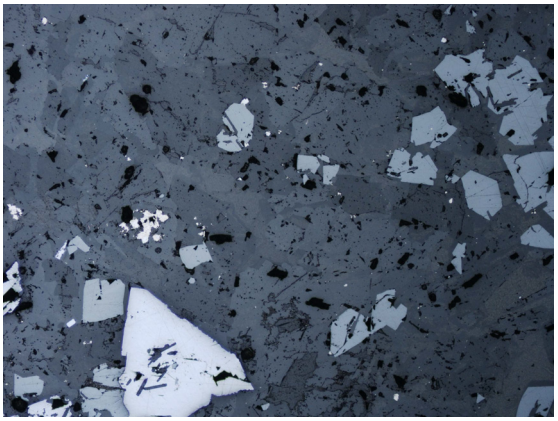

Thin Section: Fragments of sphalerite, pyrite, and galena in a dolomite host. Field of view is 4 mm.

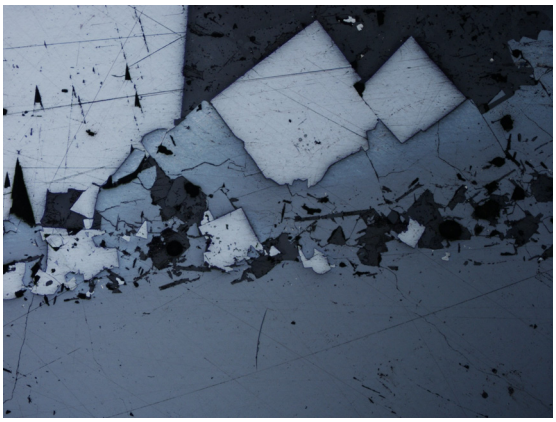

Galena cubes on and within colloform sphalerite. Field of view is 4 mm.

Hand Sample:
Sulphide minerals are concentrated in bands that separate sucrosic dolomite from light grey-brown fine-grained dolomite and calcite. Galena crystal cubes (0.1–0.2 cm) are concentrated in the bands. Honey-brown sphalerite (<0.1 cm) occurs between galena and dark brown sphalerite. Galena occurs throughout the hand sample.

Thin Section:
Large (1 cm) subhedral sphalerite are zoned, with Fe-rich layers, honey-brown layers, and Fe-rich rims. Galena grains are euhedral to subhedral that range in size from 1 to 5 mm. Pyrite (100 µm), sphalerite fragments (200–500 µm), and galena fragments (250 µm) occur within 'dirty' dolomite. Pyrite occurs in all dolomite but sphalerite and galena fragments trail off from cubic galena cluster. Galena cubes are 300 µm; sphalerite grains are 500 to 1000 µm.

Modal Distribution:
Sphalerite: 20%
Galena: 10%
Pyrite: 5%
Gangue: 65%

Appendix A2 continued.

Sample 10-MPB-R67

Deposit: HZ

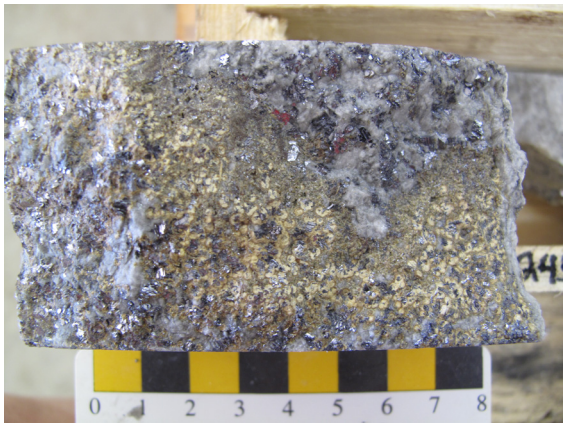

Hand Sample

Thin Section: Skeletal galena in cleiophane sphalerite. Field of view is 4 mm.

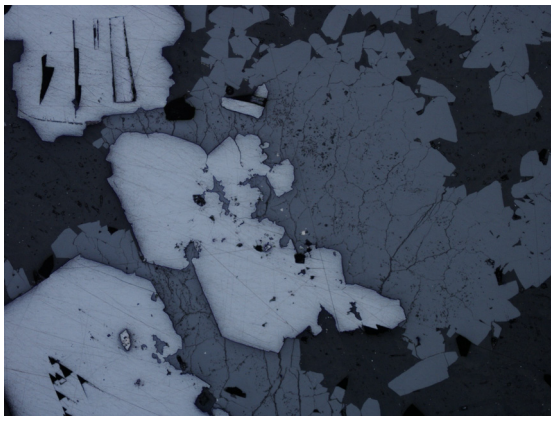

Galena cubes partially replaced by honey-brown sphalerite. Field of view is 4 mm.

Hand Sample:
Very small botryoidal sphalerite grains (0.1 cm across) interfingered with galena (0.1 cm across). Sphalerite coats the galena crystals; large calcite crystals.

Thin Section:
Dendritic galena is coated with honey-brown sphalerite grains. Galena has dissolved grain boundaries, skeletal form, size ranges from 100 to 2000 µm. Sphalerite grains range from 500 µm botryoidal fans to individual grains that are 350 µm. Dolomite grain boundaries are heavily dissolved, have sweeping extinction, and are approximately 1500 µm across. Sphalerite grains are subhedral. Possible pyrite grains are 50 µm and possible chalcopyrite grains that are 10 µm across. Sphalerite botryoids are 1000 µm across.

Modal Distribution:
Sphalerite: 35%
Galena: 30%
Pyrite/Chalcopyrite: trace
Gangue: 35%

Appendix A2 continued.

Sample 10-MPB-R68

Deposit: HZ

Hand Sample

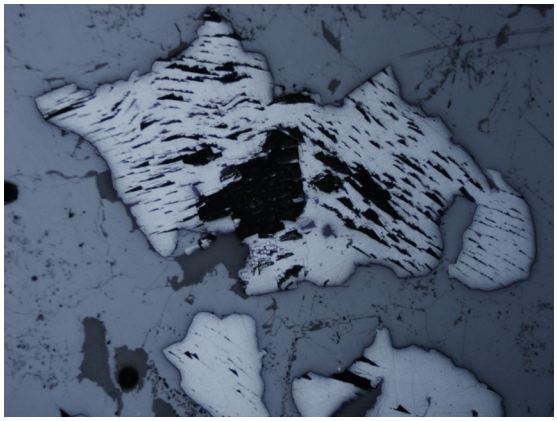

Thin Section: Galena crystals replaced by sphalerite crystals. Field of view is 4 mm.

Hand Sample:
Similar to sample 10-MPB-R67, though with more abundant honey-brown sphalerite.

Thin Section:
Anhedral calcite fills interstitial space and range in size from 500 to 750 µm. Galena crystals have curved faces, dissolved edges, and are approximately 2000 µm. Anhedral galena occurs within sphalerite or along boundaries. Honey-brown Sphalerite grains are subhedral and on average 500 to 750 µm.

Modal Distribution:
Sphalerite: 65%
Galena: 20%
Gangue: 15%

Appendix A2 continued.

Sample 10-MPB-R69

Deposit: HZ

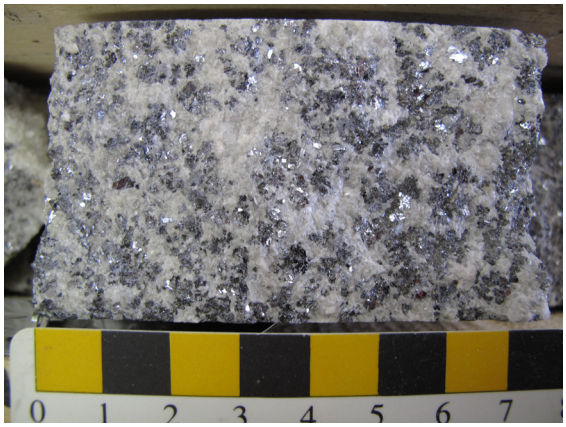

Hand Sample

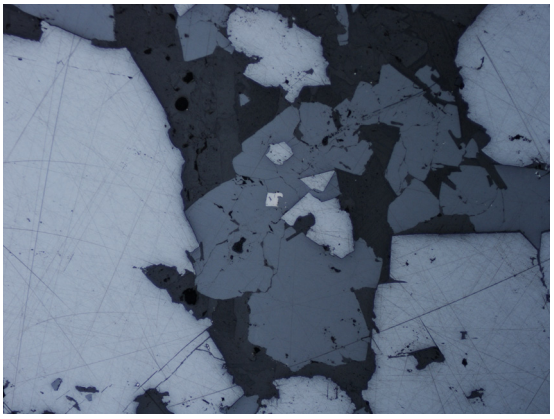

Thin Section: Sphalerite crystals containing pyrite and galena fragments. Field of view is 4 mm.

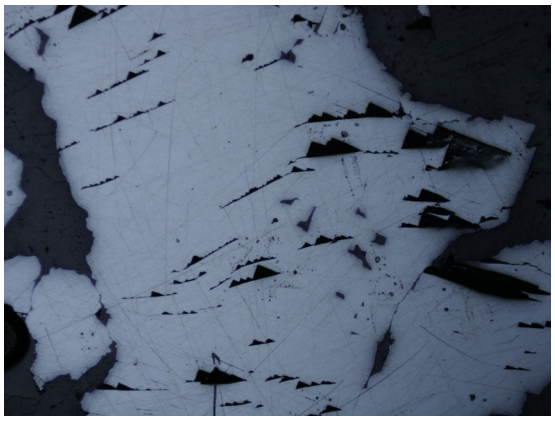

Galena crystal with some curved crystal faces. Field of view is 4 mm.

Hand Sample:
Galena occurs throughout sample, sometimes in crystal clusters. Galena grains average 0.1 cm. Calcite/dolomite grains are approximately 0.1 cm.

Thin Section:
Clusters of galena crystals occur throughout sample. Interstitial dolomite (500–1000 μm) is anhedral and has sweeping extinction. Some dolomite has curved crystal faces of saddle dolomite. Light-coloured sphalerite grains occur throughout; some fragments are 100 μm or less but most are 500 to 1000 μm. Galena ranges from anhedral to subhedral (mostly subhedral) and ranges in size from 4 mm to 1 cm with curved crystal faces. Trace pyrite occurs as 200 μm cubes with ragged edges.

Modal Distribution:
Sphalerite: 15%
Galena: 55%
Pyrite: trace
Gangue: 30%

Appendix A2 continued.

Sample 10-MPB-R70

Deposit: HZ

Hand Sample

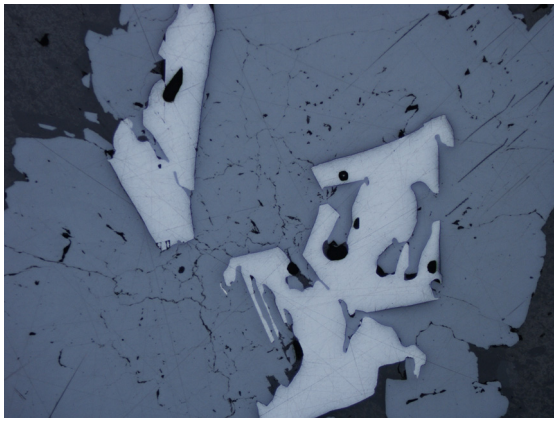

Thin Section: Sphalerite crystals containing galena fragments. Field of view is 4 mm.

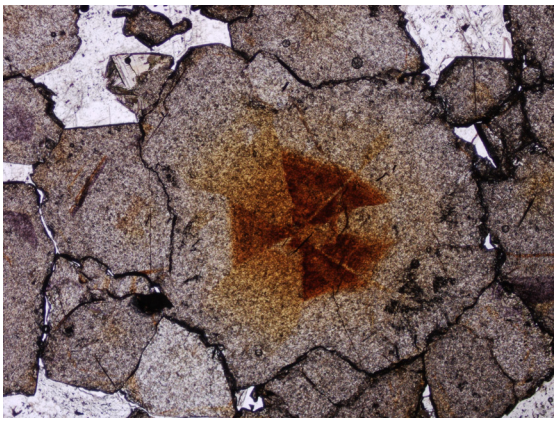

Honey-brown sphalerite crystal with a Fe-rich core. Field of view is 4 mm.

Hand Sample:
Honey-brown sphalerite crystals (0.2 cm) occur with dark brown (possibly blackjack) sphalerite. Galena crystals, 0.2 cm in size, occur throughout the sample. The sulphide minerals appear to have replaced dolomite with small veins of late-stage calcite that have crosscut all minerals.

Thin Section:
Patches of euhedral sphalerite grains (1500 µm) display zoning. Sphalerite and galena occur together. Galena crystals have heavily dissolved boundaries on which sphalerite has precipitated. Galena grains (~2500 µm) are anhedral. Sphalerite grains are 1500 by 1000 µm. Heavily zoned blackjack sphalerite contains skeletal galena (~500 µm). An isolated sphalerite crystal is 5000 µm and appears to be filling a vug. Galena does not occur within the honey-brown sphalerite, mostly occuring as skeletal grains (~300 µm). Heavily fractured sphalerite grains are 5000 µm across. Botryoidal sphalerite occurs throughout. Honey-brown sphalerite occurs as subhedral to euhedral crystals that are 500 µm across. Heavily zoned botryoidal sphalerite is in stylolitic contact with honey-brown (subhedral) grains. Bitumen occurs with the honey-brown sphalerite.

Modal Distribution:
Sphalerite: 40%
Galena: 10%
Pyrite: trace
Gangue: 50%

Appendix A2 continued.

Sample 10-MPB-R71

Deposit: M67

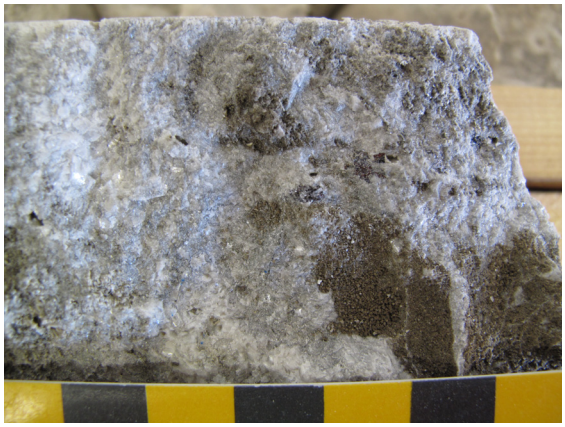

Hand Sample

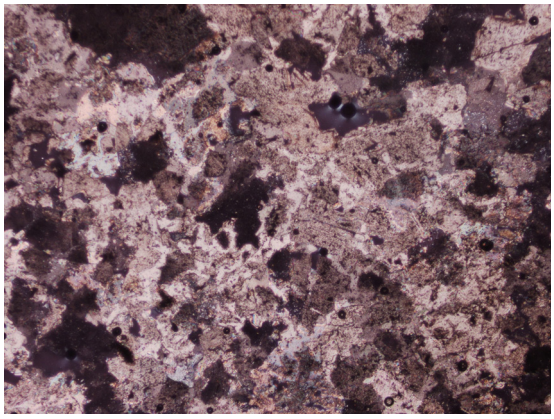

Thin Section: Dissolved crystal boundaries. All grains are anhedral. Field of view is 4 mm.

Dissolved galena crystal in dolomite. All dolomite grain boundaries appear to be slightly dissolved. Field of view is 4 mm.

Hand Sample:
Green mud (Watt Mountain Formation) with isolated galena crystals (0.3–0. 5 cm). Dark grey to bluey grey dolomite coats Watt Mountain Formation sediment. White to transparent calcite has filled interstitial space and vugs. Sample is brecciated at one end. Dolomite veins cut the green Watt Mountain Formation sediment.

Thin Section:
Galena crystals are anhedral and are approximately 1000 µm. Pyrite occurs as small isolated patches 100 µm across. Dolomite has small grains of pyrite (10 µm) throughout. Dolomite grains have dissolution features on most grain boundaries. Sphalerite may be contained as small (10 µm) fragments throughout the dolomite.

Modal Distribution:
Sphalerite: trace
Galena: 2%
Pyrite: 3%
Gangue: 95%

Appendix A2 continued.

Sample 10-MPB-R72

Deposit: M67

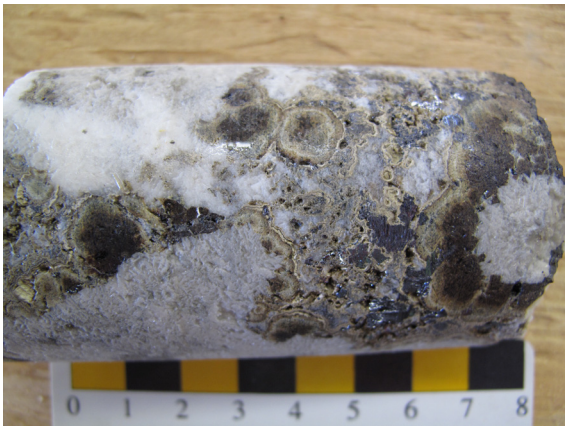

Hand Sample

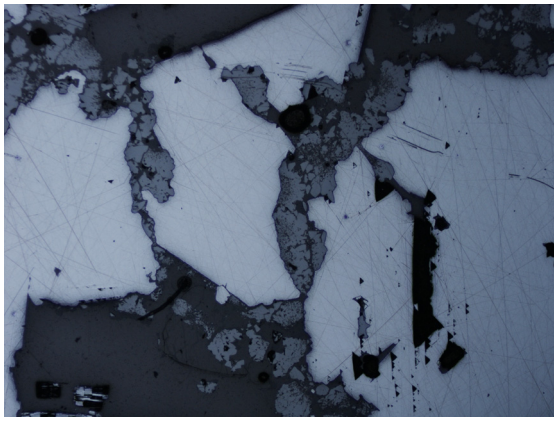

Thin Section: Sphalerite filled fractures between galena grains. Field of view is 4 mm.

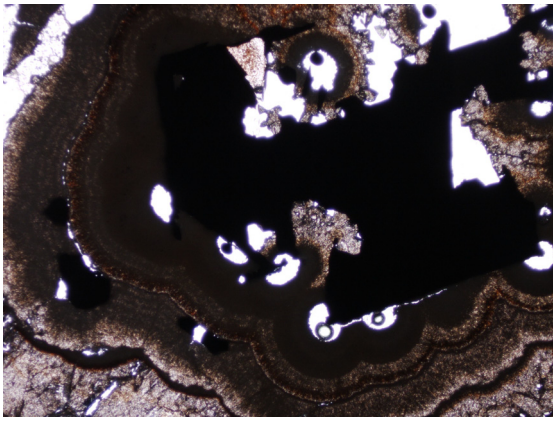

Botryoidal sphalerite formed on galena cube. Field of view is 4 mm.

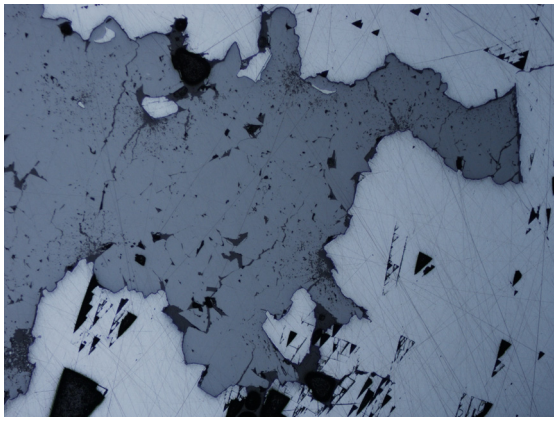

Sphalerite and galena grain boundaries. Field of view is 4 mm.

Hand Sample:
Cubic galena grains (0.2–0.3 cm) and botryoidal sphalerite with cleiophane. Sulphide minerals all occur together. Dark grey dolomite, lighter white dolomite to centre of dark grey units.

Thin Section:
Galena grain are 3000 to 4000 µm and have ragged boundaries (dissolved by sphalerite). Two phases of sphalerite mineralization (botryoidal and interstitial) occur. Sphalerite grains (100 µm) have filled fractures in the galena crystals. Botryoidal sphalerite (500–1000 µm) has grown on subhedral galena grains. Sphalerite grains are subhedral and range from 100 to 500 µm. Botryoidal sphalerite is heavily zoned and grades into layered colloform sphalerite. Layers range from 25 to 250 µm thick. Isolated pyrite cubes (25 µm) occur in botryoidal sphalerite. Isolated anhedral pyrite (10 µm) occurs within dolomite. Pyrite (10 µm) also occurs within sphalerite. Single calcite grains are 750 µm across on average, though some are 5000 µm.

Modal Distribution:
Sphalerite: 65%
Galena: 20%
Pyrite: 5%
Gangue: 10%

Appendix A2 continued.

Sample 10-MPB-R73

Deposit: M67

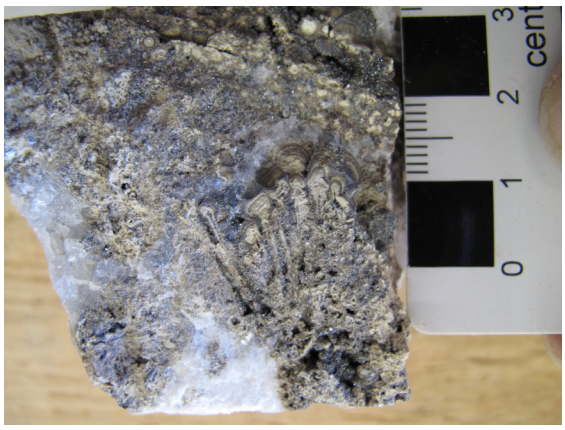

Hand Sample

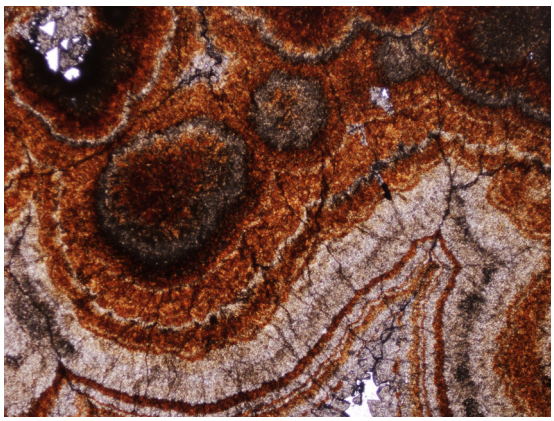

Thin Section: Botryoidal sphalerite. Field of view is 4 mm.

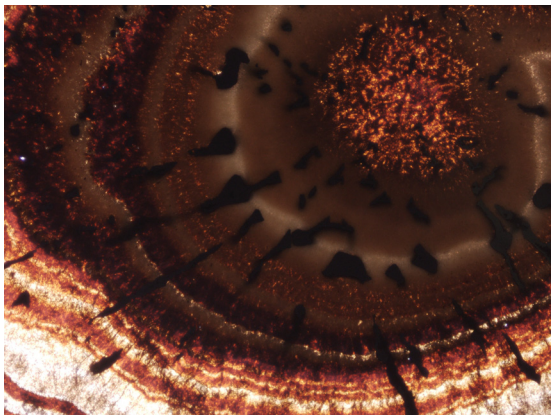

Botryoidal sphalerite with skeletal galena.
Field of view is 4 mm.

Hand Sample:
Sphalerite occurs as botryoidal forms and as isolated crystals (<0.1 cm) that coat vugs. Coarse crystalline calcite (>0.5 cm) has filled pore space and small (0.1–0.2 cm) fractures.

Thin Section:
Sphalerite is botryoidal and occurs as individual crystals (blackjack). Botryoidal fans range from 500 µm to 1.5 cm across. Individual crystals are 500 to 1000 µm. Some heavily dissolved grains of sphalerite occur in dolomite host. Layers in botryoidal sphalerite range from 1000 to 1500 µm. Skeletal galena occurs exclusively in sphalerite. Some iron-rich cores of isolated sphalerite grains were dissolved. Pyrite fragments (200 µm) occur in trace amounts. Saddle dolomite (late) grains are associated with the heavily dissolved sphalerite. Crystal faces have curved faces with sweeping extinction and are approximately 2000 µm. Early dolomite has uniform extinction and occurs as 1000 µm crystals.

Modal Distribution:
Sphalerite: 35%
Galena: 5%
Pyrite: trace
Gangue: 60%

Appendix A2 continued.

Sample 10-MPB-R74

Deposit: HZ

Hand Sample

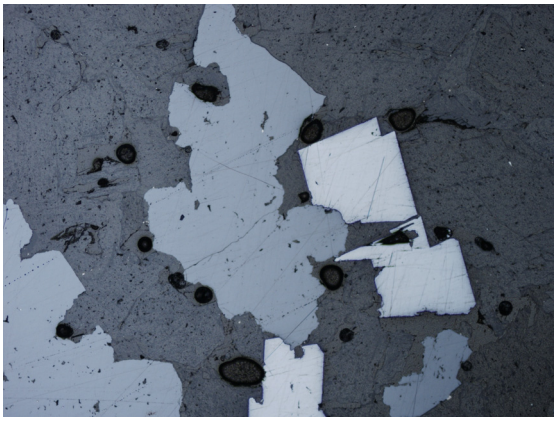

Thin Section: Ragged sphalerite with cubic galena. Field of view is 4 mm.

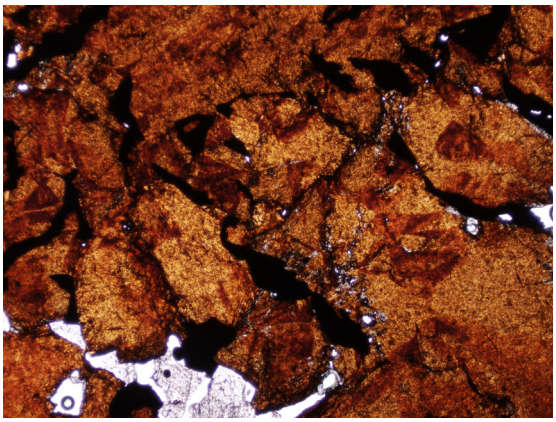

Fe-rich blackjack sphalerite. Field of view is 4 mm.

Hand Sample:
Branching (dendritic) blackjack sphalerite of 0.1 to 0.2 cm crystals, Sphalerite appears to have replaced light grey dolomite. Sphalerite clusters are 1 to 1.5 cm across.

Thin Section:
Branching, dark-red sphalerite occurs with galena (anhedral, grains are 500 by 100 µm) and pyrite. Sphalerite grains are 2500 µm and subhedral. Subhedral, elongate galena grains (500 µm) occur within dolomite. Pyrite grains are anhedral and are up to 100 µm. Cubic galena grains (500 µm) occur within dolomite.

Modal Distribution:
Sphalerite: 30%
Galena: 15%
Pyrite: 5%
Gangue: 50%

Appendix A2 continued.

Sample 10-MPB-R75

Deposit: HZ

Hand Sample

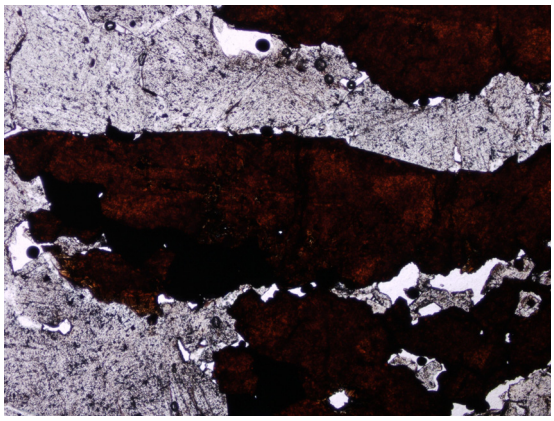

Thin Section: Dendritic Fe-rich sphalerite. Field of view is 4 mm.

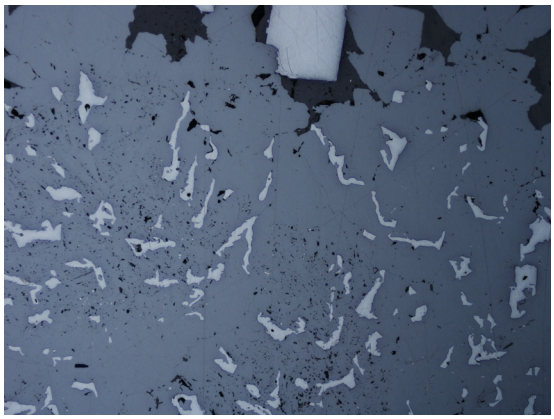

Cubic and skeletal galena. Field of view is 4 mm.

Hand Sample:
Dendritic sphalerite (0.1–0.2 cm); calcite interfingered with sphalerite.

Thin Section:
Cleiophane sphalerite containing skeletal galena. Small pyrite, sphalerite and galena fragments occur throughout dolomite. Galena fragments are cubic and 250 µm across. Isolated Fe-rich sphalerite crystals are 200 to 250 µm. Sphalerite occurs as dendritic form, individual clusters occur as 1 cm groups. Very dark sphalerite contains abundant skeletal galena. Angular, long, narrow galena fragments occur (<500 µm). Some galena crystals are subhedral 250 µm. Galena within sphalerite is anhedral. Dolomite grains are 1000 to 1500 µm. Some dolomite grains have dissolution features along grain boundaries. Dendritic sphalerite has galena along boundaries. Isolated anhedral patch of pyrite that is 250 µm across.

Modal Distribution:
Sphalerite: 45%
Galena: 10%
Pyrite: trace
Gangue: 45%

Appendix A2 continued.

Sample 10-MPB-R76

Deposit: HZ

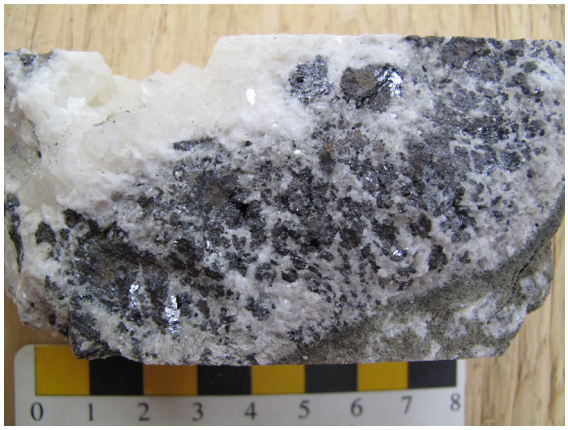

Hand Sample

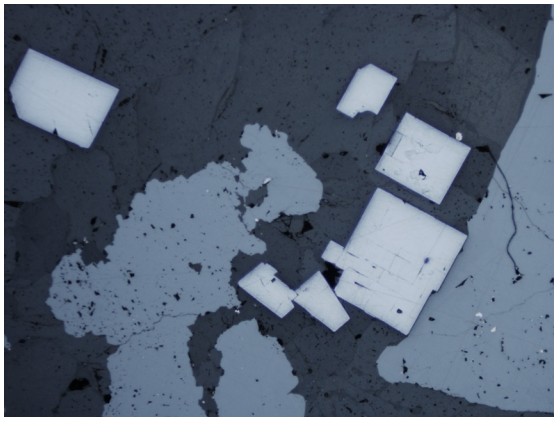

Thin Section: Cubic galena with honey-brown sphalerite. Field of view is 4 mm.

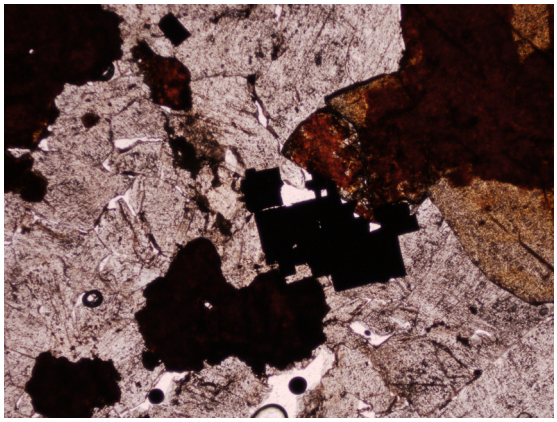

Honey-brown and blackjack sphalerite. Field of view is 4 mm.

Hand Sample:
White to light grey dolomite crystals (~0.2 cm) occur with sphalerite as 0.2 to 0.5 cm grains and has a 'clustered' appearance within the dolomite. Very fine-grained green mud (Watt Mountain Formation shale?) contains white dolomite but no mineralization.

Thin Section:
Calcite (25%) occurs as very clear, ≥2 mm grains with cleavage. Dolomite (35%) is very dirty with a large range in grain size. Isolated patches of very fine-grained dolomite correspond to brown mud clasts. Green mud (Watt Mountain Formation) contains subhedral to euhedral calcite or dolomite crystals that range in size from 50 to 100 µm. Saddle dolomite crystals are in contact with mineralization occuring as grains that range from 1500 to 2000 µm. Sphalerite (25%) occurs as anhedral, dendritic grains (2000 µm) that exhibit little to no zoning. Galena (15%) occurs as cubic, 500 µm grains or as skeletal grains in sphalerite. Within the crystalline calcite, there are semi-dissolved galena cubes (200 µm).

Modal Distribution:
Sphalerite: 25%
Galena: 15%
Gangue: 60%

Appendix A2 continued.

Sample 10-MPB-R77

Deposit: O28

Thin Section

Hand Sample:
Blackjack sphalerite hosted mainly within sparry dolomite. Sphalerite crystals are on average 2 mm. Sample contains a dirty dolomite core that is surrounded by a clean 5 mm dolomite band on which the blackjack sphalerite grew.

Thin Section:
Thin section is essentially devoid of sulphides. There are trace amounts of galena fragments and even fewer and smaller pyrite fragments. Galena occurs throughout as 0.08 mm and smaller fragments. Dolomite ranges from 3 mm saddle dolomite grains to fine-grained (devoid of sulphide fragments) grains (0.01 mm). Possibly two phases of saddle dolomite occur: one is pre-ore, one is post ore.

Modal Distribution:
Sphalerite: trace
Galena: trace
Pyrite: trace
Gangue: 100%

Appendix C1. Electron microprobe maps of grain mounts.

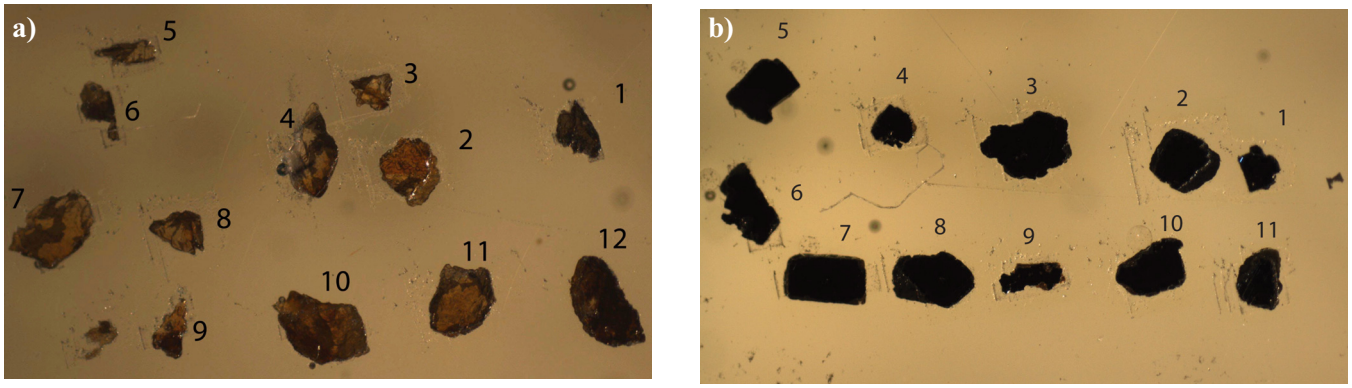

Electron microprobe maps of **(a)** sphalerite and **(b)** galena grains in the 0.25 to 0.5 mm fraction of sample 010-MPB-004.

Appendix C2. Operating conditions for the JEOL 8900 electron probe microanalyzer.

Element	Standard	Standard (wt.%)	Crystal	Beam (nA)
Cd	Cd metal	100	PET	20
Ge	Ge metal	100	TAP	20
Ag	Ag metal	100	PETH	20
Sb	Sb metal	100	PET	20
Fe	pyrite	46.55	LIFH	20
In	In metal	100	PET	20
As	arsenopyrite	45.21	TAP	20
S	sphalerite	33.02	PETH	20
Hg	cinnabar	86.22	PET	20
Mn	Mn_2O_3	69.5972	LIFH	20
Se	umangite	44.89	TAP	20
Pb	PbS	86.6	PETH	20
Zn	sphalerite	66.8	LIFH	20
Cu	Cu metal	100	LIFH	20